MV006 - Globular Ovoid Jar

An Exploration of Precision

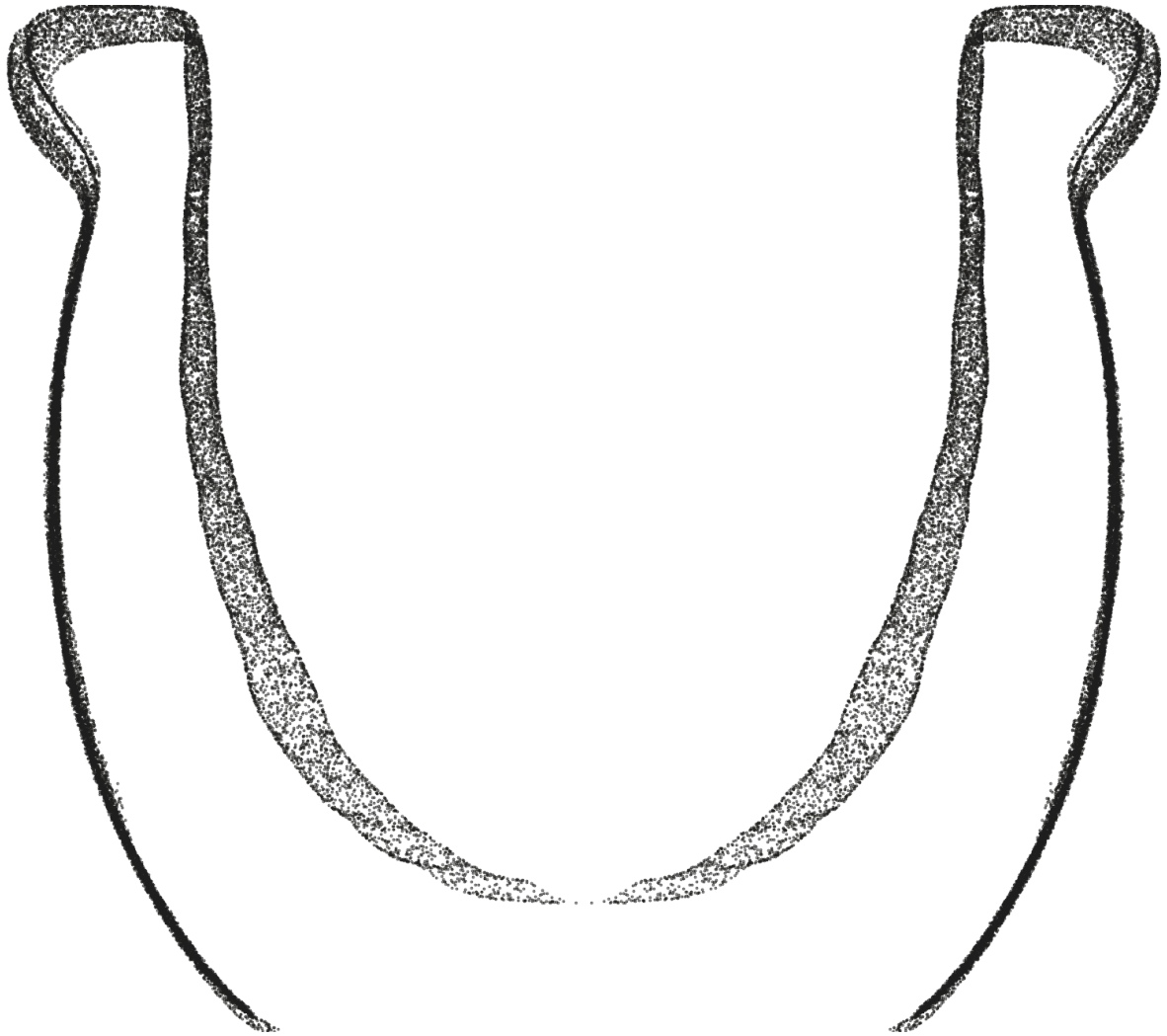

Author: Stine Gerdes, arcsci.org

Date: 2025-07-21
Version: 01.20

Petrie Museum, CC BY-NC-SA

Contents

Artifact Information

Artifact Data

Collection	Petrie Museum of Egyptian Archaeology
Provenance[1]	Petrie Museum of Egyptian Archaeology (London), recovered by Flinders Petrie
Provenience[2]	William Matthew Flinders Petrie excavation
Attribution	Predynastic Period

Museum information

Ref.	LDUCE-UC15724
Description	Basalt cylinder vase, tapering at base, rim damaged
URL	https://collections.ucl.ac.uk/Details/collect/24117

Maijers vessel classification[3]

Short classification	Globular Ovoid Jar
Long classification	The vessel is created in a closed form classified as a globular jar with a ovoid shape, a raised blunt rim.

Physical properties

Precision score[4]	11
Height (approximate)	65 mm 2.56 in
Width (approximate)	70 mm 2.76 in
Material	Basalt
Mohs Hardness[5]	6 - 7 (Basalt)
Weight	

Scan information

Source	Scanned by Artifact Foundation
Source file name	UC15724_base_0.09.stl
Scan method	Laser
Scanner	FreeScale Combo+
Rated scan accuracy	37 µm | 1.51 thou
Scan date	2024-10-07
Scanned by	Adam Young and Károly Póka

Mesh decimation	None, raw scan file used in the analysis
Number of vertices	4 352 705
Mesh density[6]	35 µm | 1.38 thou
Max vertex distance	132 µm | 5.211 thou
Min vertex distance	0 µm | 0.000 thou
Vertices per cm2	19 081 (approximated)
Vertices per in2	123 102 (approximated)

[1] The verifiable chain of custody of an artifact

[2] The location or site where an artifact was recovered

[3] Vessel artifact classification developed by W. Arnold Maijer and described in his publication Masters of Stone, ISBN 978-90-829212-0-5

[4] The precision score metric is described in Precision Score Of The Artifact, p. 61

[5] The Mohs scale is an ordinal scale, from 1 to 10, describing the materials resistance to abrasion (the ability of harder material to scratch softer material)

[6] Median distance between vertices

Alignment In The Cartesian Coordinate System

For precise and valid measurements of the vessel's geometry to be possible, the points of the scanned dataset must first and foremost be placed optimally in a Cartesian coordinate system. Several alignment methods and algorithms have been tested on a number of different vessels to determine the best way to achieve optimal alignment.

Any misalignment of the artifact will increase the error of the precision measurements, due to the distortion/ wobble effect caused by the misaligned object. To visualize this distortion, we can consider a representation of the three-dimensional point cloud data, folded to a two-dimensional plane. This folded representation is obtained by rotating all scanned points around an assumed center axis to $y = 0$, $x > 0$, thus resulting in a two-dimensional profile representation of all scanned vertices in the object.

Figure 1 illustrates this effect on a ideal ellipsoid. In the first image, the ellipsoid is perfectly aligned, resulting in a narrow and precise two-dimensional folded profile. As misalignments are introduced, the two-dimensional profile increases in width, visually showing the distortion, causing the error in the precision measurements to increase. While easy to understand visually, this distortion can also be objectively quantified, and as such used to compare the fitness of different assumed center axes against each other, and further to create an automated and solid process for optimal Cartesian alignment of the scan data.

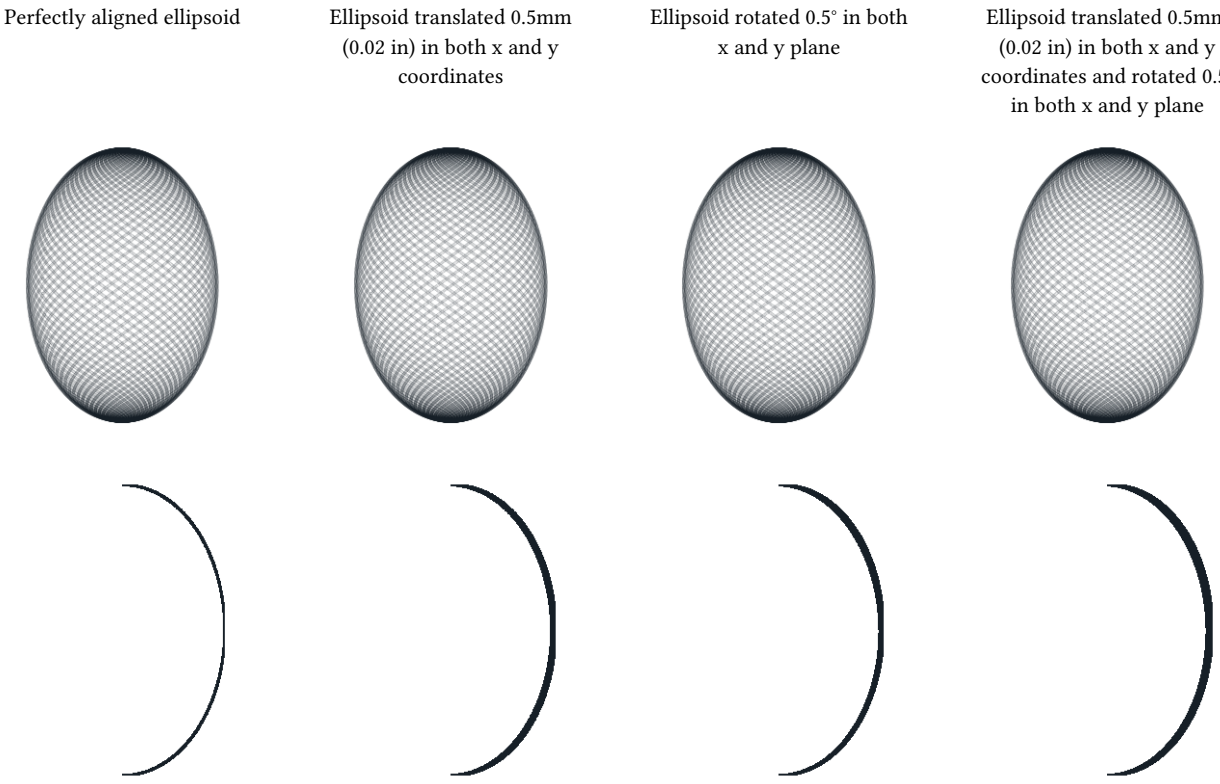

Figure 1: Distortion caused by a misalignment of the artifact

In contemporary metrology analysis of modern production objects, it is common to align the object in a Cartesian coordinate system by fitting a flat surface of the object to a reference plane in the coordinate system, cylindrical features to an ideal cylinder etc., or by using specific markers placed on the object in the design process. This methodology, however, is inadequate for the ancient objects in question. Most scanned artifacts, do not have a valid flat surface which could be aligned to a plane in the Cartesian coordinate system; most surfaces seem to be curved. Some artifacts do have a flat base, however this is often a worn area of the artifact and practical tests have shown that alignment to such surfaces will not produce optimal alignment of the scan data.

As conventional methods of alignment do not always yield good results with these types of artifacts, a more adequate method of alignment has been developed to enable precise measurements and statistical analysis of the scan data.

To find the optimal position of the vessel in the coordinate system, a range of rotation and translation tests are carried out to find the best fit of the central axis.

Based on the assumption that the analyzed object was created using a rotational process, and thus have symmetry around a central axis, the alignment of the artifact is carried out in a two-step process. An overview of this process is given below.

The artifact is placed in a Cartesian coordinate system, in an initially unaligned state. The first step in the alignment process estimates the central rotational axis of the vessel, by analyzing the coaxiality of thin cross-section slices of the vessel. The slices will be as thin as possible based on the mesh density of the scan, while still ensuring enough data points in each slice to be statistically valid.

For each slice, circular regression[7] (estimate of best fit circle) is used to estimate the center point of this slice. Combined over the total Z-axis range of the vessel, these center points provide us with an indicator of the incline and position of the vessel's central axis.

The next step will optimize the center axis alignment by progressively minimizing the deviation (perpendicular to the surface curvature) of the two-dimensional profile, see Figure 1. By ascertaining and comparing the resulting fit of many thousands of different potential rotations, the best fit alignment of the scan data can be estimated, and an optimal center axis (in relation to the data points) can be reconstructed. The actual three-dimensional point-cloud is then aligned to this axis, by rotating and translating the scanned data points to match the Z-axis of the Cartesian coordinate system.

To enable extensive analysis of the full surface of the artifact, the mesh is split into exterior and interior surfaces. The exterior surface is aligned independently of interior data points, providing a baseline for exterior quality assessment. The interior surface is represented by two alignments:

- Aligned with the exterior mesh to analyze concentricity, and
- Aligned separately to assess its precision and compare the true tilt/displacement between interior and exterior surfaces.

[7] Circle regression algorithm used: Kenichi Kanatani, Prasanna Rangarajan, "Hyper least squares fitting of circles and ellipses" Computational Statistics & Data Analysis, Vol. 55, pages 2197-2208, (2011)

Statistics used throughout the report

This section provides an overview of the key statistical and model-evaluation metrics employed throughout the report to analyze dataset variability, model fit, and predictive accuracy.

Each measure is introduced with its mathematical formulation, practical interpretation, and explicit reference to how it is calculated in the context of the evaluated models and residuals. Together, these metrics quantify:

- Data variability (e.g., MAD, Standard Deviation, Range).
- Model accuracy (e.g., MSD, RMSD).
- Robustness vs. sensitivity to extreme values and central tendencies.

Mean Squared Deviation (MSD), also known as Mean Squared Error (MSE).

$$\mathrm{MSD} = \frac{\sum_{i=1}^{n} (y_i - \hat{y})^2}{n}$$

The Mean Squared Deviation (MSD) measures the average magnitude of squared differences between observed (y_i) and predicted ($\hat{y}$) values, calculated as the mean of squared residuals, and is a used as a measure of discrepancy in regression and model-fitting contexts.

This measure amplifies the influence of larger deviations through squaring, emphasizes imperfections in the observed data, but retains sensitivity to outliers.

Root Mean Squared Deviation (RMSD), also known as Root Mean Squared Error (RMSE).

$$\mathrm{RMSD} = \sqrt{\frac{\sum_{i=1}^{n} (y_i - \hat{y})^2}{n}}$$

The Root Mean Square Deviation (RMSD) measures the magnitude of differences between observed (y_i) and predicted ($\hat{y}$) values by calculating the square root of the average of squared residuals.

RMSD is a commonly used measure of discrepancy in regression and model-fitting contexts. It quantifies the average magnitude of residuals while retaining sensitivity to larger deviations (via squaring), making it particularly useful for evaluating model accuracy.

Standard Deviation (SD)

$$s = \sqrt{\frac{\sum_{i=1}^{n} (y_i - \bar{y})^2}{n-1}}$$

The Standard Deviation measures the spread of data (y_i) around the mean ($\bar{y}$) by calculating the square root of the average of squared differences between each value and the mean.

It is sensitive to outliers as it amplifies their influence through squaring, in contrast to MAD.

Throughout this report, the Standard Deviation is calculated using the absolute residuals from regression models.

Median Absolute Deviation (MedianAD)

$$\mathrm{MedianAD} = \mathrm{median}(|y_i - \mathrm{median}(y)|)$$

The Median Absolute Deviation (MAD) measures the spread of data around the median by calculating the median of absolute differences between each value and the median.

MAD is a robust measure of spread, analogous to the interquartile range (a robust measure centered on the middle 50% of data), and differs from the standard deviation in that it minimizes the impact of outliers.

Throughout this report, the MAD is calculated using the absolute values of residuals from regression models.

Range

$$\max(y_i) - \min(y_i)$$

The Range measures the spread of a dataset by calculating the difference between the maximum and minimum values.

The Range is a simple measure of spread, capturing the full extent of variability. Range is very sensitive to extreme values, as it is entirely determined by the two most extreme data points.

Throughout this report, the Range is calculated using the full range of residuals from regression models.

Precision

To explore the manufacturing precision of the artifact in depth, the following analysis have been carried out:

- Circularity around the axis of symmetry is examined in detail at selected cross-sections.
- Overall circularity around the axis of symmetry is measured for the full height of the vessel (areas of the vessel with extensive damage are not taken into account for this metric).
- Concentricity of the vessel between selected cross-sections are examined in detail to determine if the existence of an axis of rotation in the manufacture of the object can be established.
- The coaxiality of the vessel is analyzed to explore the precision of the central axis of the object.
- The surface variability is analyzed and visualized on through a heatmap.

Circularity

Circularity is the measurement of how round the surface of an object is, optionally in reference to a datum axis. The *circularity tolerance* is the radial distance of two circles, each with their centers in the datum axis, and each of them conforming, respectively, to the minimum and maximum deviations of the data-set to a true circle, see Figure 2.

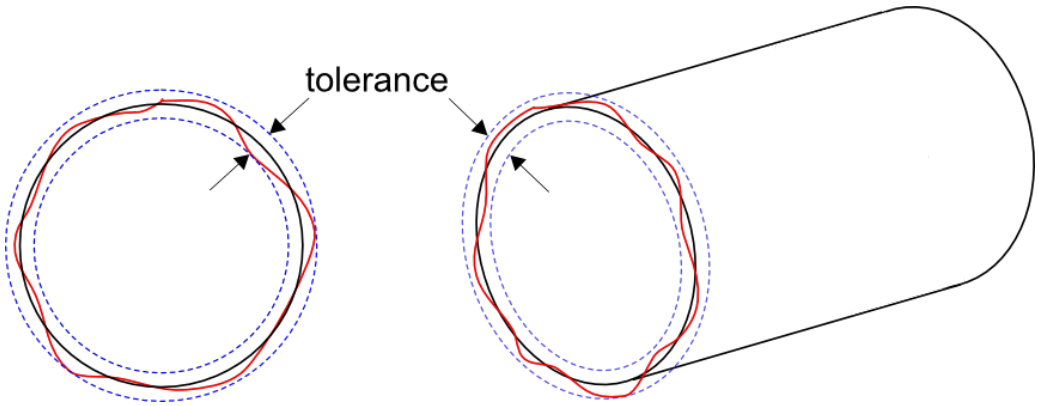

Figure 2: Circularity tolerance.

Circularity is examined at different cross-sections of the vessel, using the established Z-axis as the datum axis (axis of symmetry). The distance between the scanned points in the local datum plane is measured to determine the range between the two concentric circles encompassing the measured points, see Figure 3.

Referencing all of the individual circularity measurements to the global (reconstructed) axis of symmetry of the object, allows us to ascertain not only circularity of local features of the object, but how well circularity was *maintained* over the entire manufacturing process. This is an important distinction, which may be able to provide valuable insights into requirements of the construction methods. For reference, and seeing that the variance in local circularity also holds interest, measurements of circularity of the vessel without reference to the axis of symmetry can additionally be found in the Concentricity, p. 33.

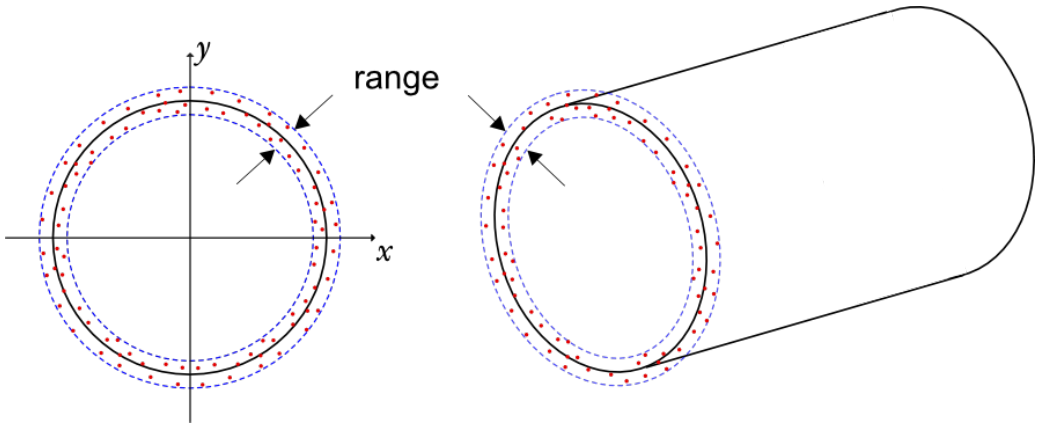

Figure 3: Circularity measurements.

If the circularity is determined from slices of the vessel exclusively in the *Z-plane* (actually measuring the cylindricity of a very thin slices of the vessel, in an attempt to approximate circularity), this would - in some areas - introduce significant distortion (increasing measurement errors) in the samples, due to the curvature of the vessel's surface.

Each sample slice of the vessel is therefore obtained perpendicular to the surface curvature, see Figure 6 to Figure 18. The measurements are taken conservatively without filtration of potential outliers.

To explore the potential distortion caused by obtaining samples in the Z-plane only, please refer to Appendix A, where measurements in the Z-plane and measurements perpendicular to surface curvature are compared side by side.

Detailed circularity measurements of selected points

Circularity measurements across a range of selected slices of the vessel (see Table 1) have been analyzed in-depth, and detailed plots of each measurement is provided. Furthermore, full circularity measurements are shown for each available scanned surface including a detailed plot to visualize the circularity of all areas of the vessel.

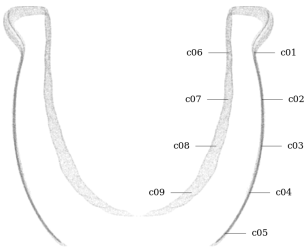

Figure 4: Circularity measurement sample locations, full mesh aligned with exterior surface

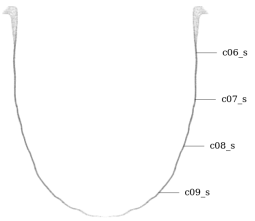

Figure 5: Circularity measurement sample location, separately aligned interior mesh

Metric

Tag	Area	Measured deviation[8]	Residuals				Sample size	Slice		
			Range	RMSD[9]	MAD[10]	SD		Height	Z coord.	Radius[11]
		mm	mm	mm	mm	mm		mm	mm	mm
c01	exterior	Ø62.863±0.516	1.012	0.276	0.111	0.149	1763	0.050	52.209	31.432
c02	exterior	Ø67.109±0.436	0.812	0.167	0.060	0.094	1960	0.050	39.545	33.555
c03	exterior	Ø66.558±0.503	0.818	0.191	0.076	0.117	2010	0.050	26.881	33.279
c04	exterior	Ø60.183±0.756	1.124	0.187	0.075	0.116	1645	0.050	14.218	30.091
c05	exterior	Ø47.151±0.437	0.714	0.167	0.078	0.107	1108	0.050	3.154	23.576
c06	interior	Ø49.366±0.754	1.408	0.460	0.155	0.203	1499	0.050	52.209	24.683
c06_s	interior sep.	Ø49.324±0.195	0.323	0.073	0.030	0.043	1434	0.050	52.209	24.662
c07	interior	Ø48.678±1.141	2.165	0.761	0.217	0.327	1447	0.050	39.545	24.339
c07_s	interior sep.	Ø48.756±0.141	0.255	0.056	0.024	0.031	1429	0.050	39.545	24.378
c08	interior	Ø42.346±1.493	2.937	1.017	0.385	0.455	1123	0.050	26.881	21.173
c08_s	interior sep.	Ø42.516±0.153	0.248	0.046	0.020	0.028	1160	0.050	26.881	21.258
c09	interior	Ø28.936±1.626	2.778	0.999	0.298	0.430	698	0.050	14.218	14.468
c09_s	interior sep.	Ø28.916±0.148	0.292	0.059	0.017	0.036	621	0.050	14.218	14.458

Imperial

Tag	Area	Measured deviation[8]	Residuals				Sample size	Slice		
			Range	RMSD[9]	MAD[10]	SD		Height	Z coord.	Radius[11]
		in	in	in	in	in		in	in	in
c01	exterior	Ø2.4749±0.0203	0.0398	0.0109	0.0044	0.0059	1763	0.0020	2.0555	1.2375
c02	exterior	Ø2.6421±0.0172	0.0320	0.0066	0.0024	0.0037	1960	0.0020	1.5569	1.3210
c03	exterior	Ø2.6204±0.0198	0.0322	0.0075	0.0030	0.0046	2010	0.0020	1.0583	1.3102
c04	exterior	Ø2.3694±0.0298	0.0442	0.0073	0.0030	0.0045	1645	0.0020	0.5598	1.1847
c05	exterior	Ø1.8564±0.0172	0.0281	0.0066	0.0031	0.0042	1108	0.0020	0.1242	0.9282
c06	interior	Ø1.9435±0.0297	0.0555	0.0181	0.0061	0.0080	1499	0.0020	2.0555	0.9718
c06_s	interior sep.	Ø1.9419±0.0077	0.0127	0.0029	0.0012	0.0017	1434	0.0020	2.0555	0.9709
c07	interior	Ø1.9164±0.0449	0.0853	0.0300	0.0085	0.0129	1447	0.0020	1.5569	0.9582
c07_s	interior sep.	Ø1.9195±0.0055	0.0100	0.0022	0.0010	0.0012	1429	0.0020	1.5569	0.9598
c08	interior	Ø1.6672±0.0588	0.1156	0.0400	0.0152	0.0179	1123	0.0020	1.0583	0.8336
c08_s	interior sep.	Ø1.6739±0.0060	0.0098	0.0018	0.0008	0.0011	1160	0.0020	1.0583	0.8369
c09	interior	Ø1.1392±0.0640	0.1094	0.0393	0.0117	0.0169	698	0.0020	0.5598	0.5696
c09_s	interior sep.	Ø1.1384±0.0058	0.0115	0.0023	0.0007	0.0014	621	0.0020	0.5598	0.5692

Table 1: Detailed circularity measurements at selected samples of MV006.

Figure 6 to Figure 18 shows a detailed plots of each circularity measurement.

[8]Sample diameter Ø± maximum measured deviation from measured radius
[9]Root mean square deviation (RMSD) also called Root mean square error (RMSE)
[10]Median absolute deviation
[11]Median sample radius from z-axis

Graphical overview of circularity measurement c01

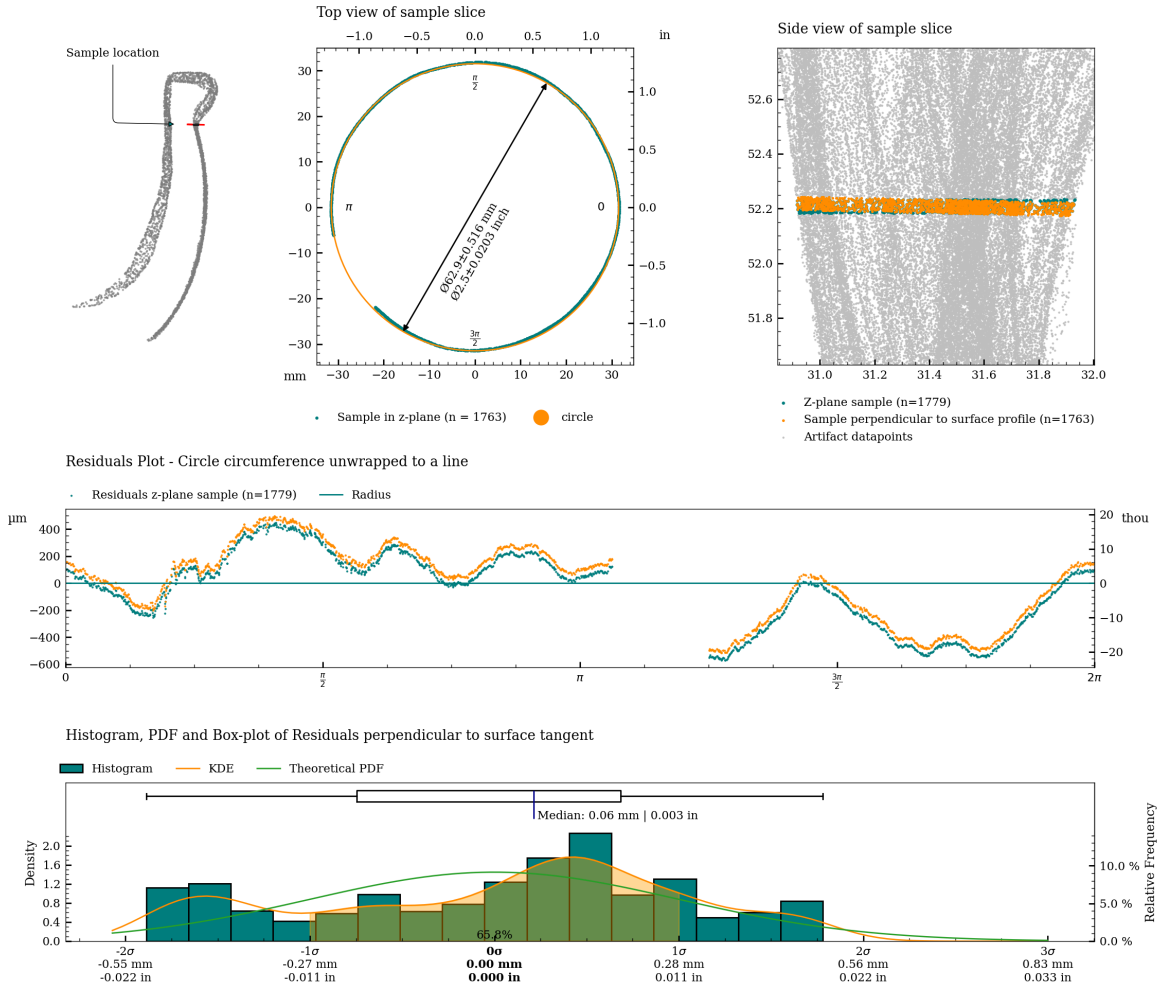

Figure 6: Charts with statistics for the measurement of c01.

Graphical overview of circularity measurement c02

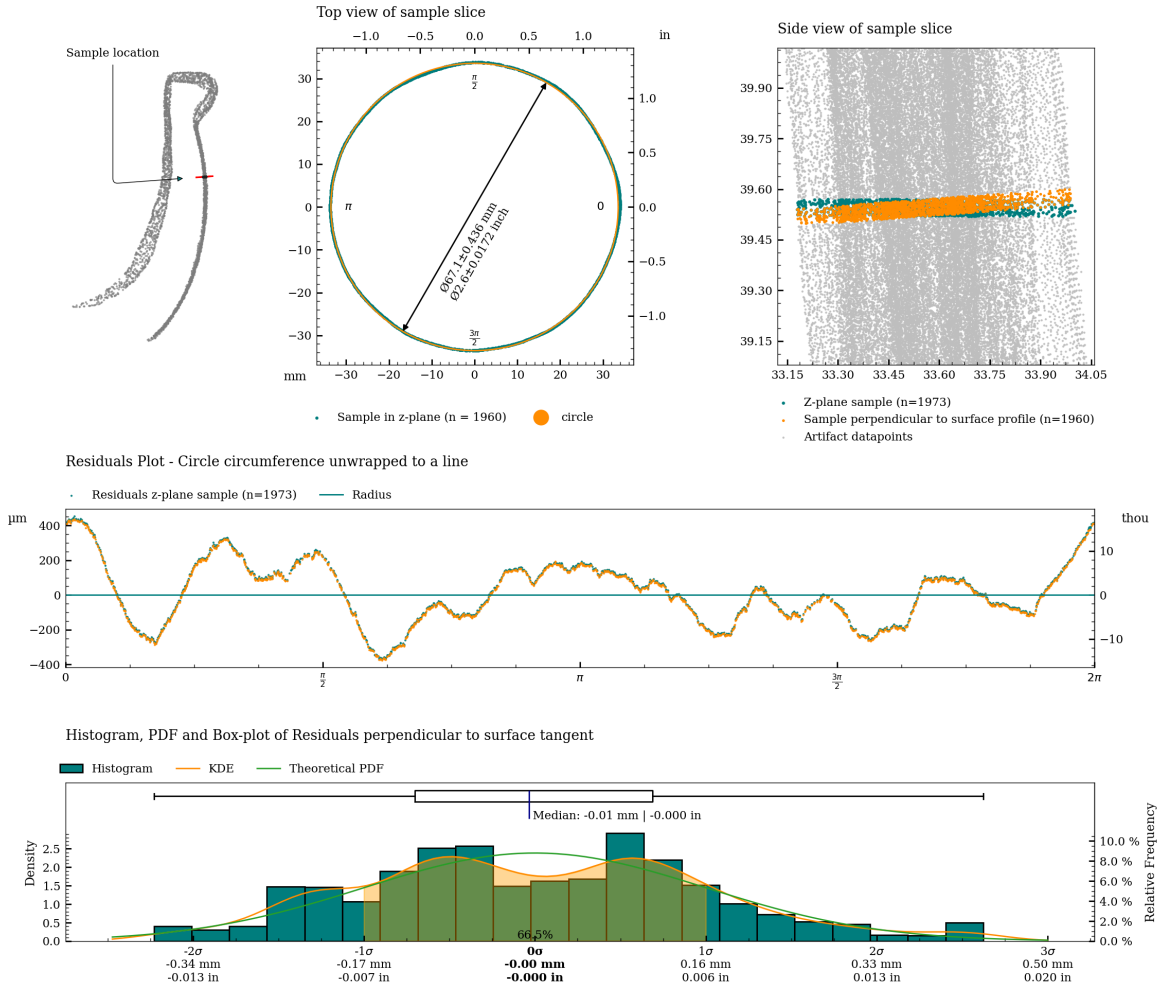

Figure 7: Charts with statistics for the measurement of c02.

Graphical overview of circularity measurement c03

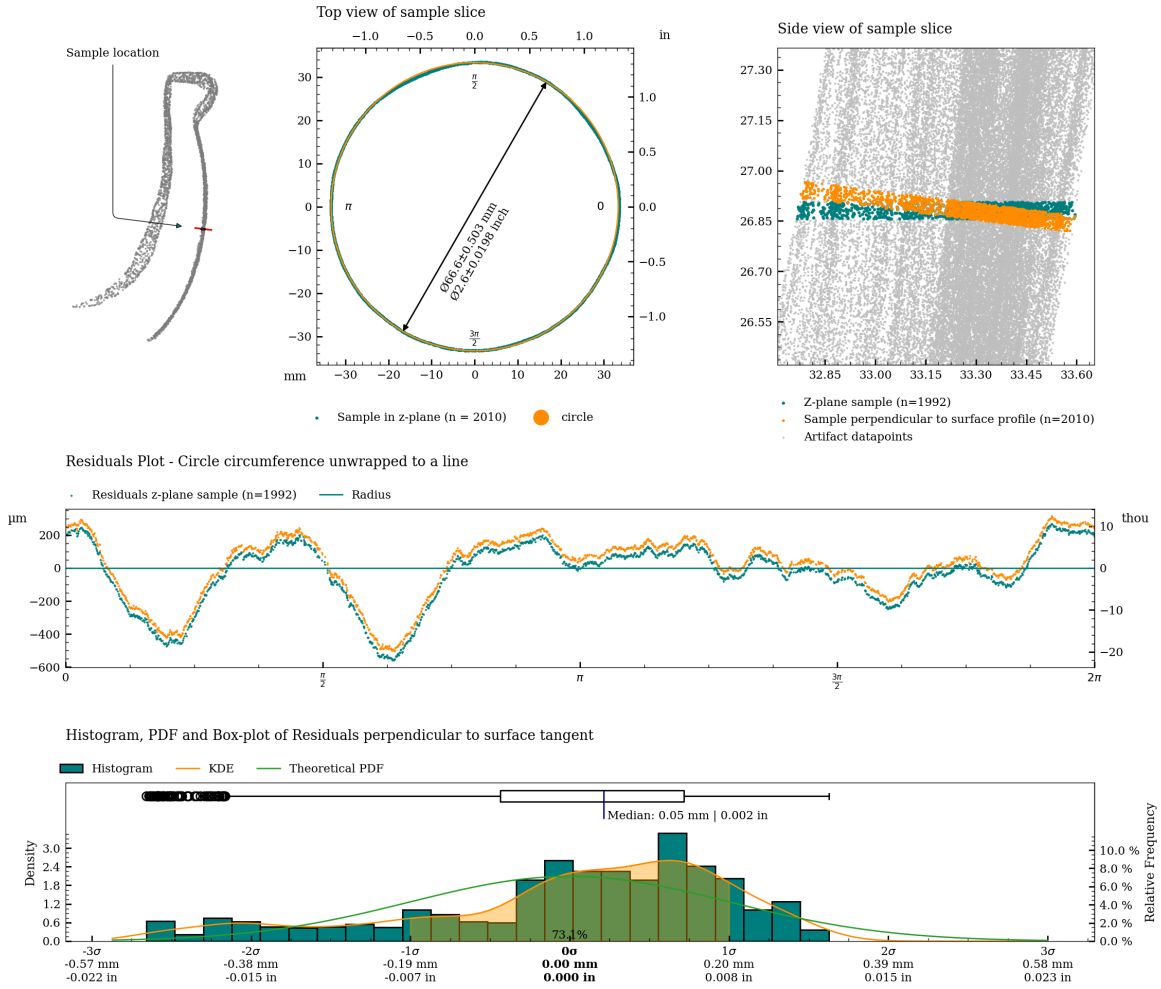

Figure 8: Charts with statistics for the measurement of c03.

Graphical overview of circularity measurement c04

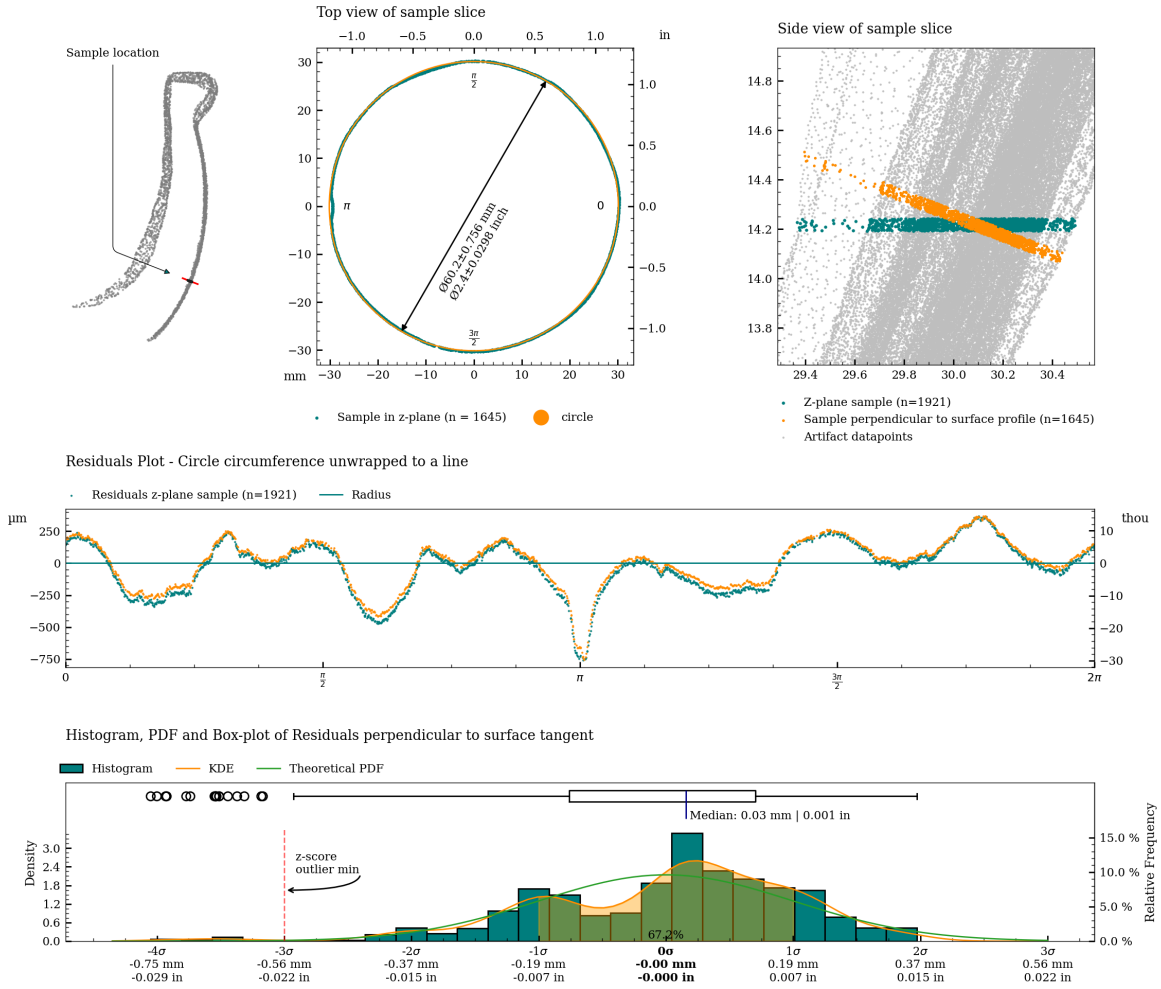

Figure 9: Charts with statistics for the measurement of c04.

Graphical overview of circularity measurement c05

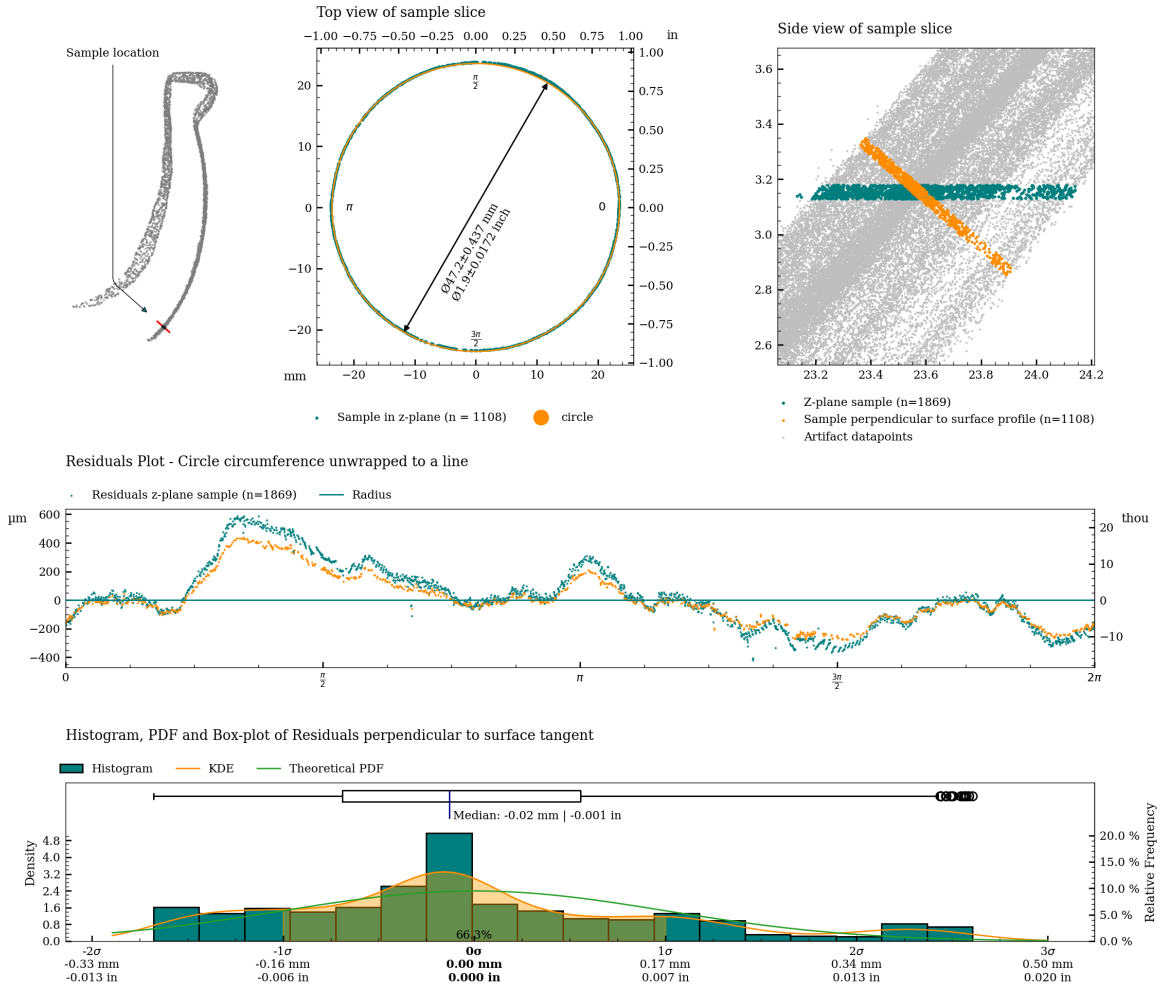

Figure 10: Charts with statistics for the measurement of c05.

Graphical overview of circularity measurement c06

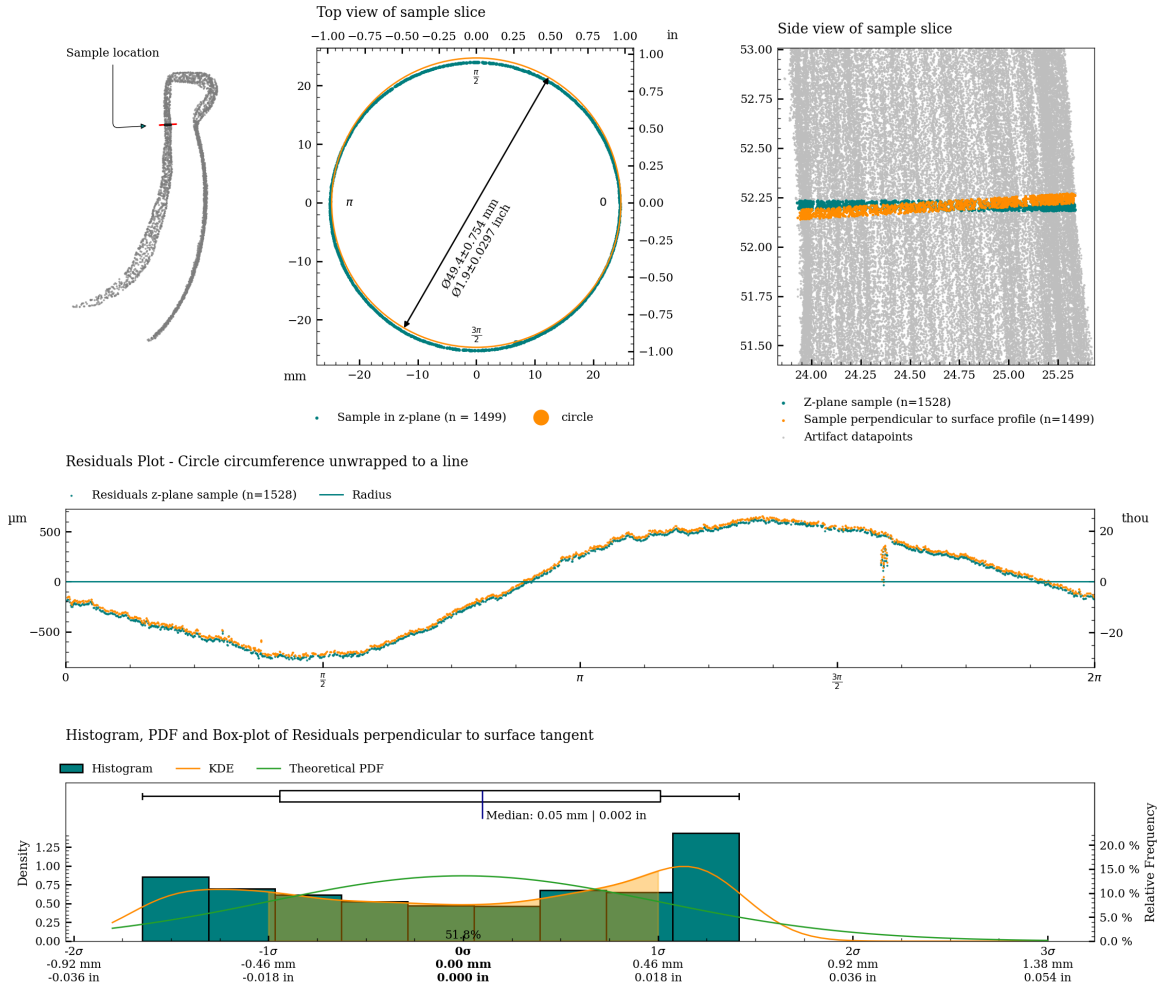

Figure 11: Charts with statistics for the measurement of c06.

Graphical overview of circularity measurement c06_s

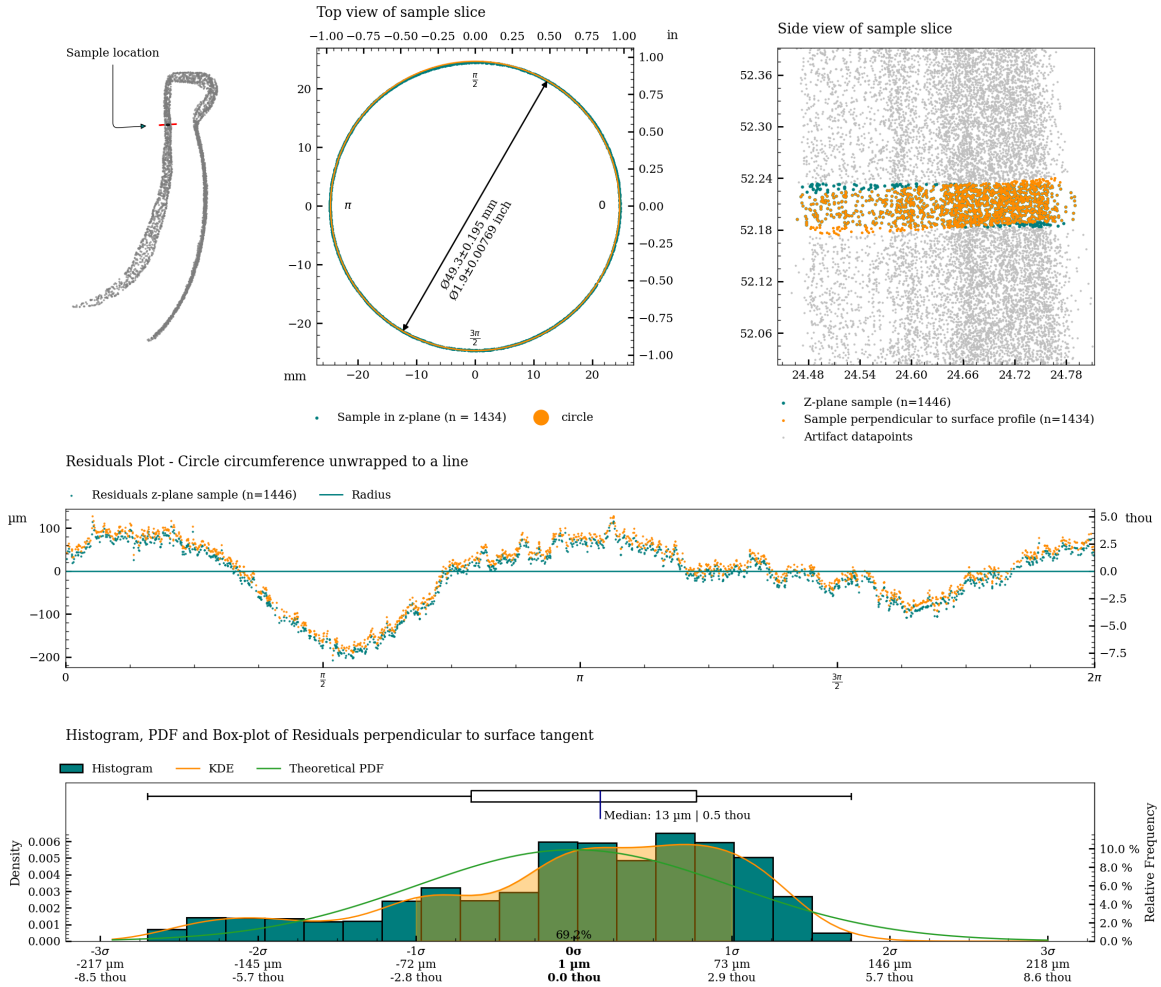

Figure 12: Charts with statistics for the measurement of c06_s.

Graphical overview of circularity measurement c07

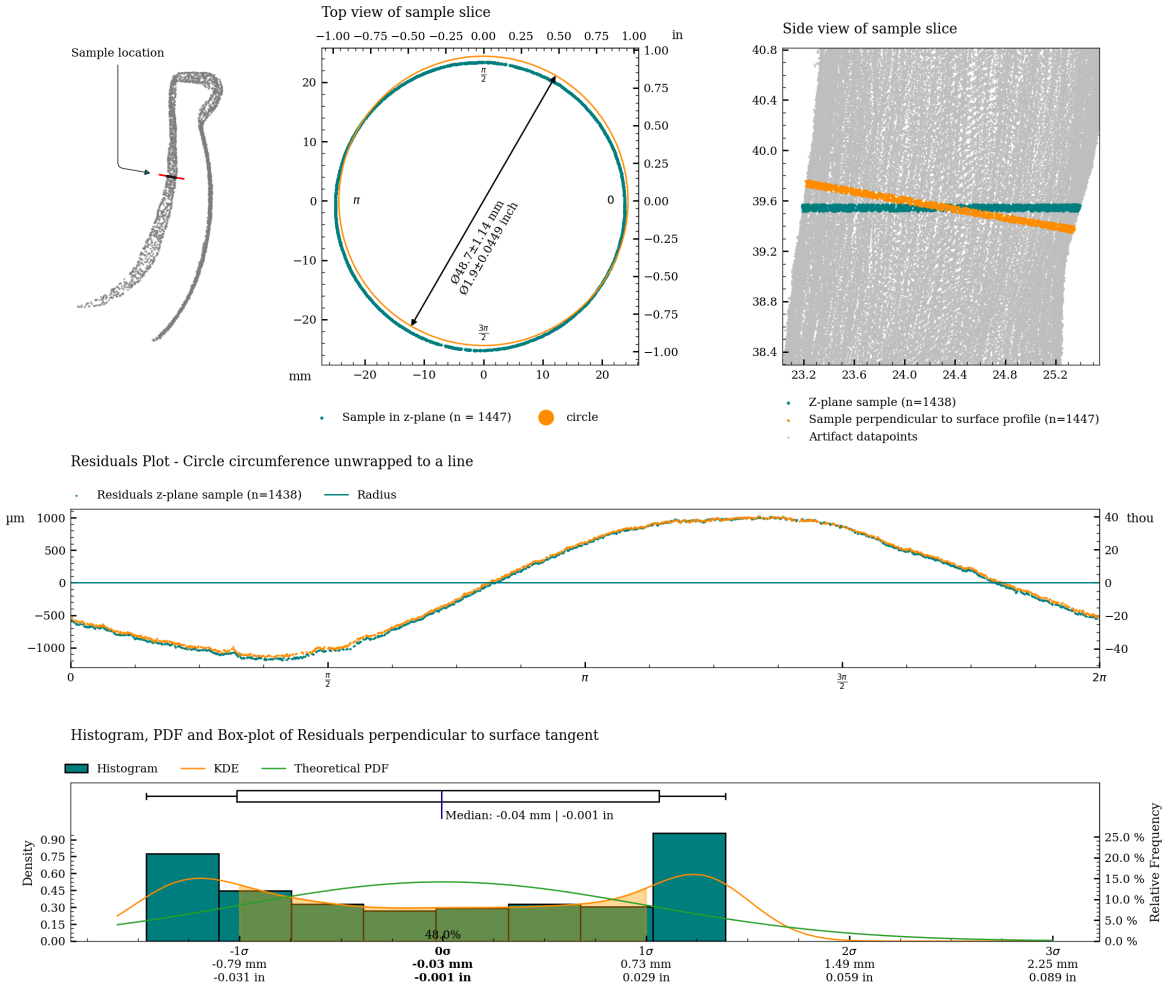

Figure 13: Charts with statistics for the measurement of c07.

Graphical overview of circularity measurement c07_s

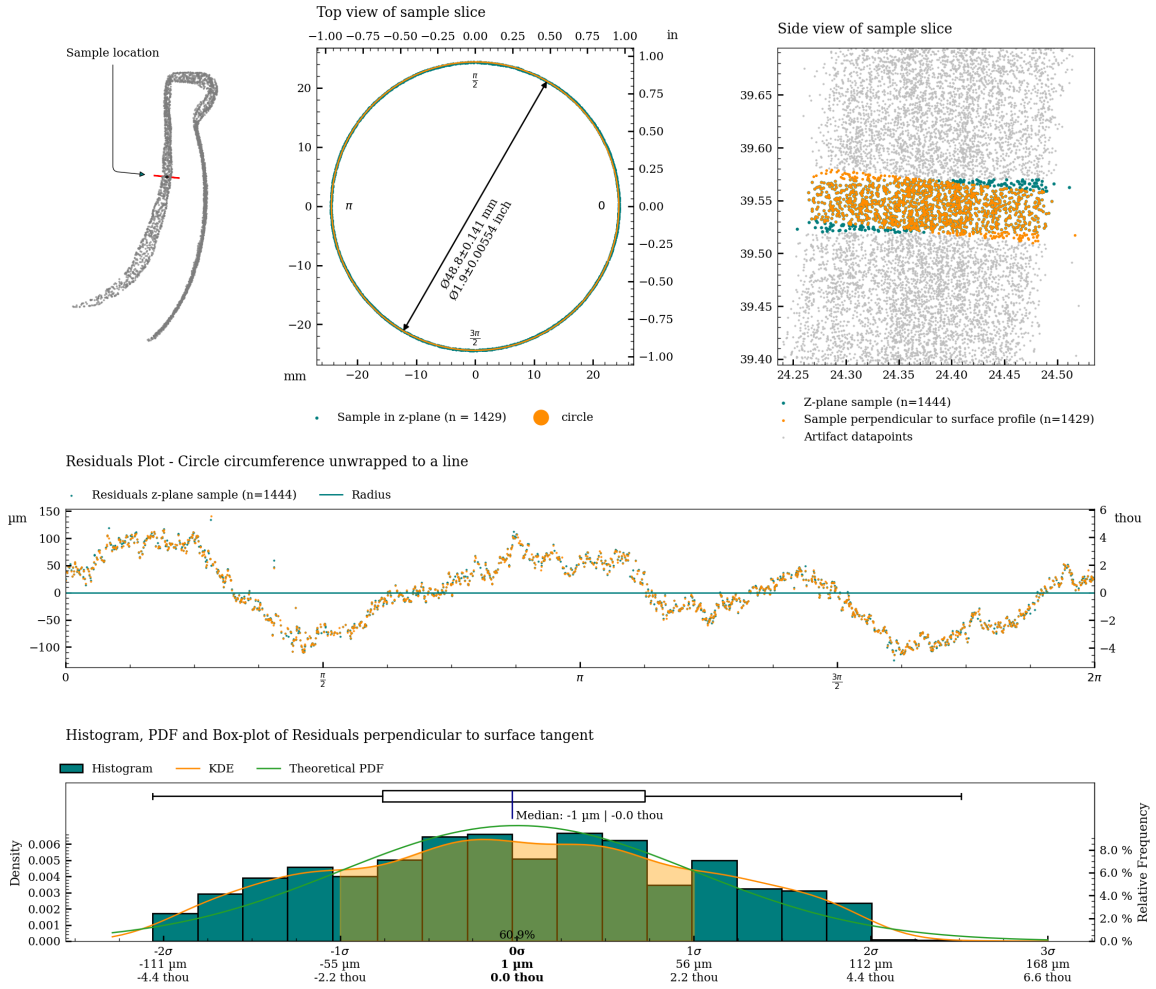

Figure 14: Charts with statistics for the measurement of c07_s.

Graphical overview of circularity measurement c08

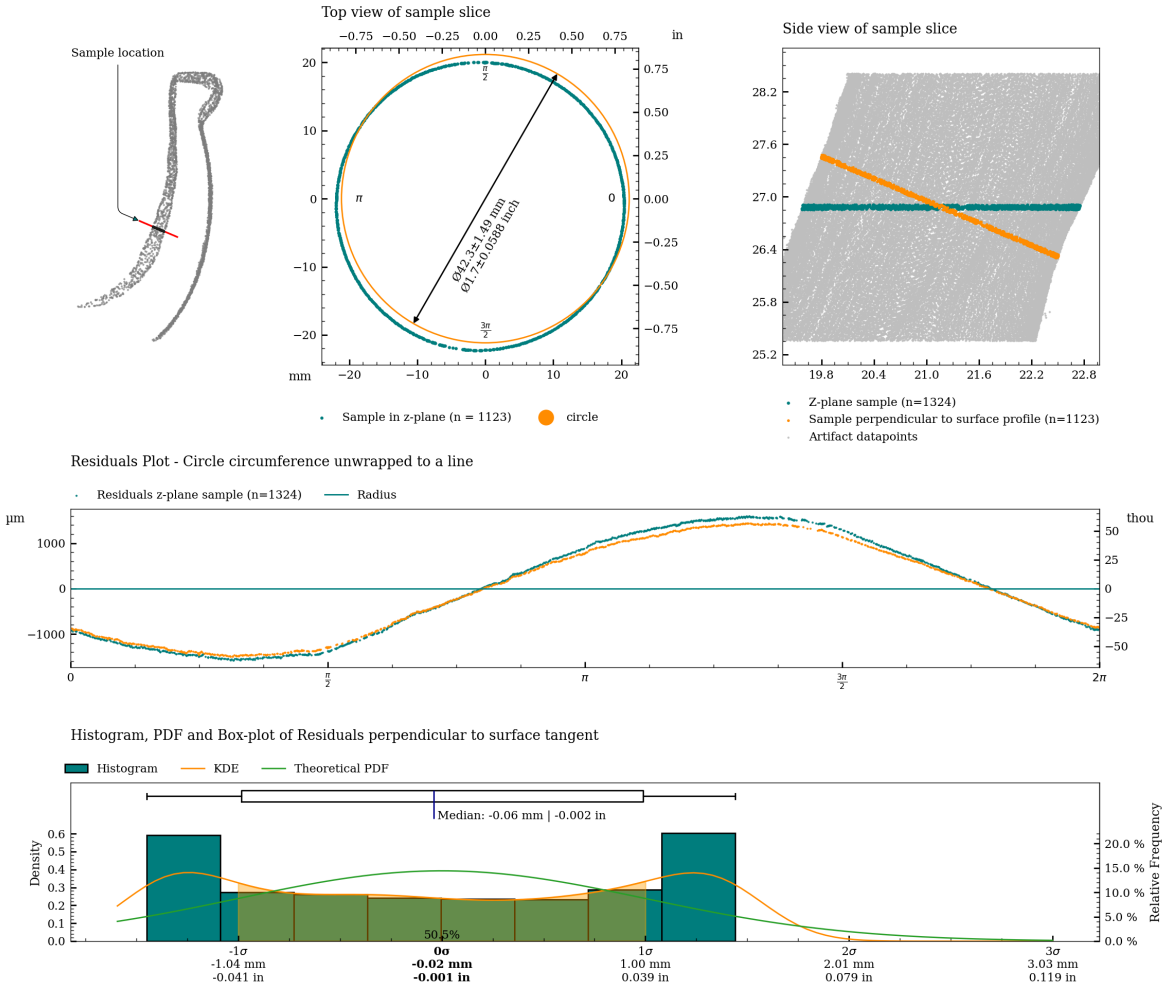

Figure 15: Charts with statistics for the measurement of c08.

Graphical overview of circularity measurement c08_s

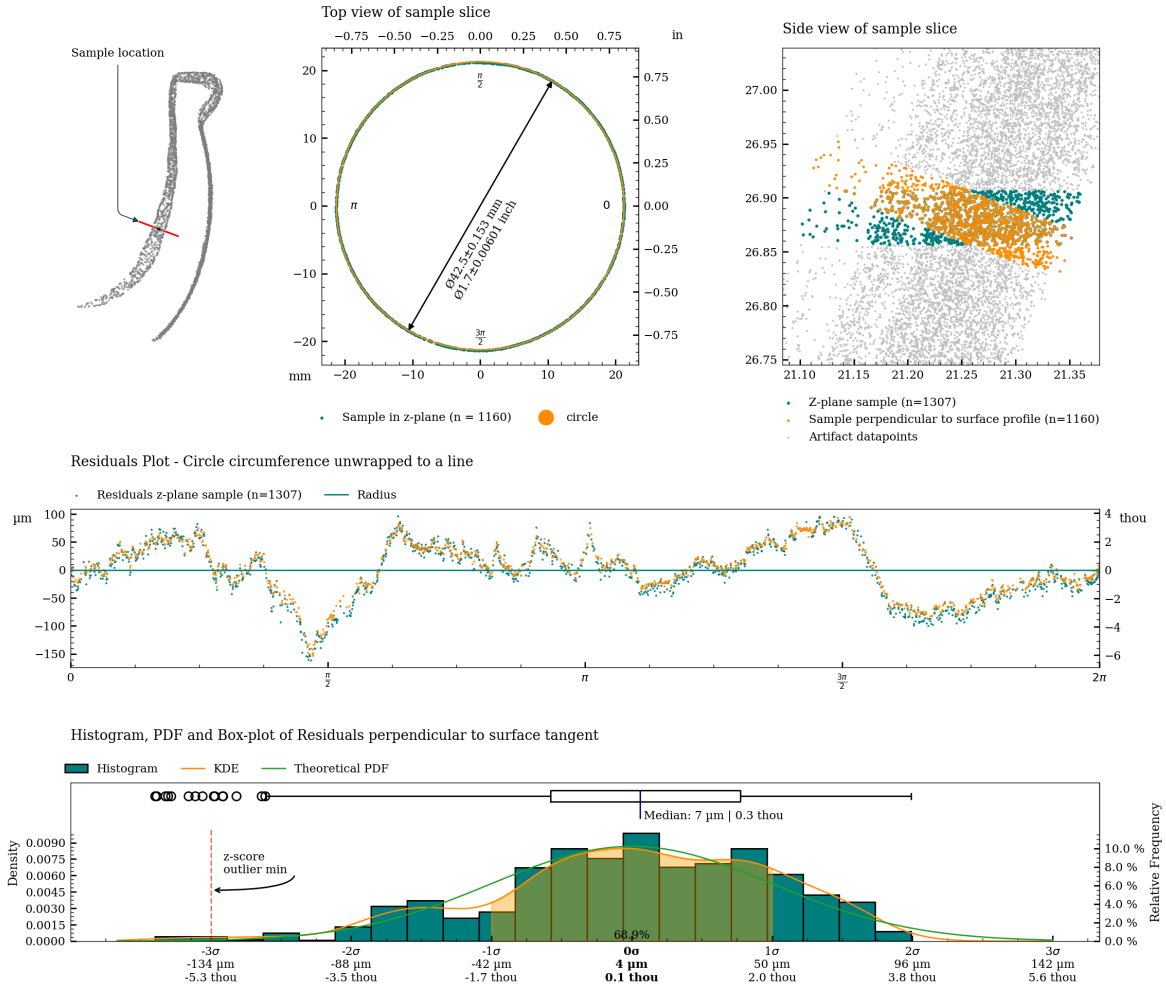

Figure 16: Charts with statistics for the measurement of c08_s.

Graphical overview of circularity measurement c09

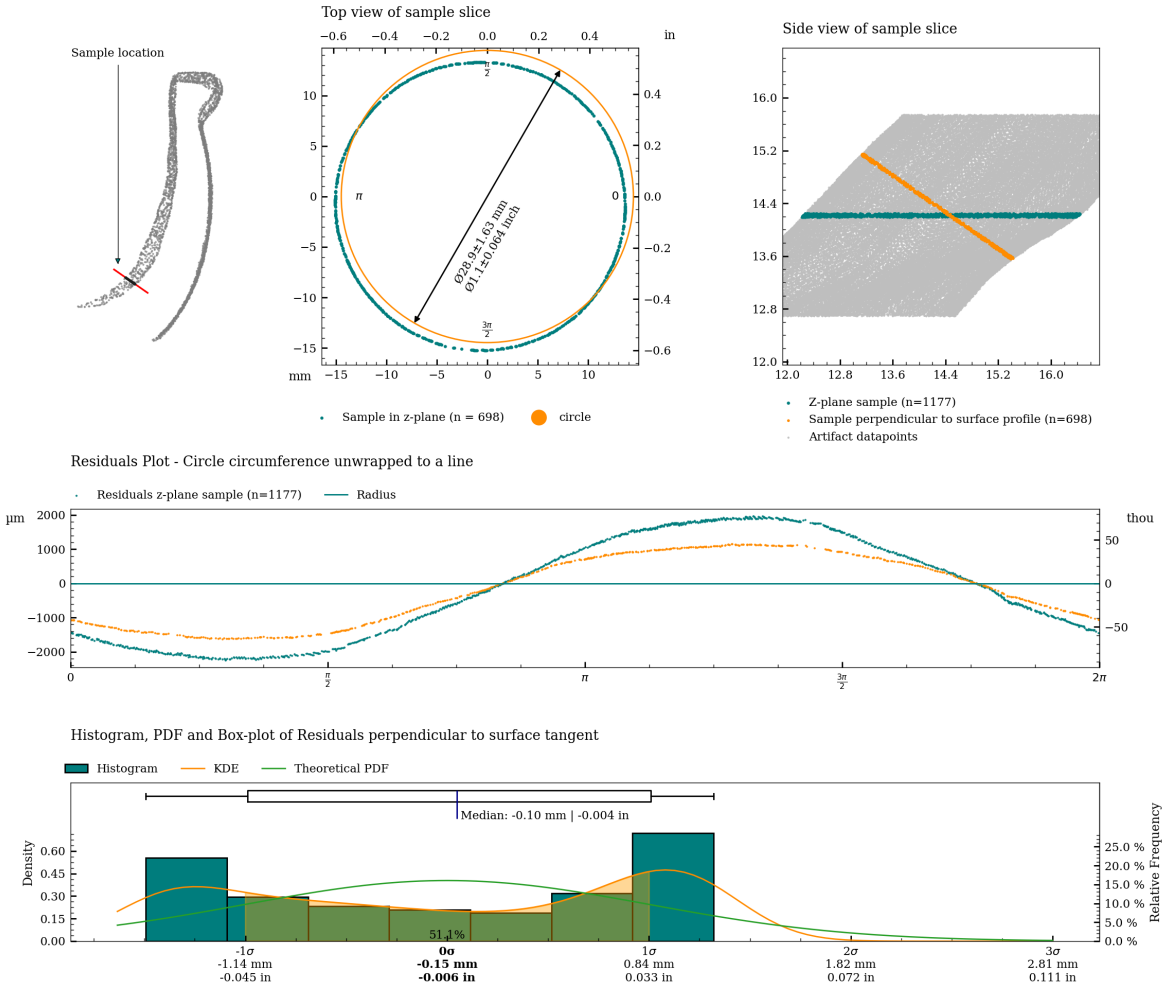

Figure 17: Charts with statistics for the measurement of c09.

Graphical overview of circularity measurement c09_s

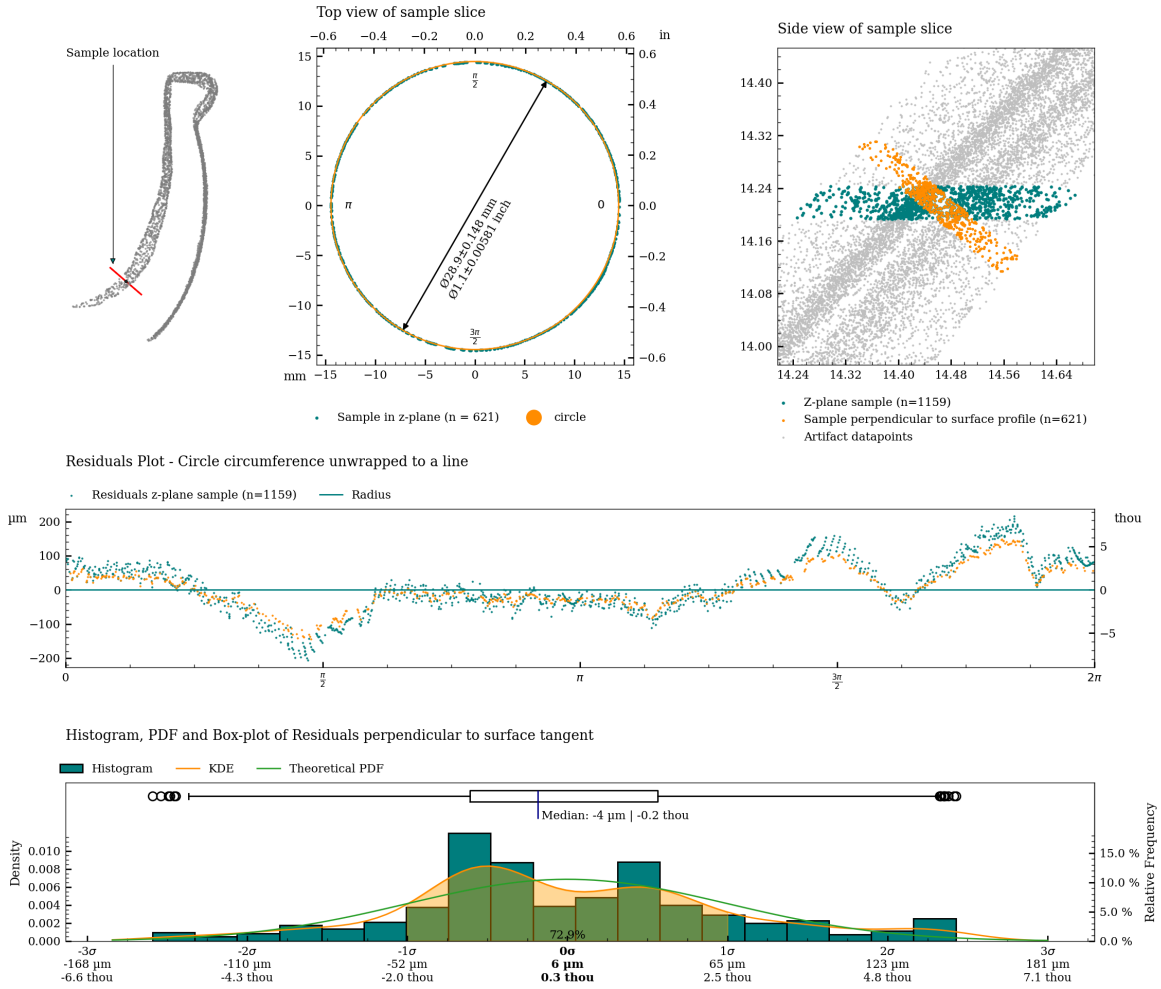

Figure 18: Charts with statistics for the measurement of c09_s.

Table 2 shows statistical measures of the circularity of the vessel, measured along the full height (areas on the artifact scan containing damaged parts have been removed to the best extent possible to reduce the influence of the measurement).

Metric

Area	Range			Standard Deviation			RMSD			Slices	Slice height
	Median	Min.	Max.	Median	Min.	Max.	Median	Min.	Max.		
	mm	mm	mm	mm	mm	mm	mm	mm	mm		mm
Exterior	0.854	0.567	2.229	0.114	0.068	0.335	0.193	0.143	0.728	1167	0.050
Interior	2.243	1.023	3.626	0.338	0.128	0.533	0.745	0.283	1.119	870	0.050
Interior separate	0.270	0.150	0.939	0.031	0.018	0.073	0.055	0.028	0.101	882	0.050

Imperial

Area	Range			Standard Deviation			RMSD			Slices	Slice height
	Median	Min.	Max.	Median	Min.	Max.	Median	Min.	Max.		
	in	in	in	in	in	in	in	in	in		in
Exterior	0.854	0.567	2.229	0.114	0.068	0.335	0.193	0.143	0.728	1167	0.050
Interior	2.243	1.023	3.626	0.338	0.128	0.533	0.745	0.283	1.119	870	0.050
Interior separate	0.270	0.150	0.939	0.031	0.018	0.073	0.055	0.028	0.101	882	0.050

Table 2: Perpendicular Circularity analysis of MV006.

Circularity analysis of exterior surface

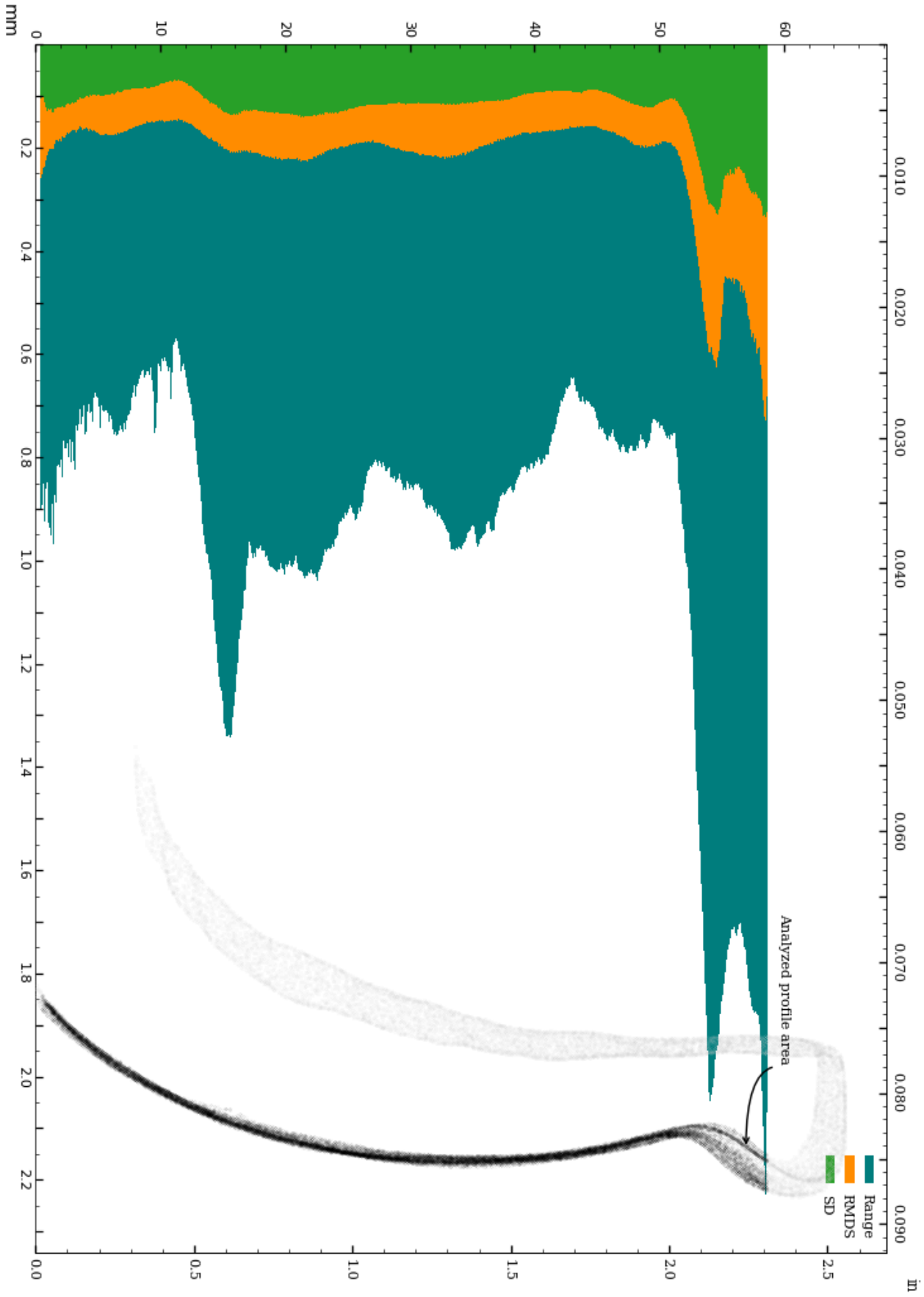

Figure 19: Circularity of exterior surface.

Circularity analysis of exterior surface, Standard Deviation and Root Mean Squared Deviation

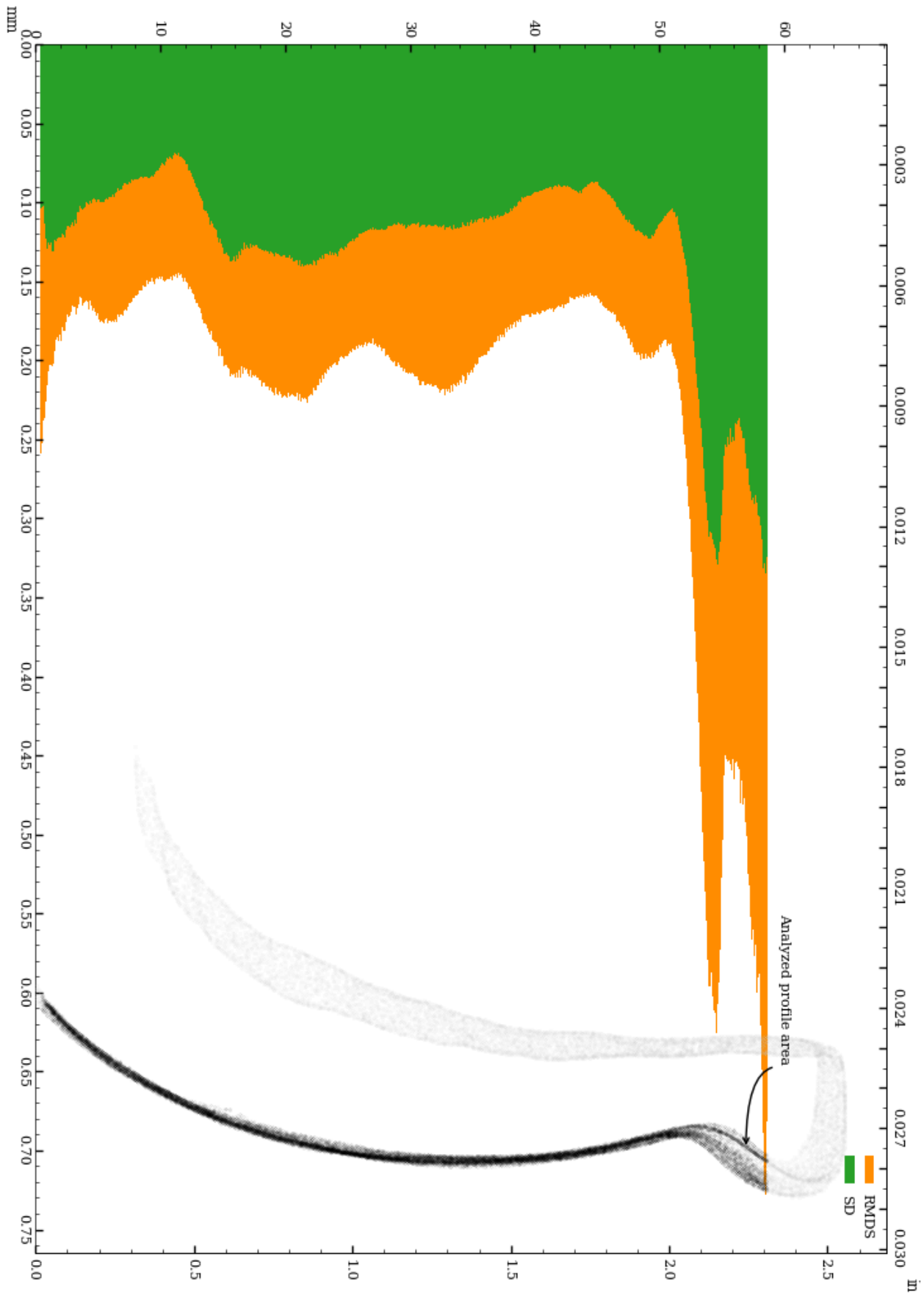

Figure 20: Vessel circularity of exterior surface, standard deviation and median absolute deviation.

The distributions of the circularity measurements across 1167 slices of the exterior surface are shown below.

Range measurement distribution across 1167 slices of exterior surface

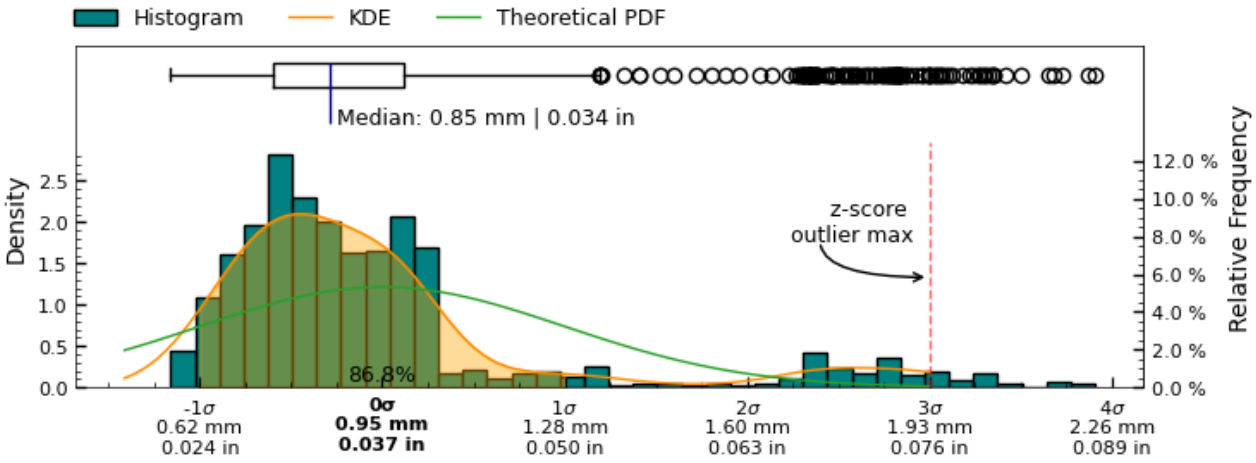

Figure 21: Range measurement distribution across measured slices of exterior surface

Standard Deviation measurement distribution across 1167 slices of exterior surface

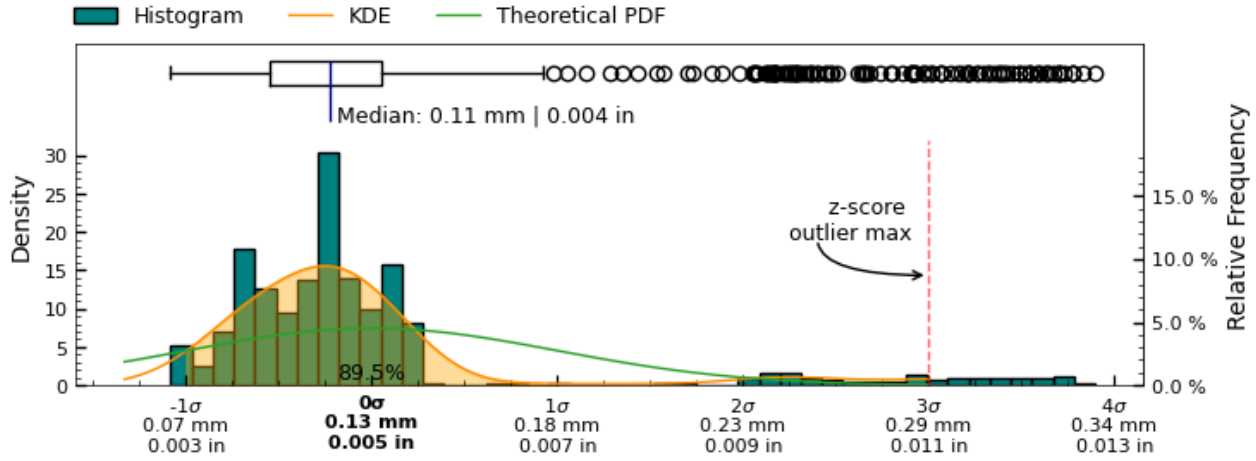

Figure 22: Standard Deviation measurement distribution across measured slices of “ + exterior + “ surface

Root Mean Squared Deviation measurement distribution across 1167 slices of exterior surface

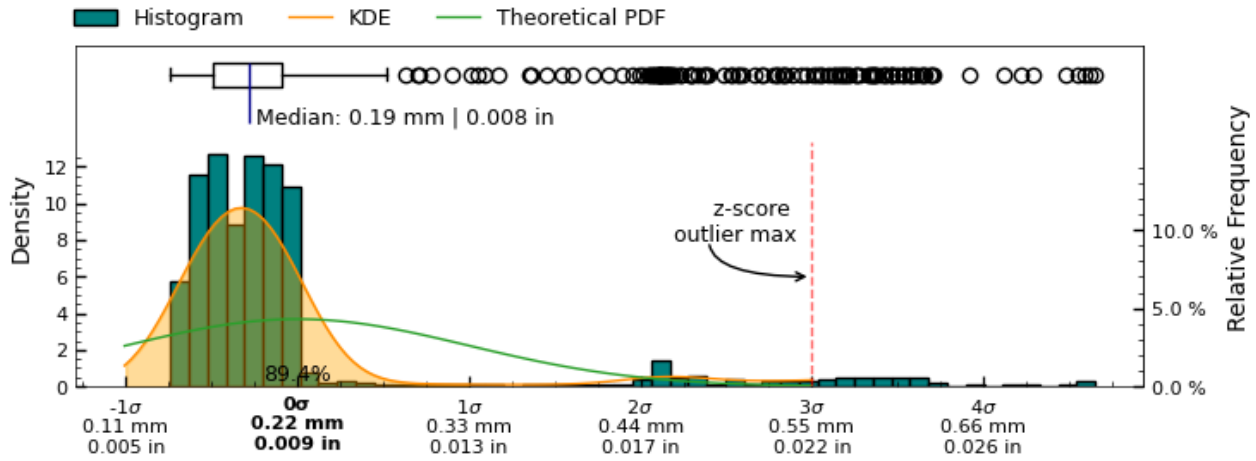

Figure 23: Root Mean Squared Deviation measurement distribution across measured slices of exterior surface

Circularity analysis of interior surface

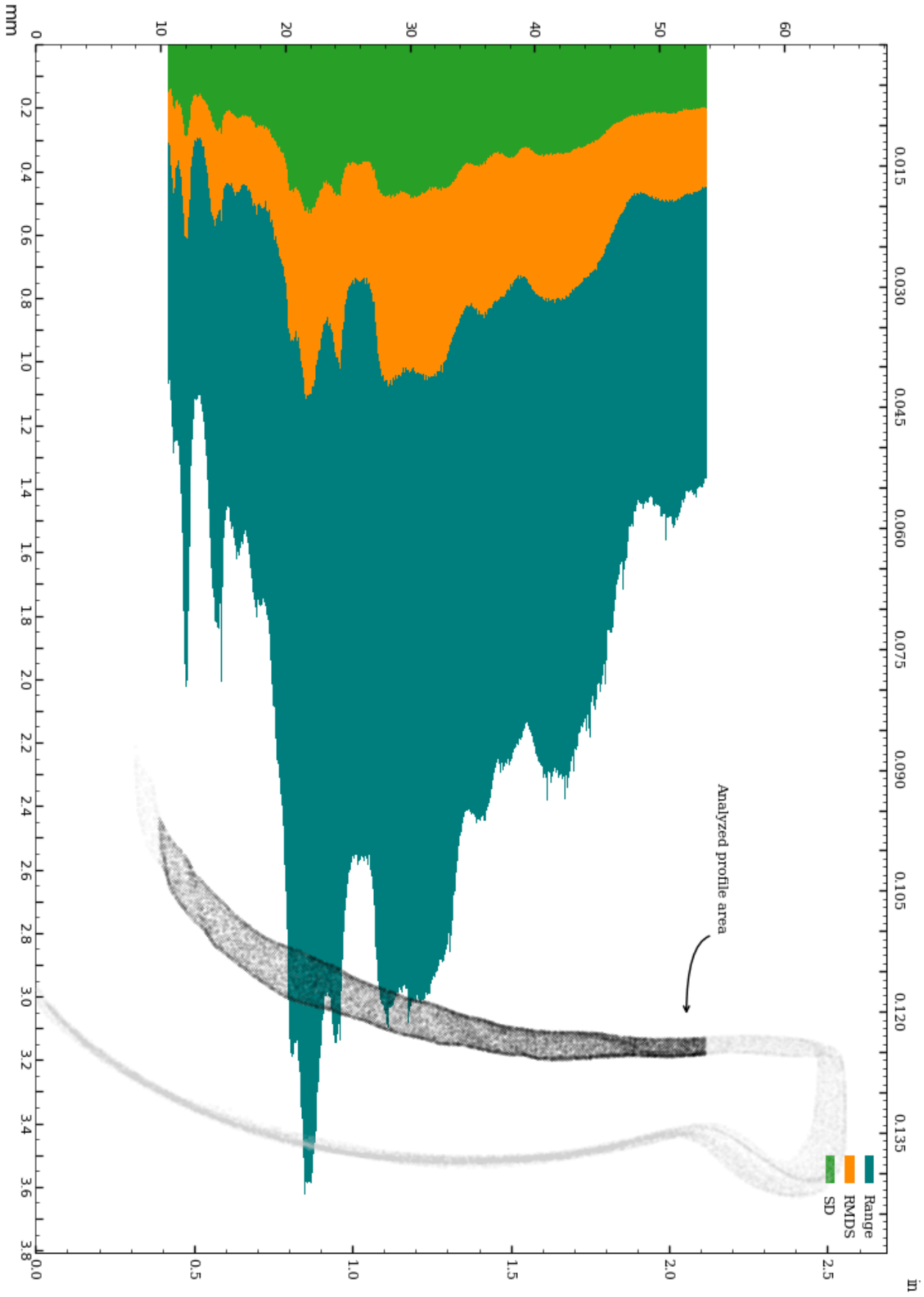

Figure 24: Circularity of interior surface.

Circularity analysis of interior surface, Standard Deviation and Root Mean Squared Deviation

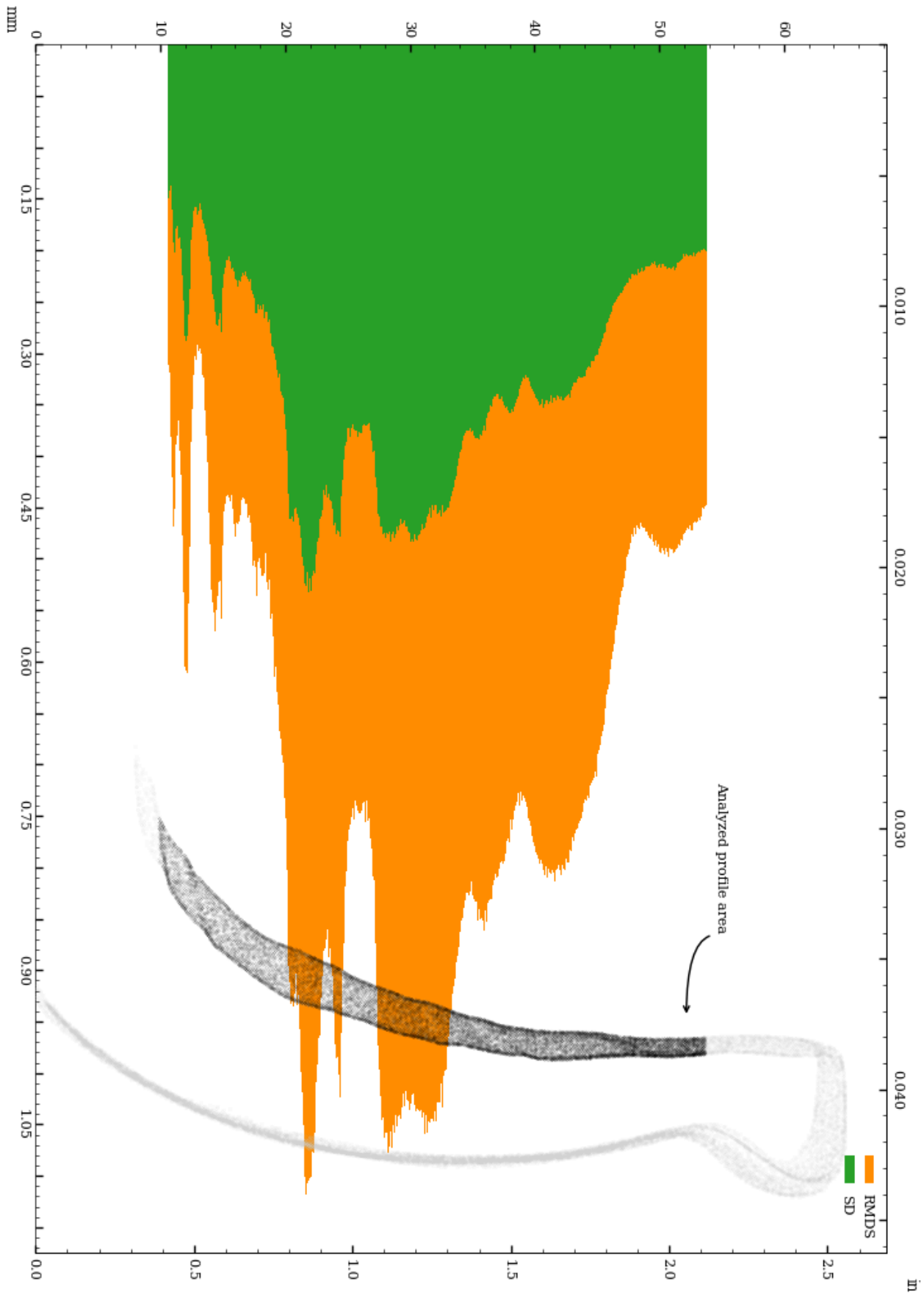

Figure 25: Vessel circularity of interior surface, standard deviation and median absolute deviation.

The distributions of the circularity measurements across 870 slices of the interior surface are shown below.

Range measurement distribution across 870 slices of interior surface

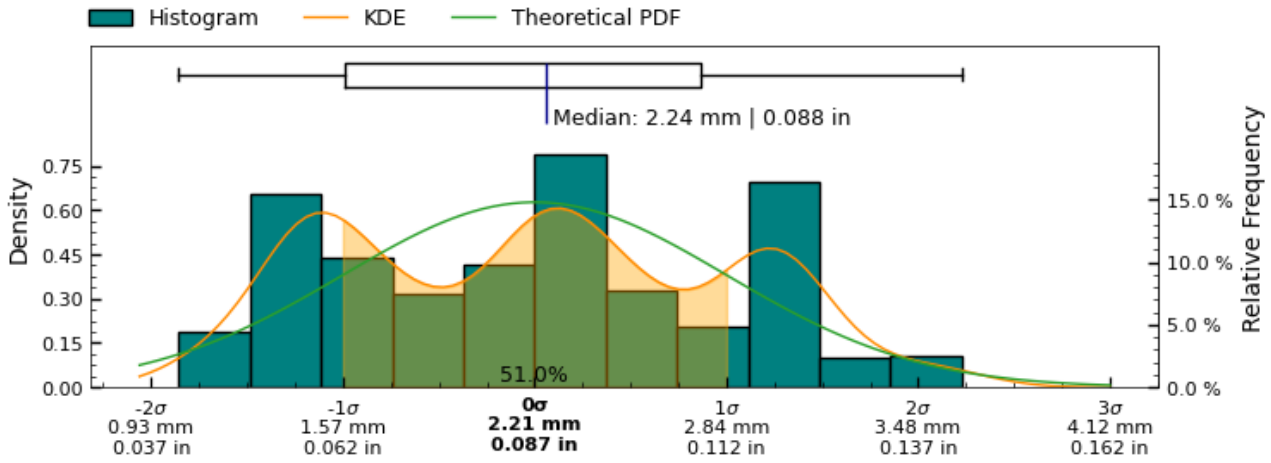

Figure 26: Range measurement distribution across measured slices of interior surface

Standard Deviation measurement distribution across 870 slices of interior surface

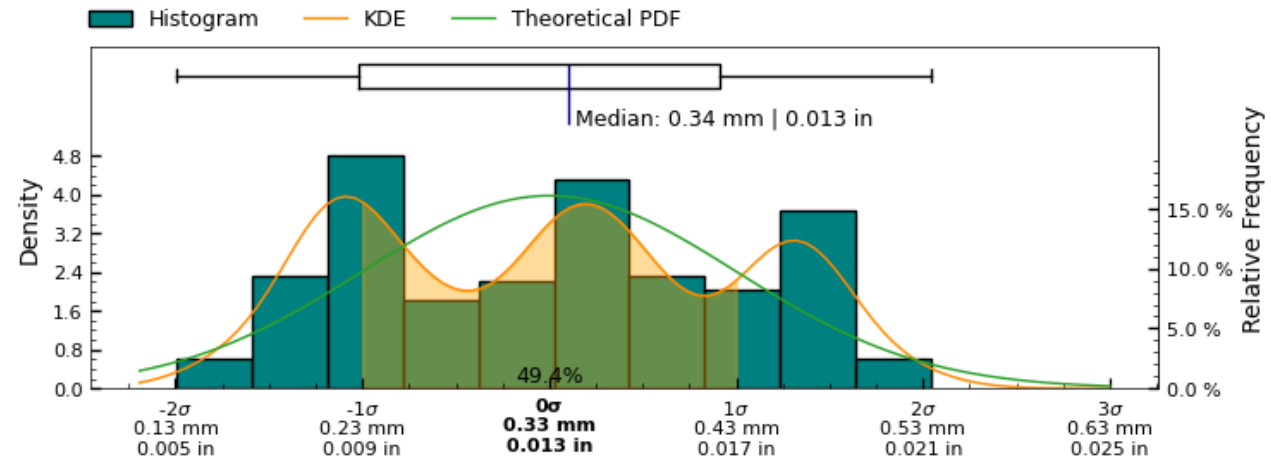

Figure 27: Standard Deviation measurement distribution across measured slices of “ + interior + “ surface

Root Mean Squared Deviation measurement distribution across 870 slices of interior surface

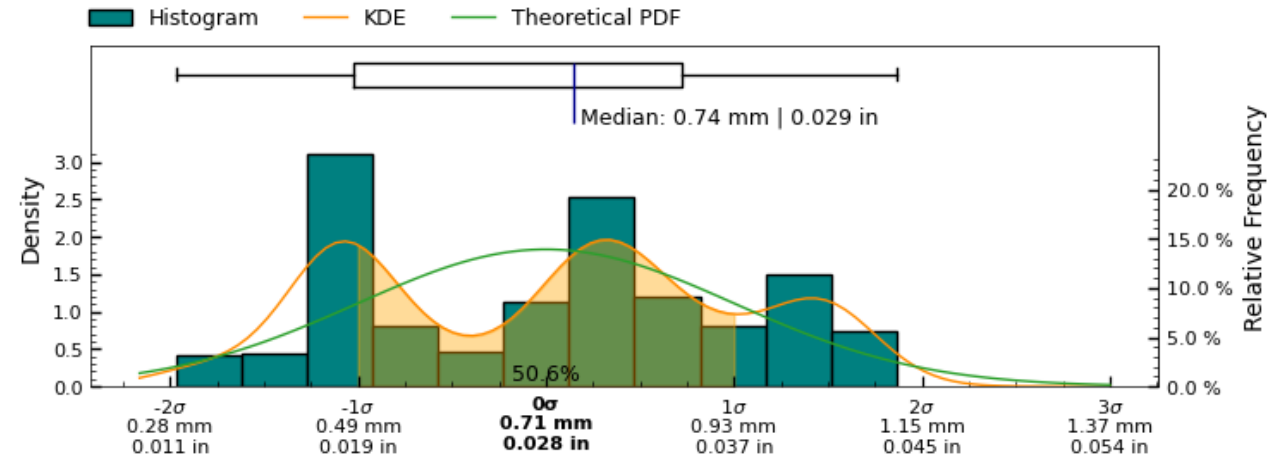

Figure 28: Root Mean Squared Deviation measurement distribution across measured slices of interior surface

Circularity analysis of interior separately aligned surface

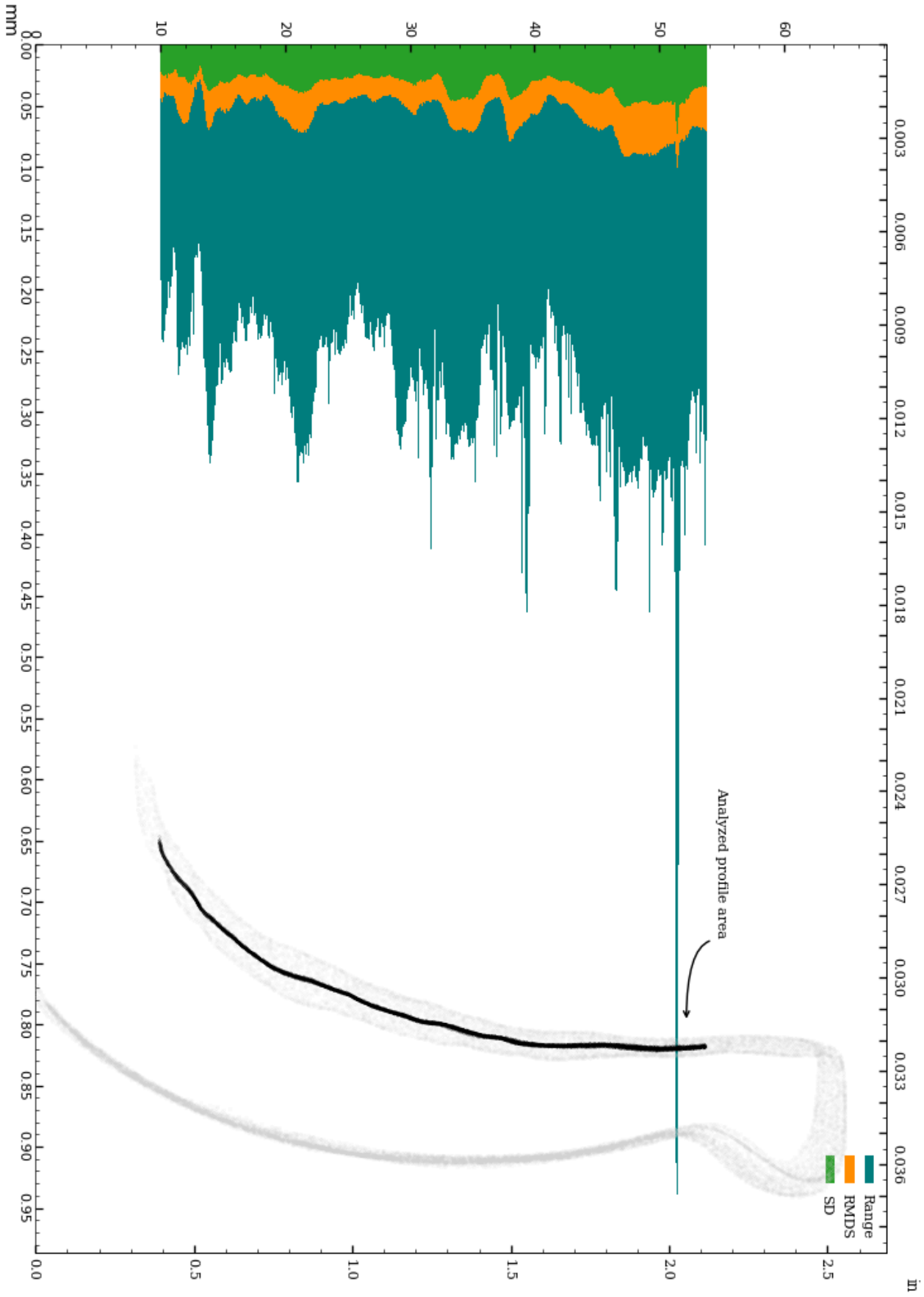

Figure 29: Circularity of interior_separate surface.

Circularity analysis of interior separately aligned surface, Standard Deviation and Root Mean Squared Deviation

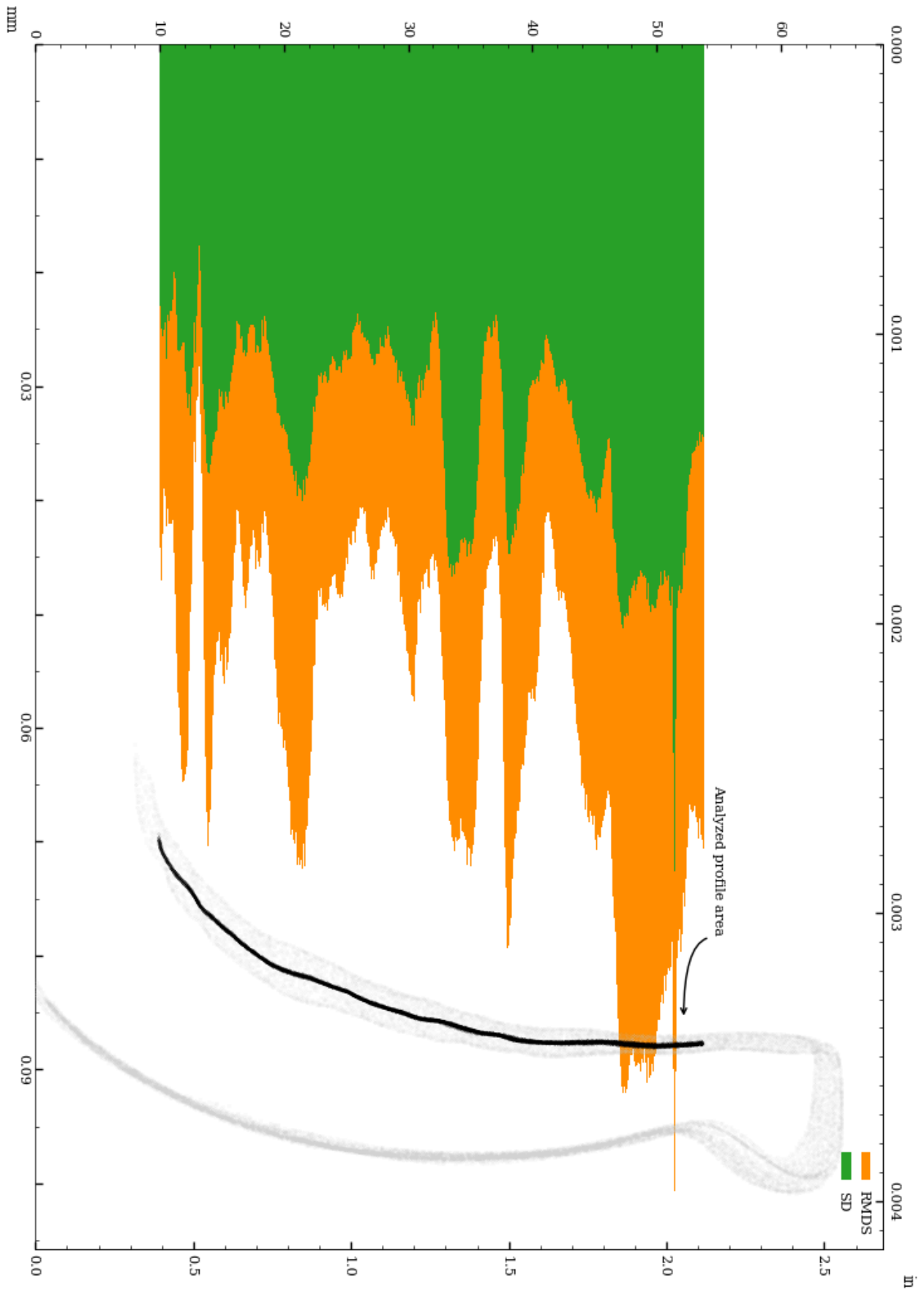

Figure 30: Vessel circularity of interior_separate surface, standard deviation and median absolute deviation.

The distributions of the circularity measurements across 882 slices of the interior_separate surface are shown below.

Range measurement distribution across 882 slices of interior separately aligned surface

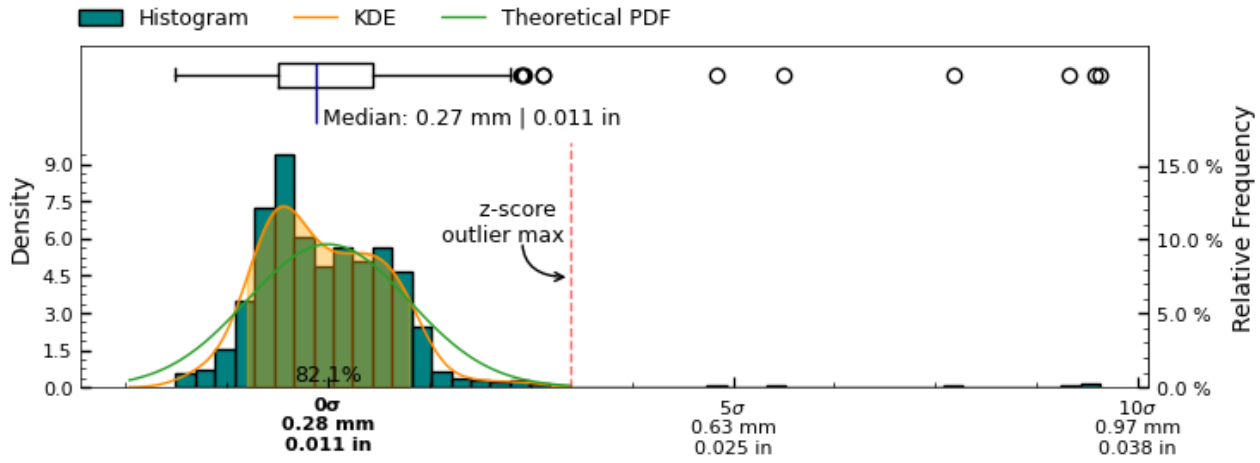

Figure 31: Range measurement distribution across measured slices of interior_separate surface

Standard Deviation measurement distribution across 882 slices of interior separately aligned surface

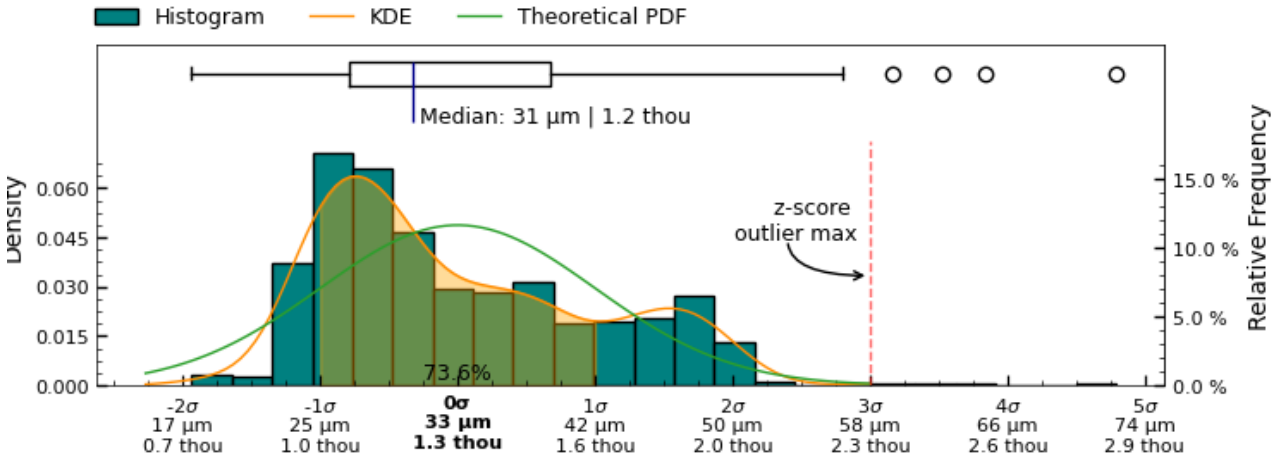

Figure 32: Standard Deviation measurement distribution across measured slices of “ + interior_separate + “ surface

Root Mean Squared Deviation measurement distribution across 882 slices of interior separately aligned surface

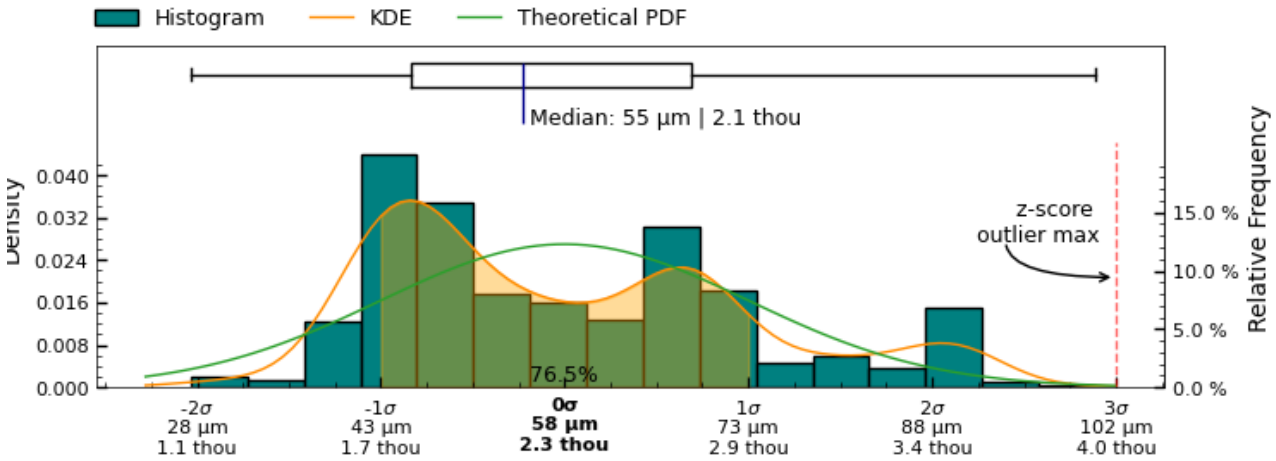

Figure 33: Root Mean Squared Deviation measurement distribution across measured slices of interior separately aligned surface

Concentricity

The concentricity metric describes the deviation in the center-point of the referenced features. As such, it is a measure to determine if several features of the object share the same center point/axis, and how closely. See Figure 34 for a visual representation of this metric.

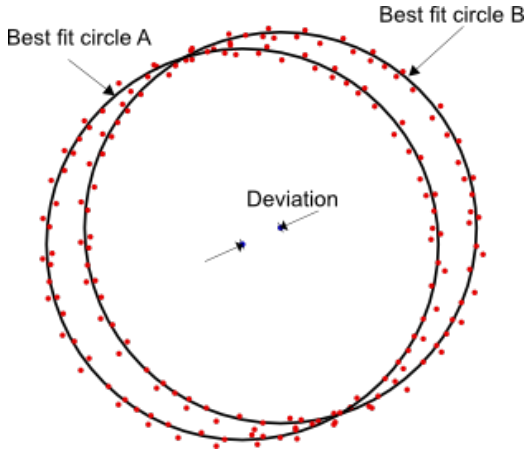

Figure 34: Concentricity measures the deviation (distance) between the center of two circles.

Determination of concentricity has been carried out by establishing the best fit circles of sample slices, using RANSAC (Random sample consensus) algorithm for outlier detection of a least squares circle regression on the scanned data-points at each cross-section, to estimate centers of each cross-section.

The concentricity between both the interior and exterior circular cross-sections is explored for cross-section measurements with the same Z-coordinates.

Additionally, the concentricity between each cross-section measurement defined in Figure 4 and the datum axis $(x, y) = (0, 0)$ has been calculated to establish the deviation of the feature center from the datum axis.

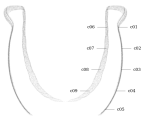

Figure 35: Circularity measurement sample locations, full mesh aligned to exterior surface

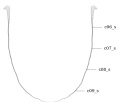

Figure 36: Circularity measurement sample location, separately aligned interior mesh

Metric

Tag	Reference	Deviation	Sample size	Circle fit residuals analysis for sample listed in Tag column						
				Range full	Range inliers	RMSD full	RMDS inliers	SD full	SD inliers	Center (x,y)
		mm		mm	mm	mm	mm	mm	mm	µm
c01	z-axis	0.305	1763	1.805	1.805	0.482	0.482	0.238	0.238	−66, 297
c02	z-axis	0.066	1960	0.834	0.834	0.186	0.186	0.107	0.107	45, 48
c03	z-axis	0.067	2010	0.809	0.803	0.212	0.210	0.128	0.126	−40, −54
c04	z-axis	0.084	1645	1.066	0.943	0.190	0.180	0.121	0.111	66, −52
c05	z-axis	0.137	1108	0.966	0.966	0.228	0.228	0.143	0.143	−26, 134
c06	z-axis	0.638	1499	2.976	2.976	1.037	1.042	0.455	0.457	−196, −607
c06_s	z-axis	0.018	1434	0.361	0.361	0.076	0.076	0.046	0.046	5, −18
c07	z-axis	1.041	1447	4.519	4.519	1.623	1.623	0.696	0.696	−556, −880
c07_s	z-axis	0.021	1429	0.295	0.295	0.062	0.062	0.035	0.035	−6, 20
c08	z-axis	1.316	1123	5.647	5.647	1.992	1.989	0.888	0.890	−778, −1061
c08_s	z-axis	0.016	1160	0.242	0.204	0.046	0.043	0.028	0.025	−16, 3
c09	z-axis	1.157	698	4.928	4.928	1.743	1.743	0.731	0.731	−683, −933
c09_s	z-axis	0.046	621	0.310	0.297	0.062	0.059	0.043	0.040	33, −32
c01	c06_s	0.323								−70, 315
c02	c07_s	0.058								51, 28
c03	c08_s	0.062								−24, −57
c04	c09_s	0.039								33, −20

Imperial

Tag	Reference	Deviation	Sample size	Circle fit residuals analysis for sample listed in Tag column						
				Range full	Range inliers	RMSD full	RMDS inliers	SD full	SD inliers	Center (x,y)
		in		in	in	in	in	in	in	thou
c01	z-axis	0.0120	1763	0.0711	0.0711	0.0190	0.0190	0.0094	0.0094	−2.6, 11.7
c02	z-axis	0.0026	1960	0.0328	0.0328	0.0073	0.0073	0.0042	0.0042	1.8, 1.9
c03	z-axis	0.0026	2010	0.0319	0.0316	0.0083	0.0083	0.0050	0.0050	−1.6, −2.1
c04	z-axis	0.0033	1645	0.0420	0.0371	0.0075	0.0071	0.0048	0.0044	2.6, −2.1
c05	z-axis	0.0054	1108	0.0380	0.0380	0.0090	0.0090	0.0056	0.0056	−1.0, 5.3
c06	z-axis	0.0251	1499	0.1172	0.1172	0.0408	0.0410	0.0179	0.0180	−7.7, −23.9
c06_s	z-axis	0.0007	1434	0.0142	0.0142	0.0030	0.0030	0.0018	0.0018	0.2, −0.7
c07	z-axis	0.0410	1447	0.1779	0.1779	0.0639	0.0639	0.0274	0.0274	−21.9, −34.7
c07_s	z-axis	0.0008	1429	0.0116	0.0116	0.0024	0.0024	0.0014	0.0014	−0.2, 0.8
c08	z-axis	0.0518	1123	0.2223	0.2223	0.0784	0.0783	0.0350	0.0350	−30.6, −41.8
c08_s	z-axis	0.0006	1160	0.0095	0.0080	0.0018	0.0017	0.0011	0.0010	−0.6, 0.1
c09	z-axis	0.0455	698	0.1940	0.1940	0.0686	0.0686	0.0288	0.0288	−26.9, −36.7
c09_s	z-axis	0.0018	621	0.0122	0.0117	0.0025	0.0023	0.0017	0.0016	1.3, −1.3
c01	c06_s	0.0127								−2.8, 12.4
c02	c07_s	0.0023								2.0, 1.1
c03	c08_s	0.0024								−1.0, −2.2
c04	c09_s	0.0015								1.3, −0.8

Table 3: Concentricity analysis of MV006.

Concentricity analysis of c01

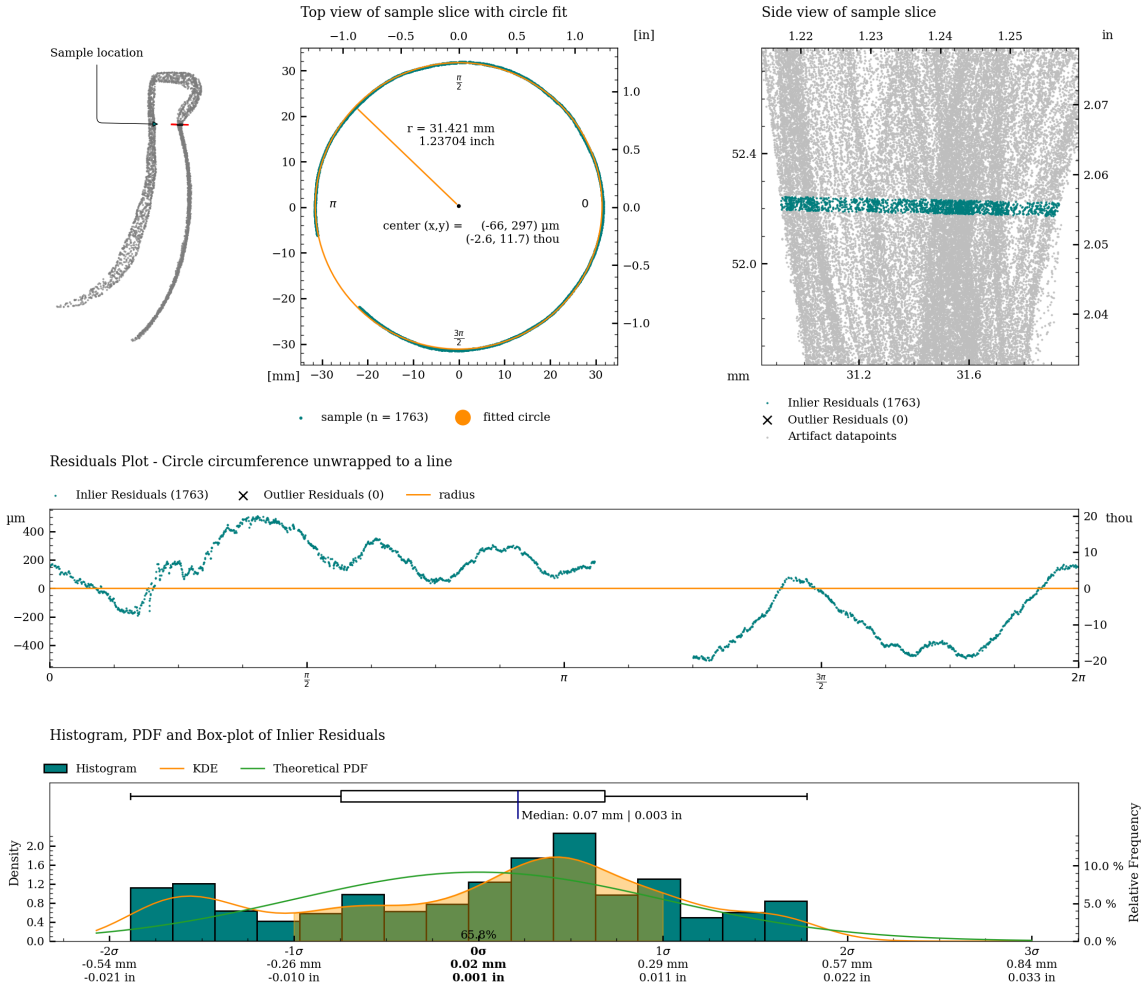

Figure 37: Detailed plot of concentricity measurement for c01.

Concentricity analysis of c02

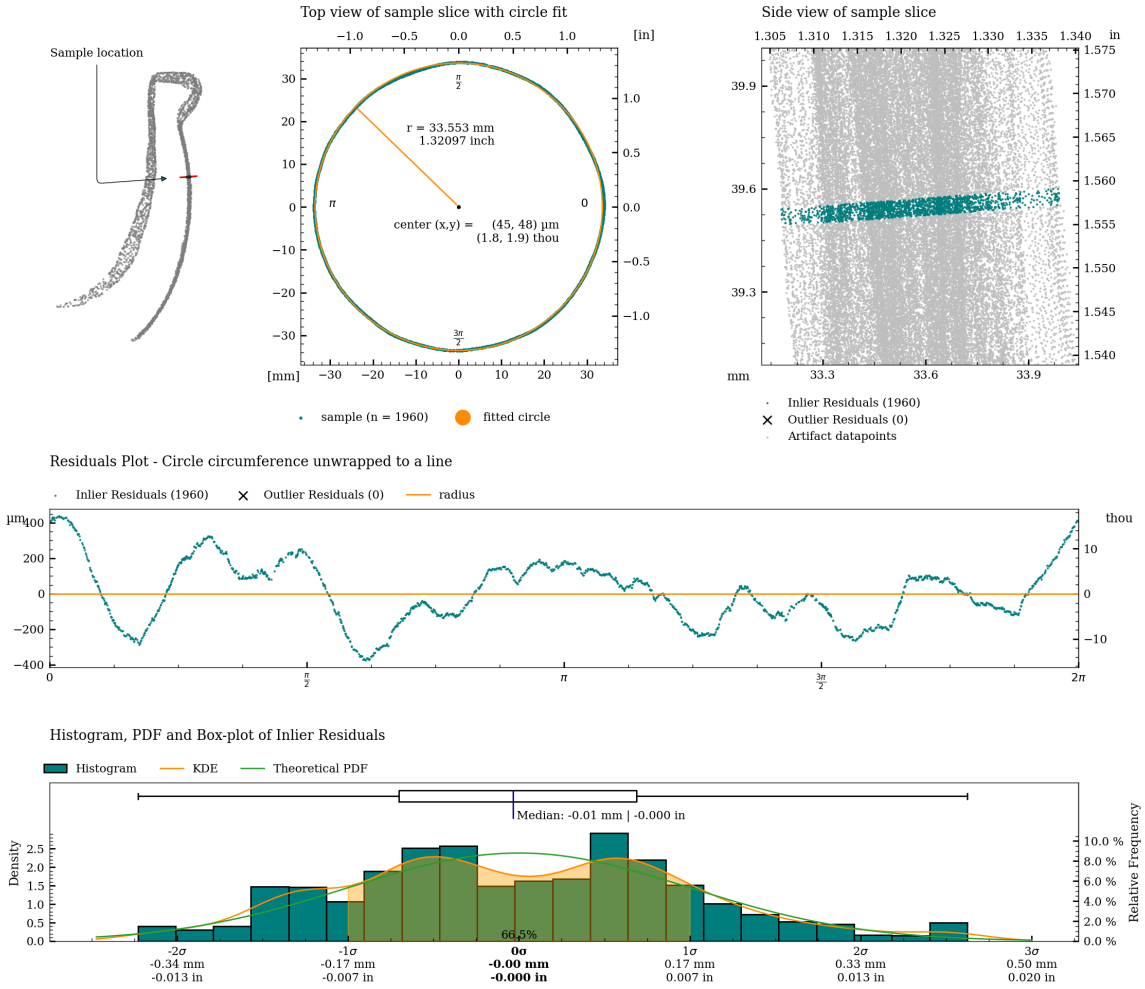

Figure 38: Detailed plot of concentricity measurement for c02.

Concentricity analysis of c03

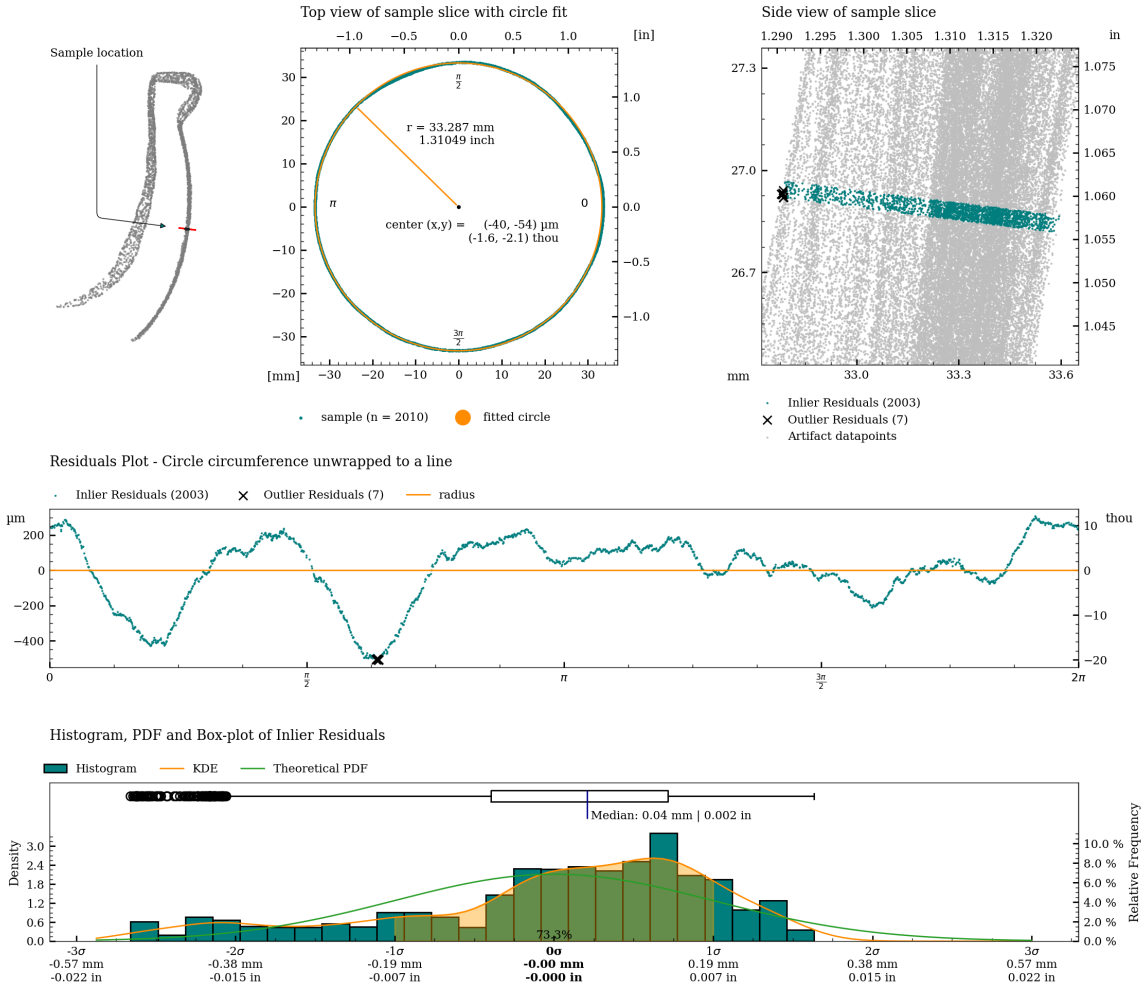

Figure 39: Detailed plot of concentricity measurement for c03.

Concentricity analysis of c04

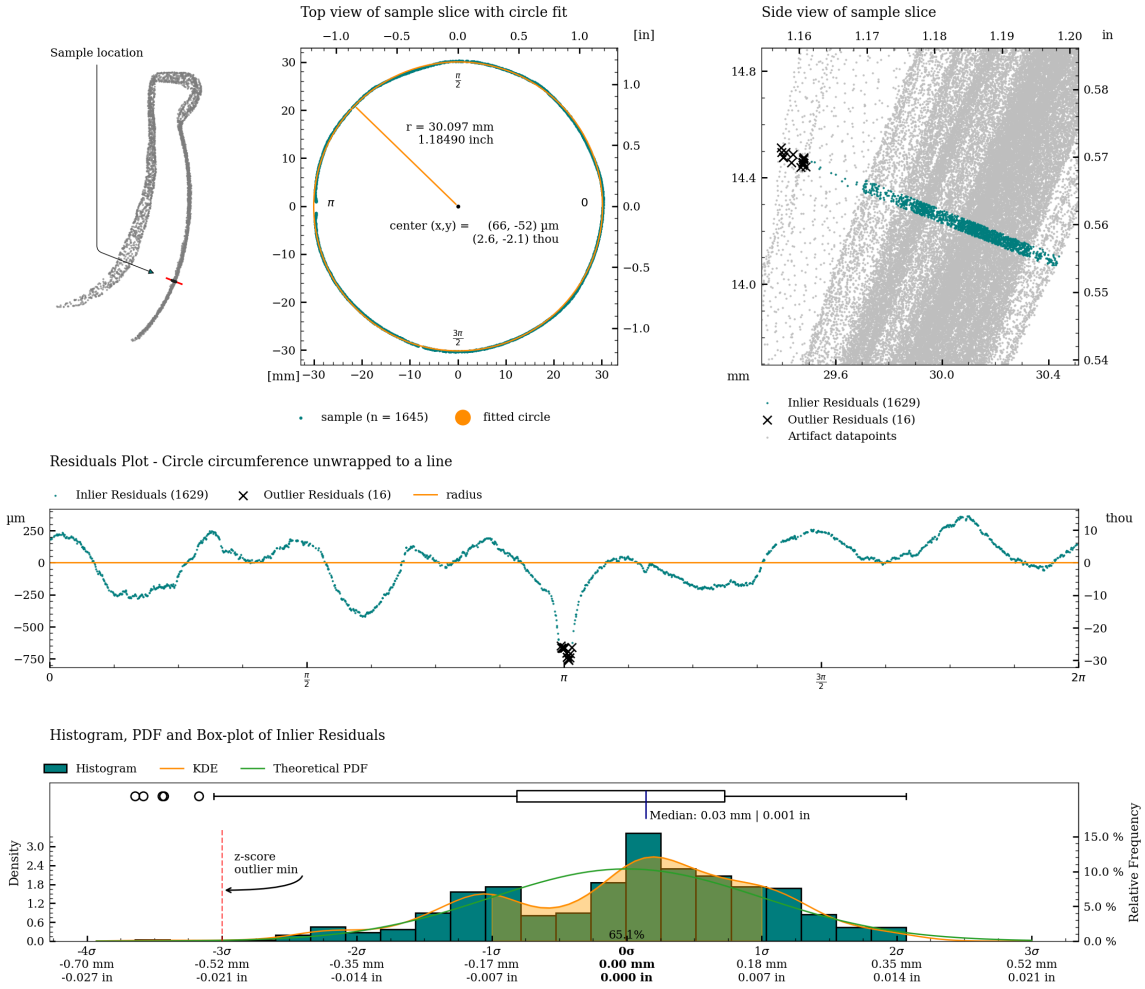

Figure 40: Detailed plot of concentricity measurement for c04.

Concentricity analysis of c05

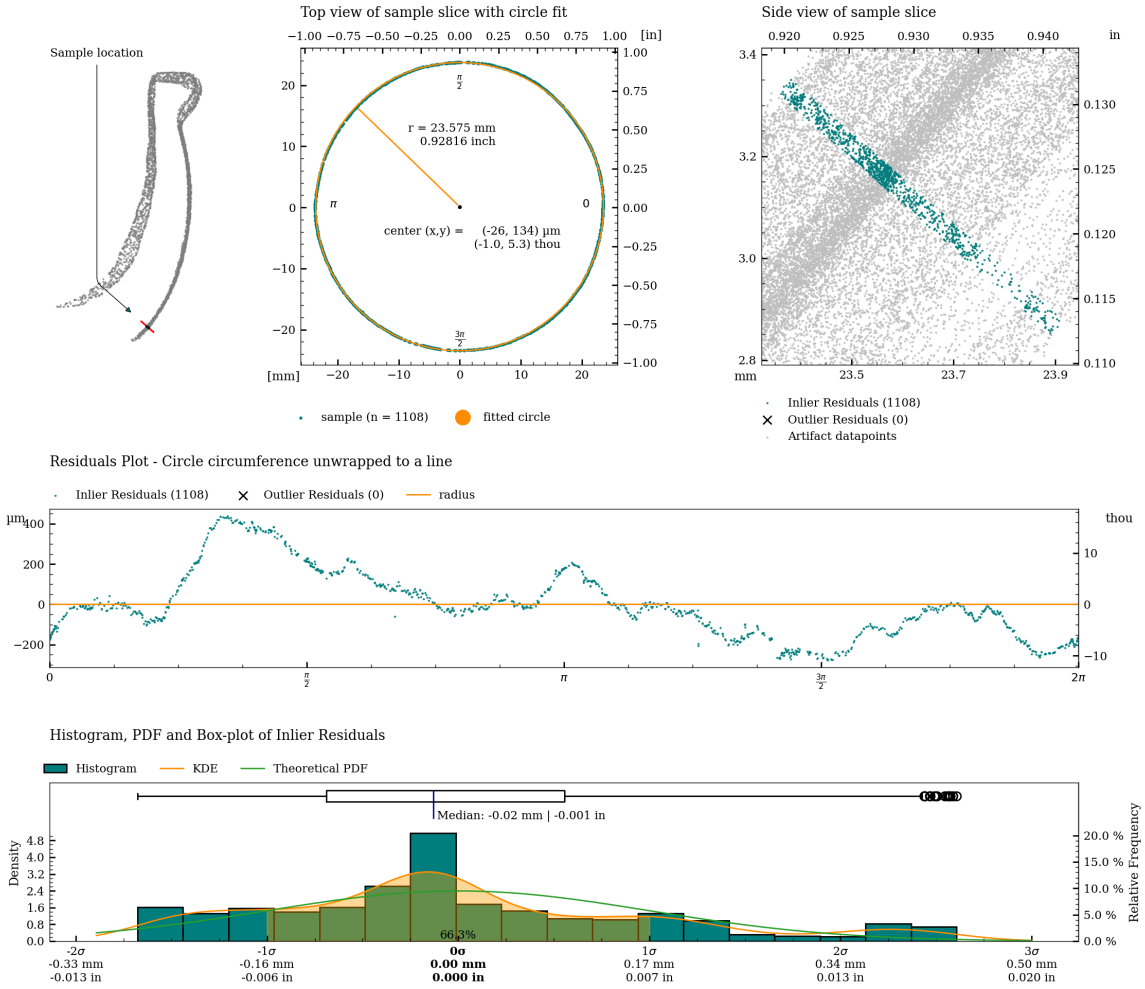

Figure 41: Detailed plot of concentricity measurement for c05.

Concentricity analysis of c06

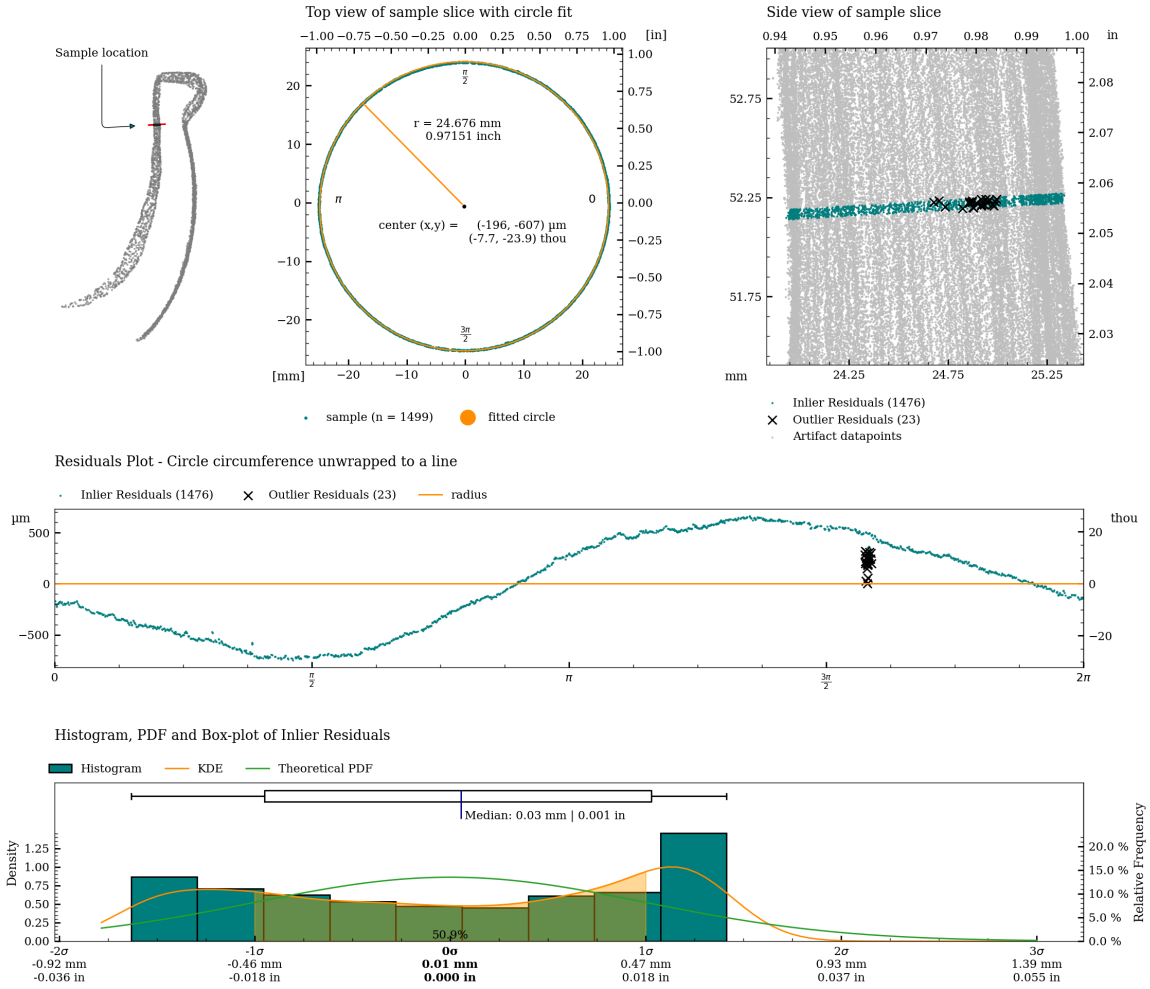

Figure 42: Detailed plot of concentricity measurement for c06.

Concentricity analysis of c06_s

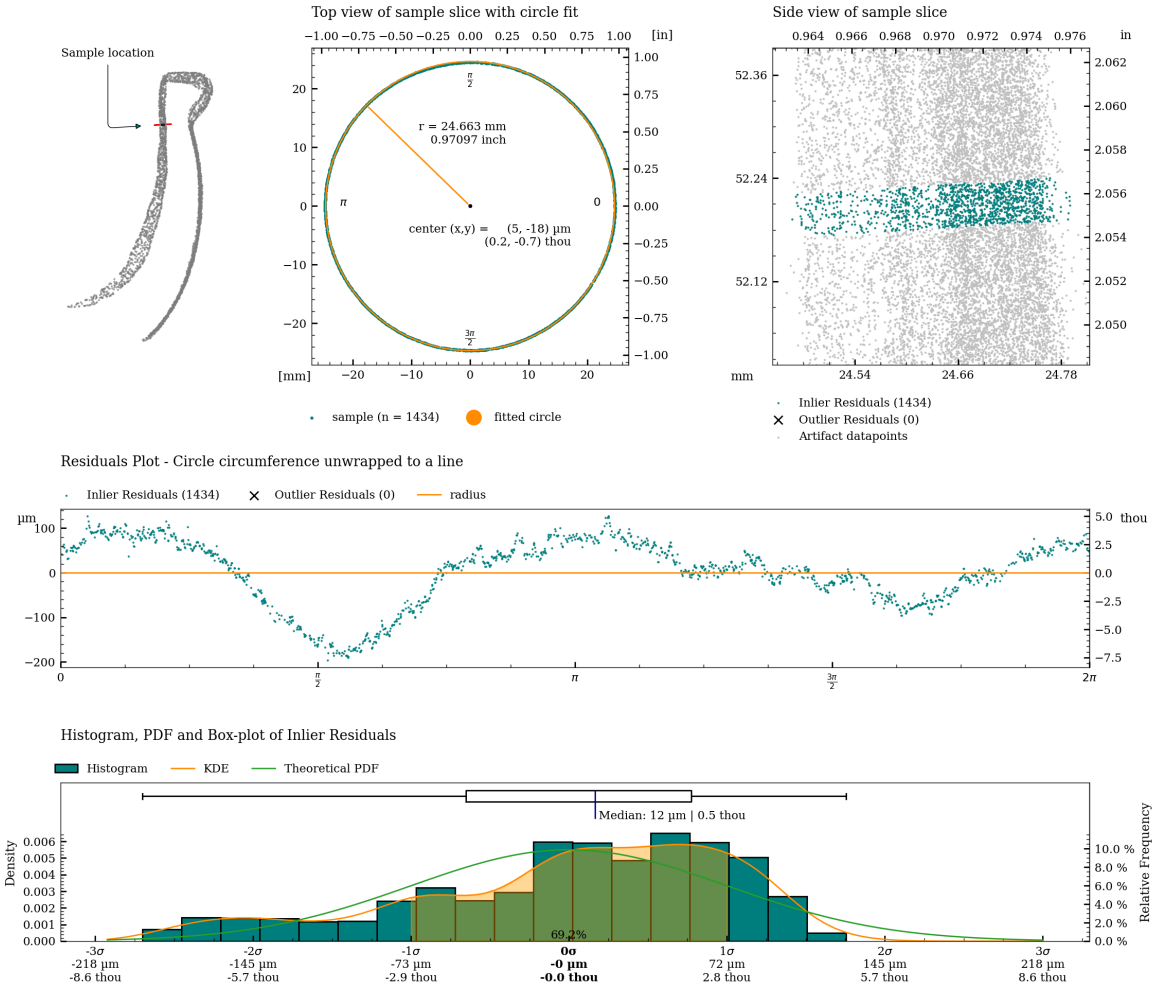

Figure 43: Detailed plot of concentricity measurement for c06_s.

Concentricity analysis of c07

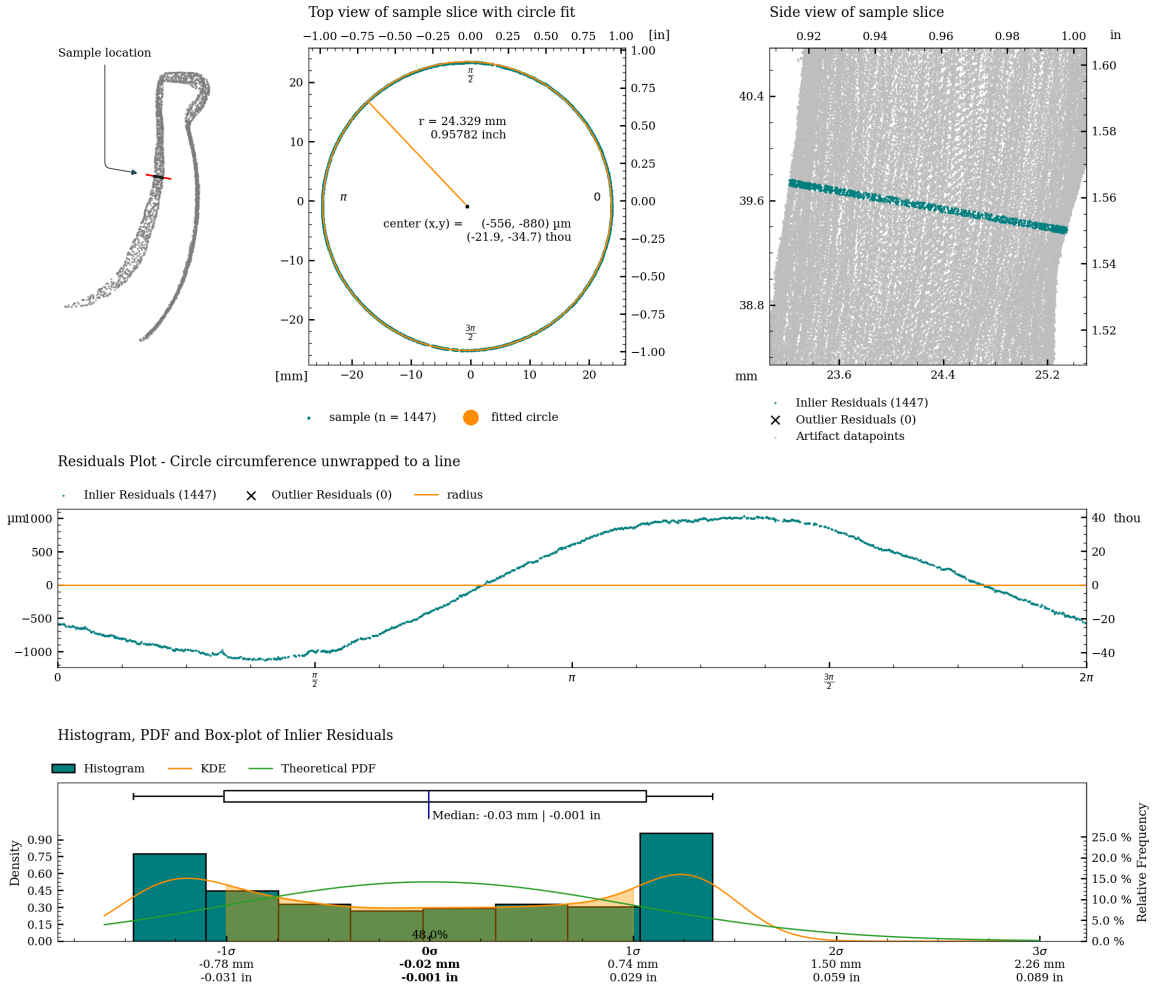

Figure 44: Detailed plot of concentricity measurement for c07.

Concentricity analysis of c07_s

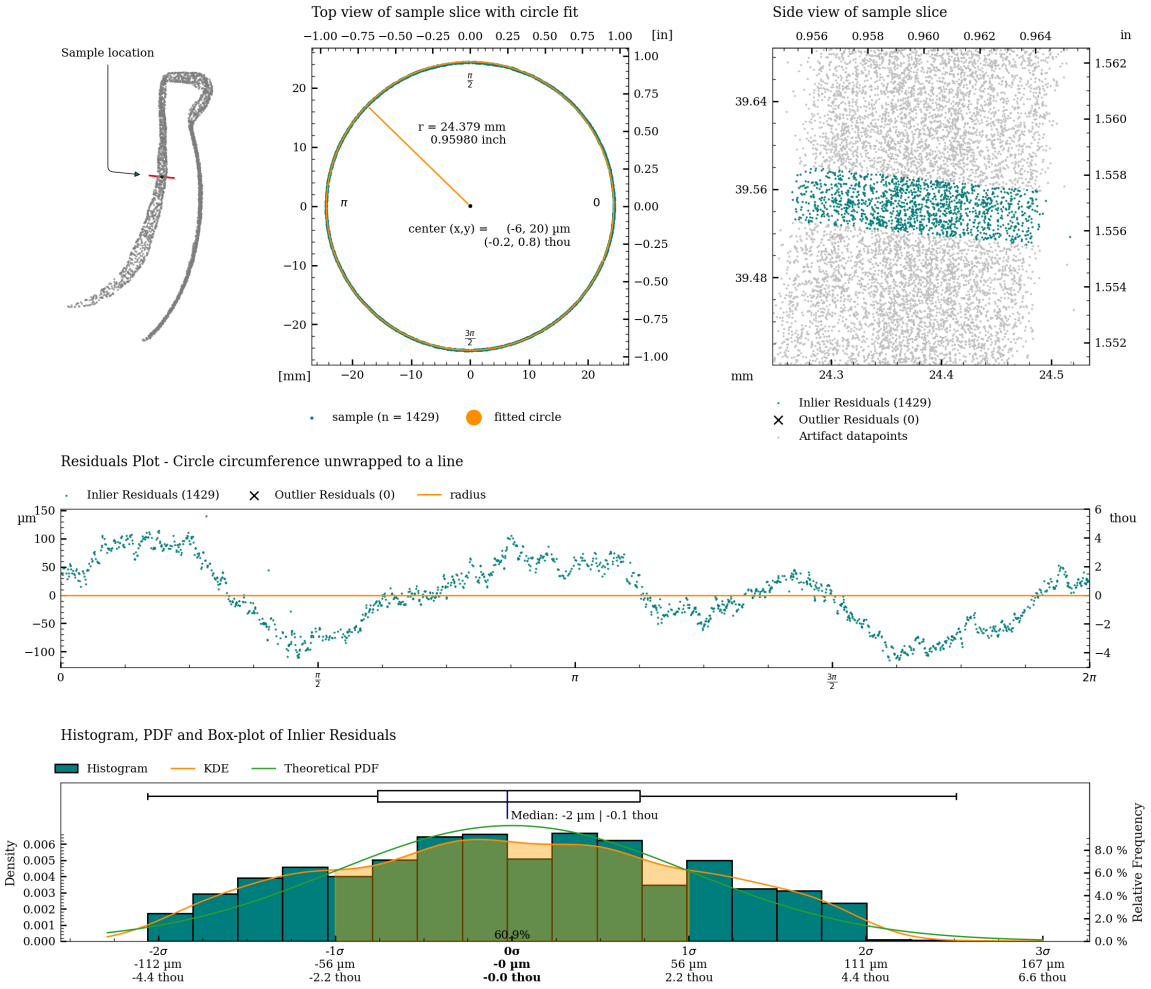

Figure 45: Detailed plot of concentricity measurement for c07_s.

Concentricity analysis of c08

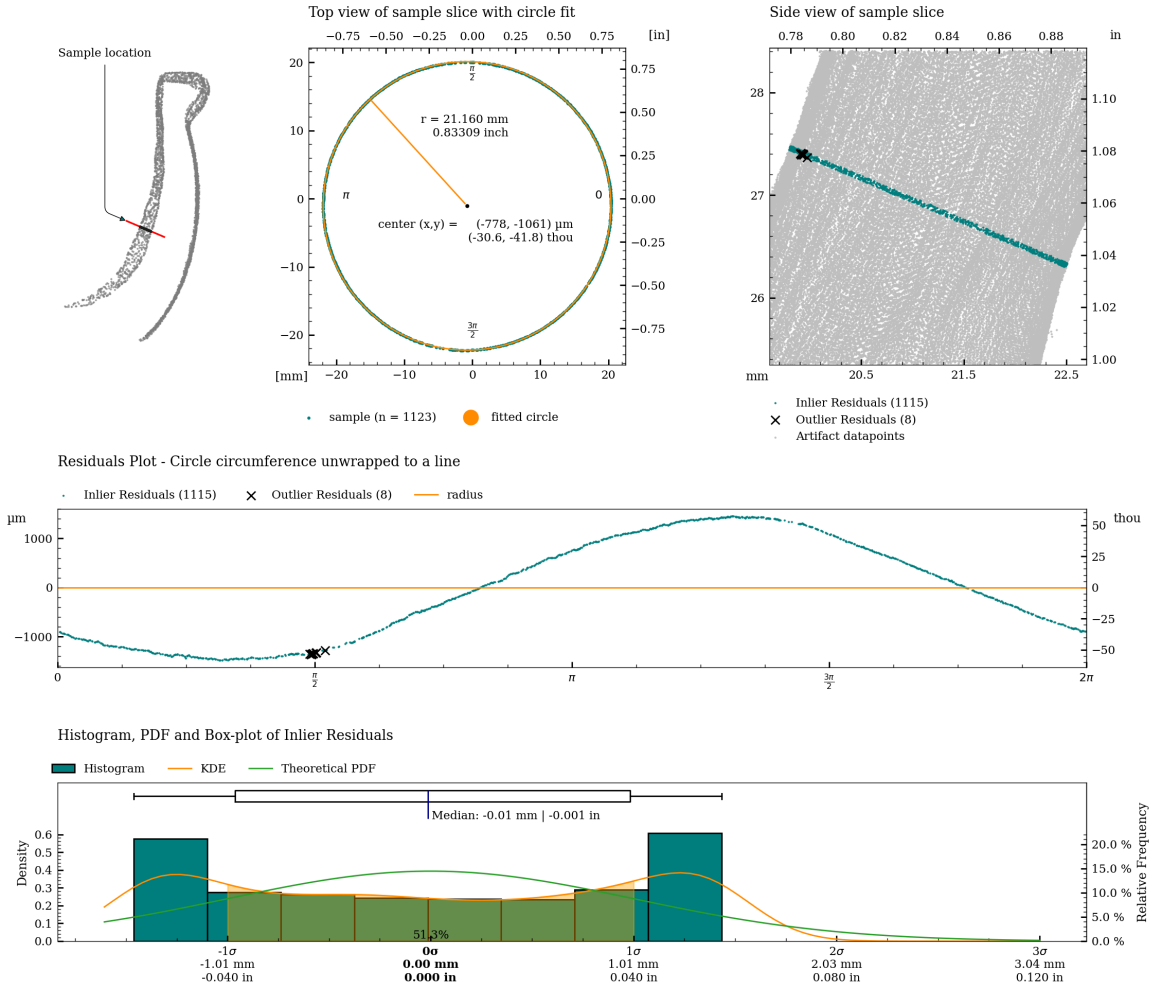

Figure 46: Detailed plot of concentricity measurement for c08.

Concentricity analysis of c08_s

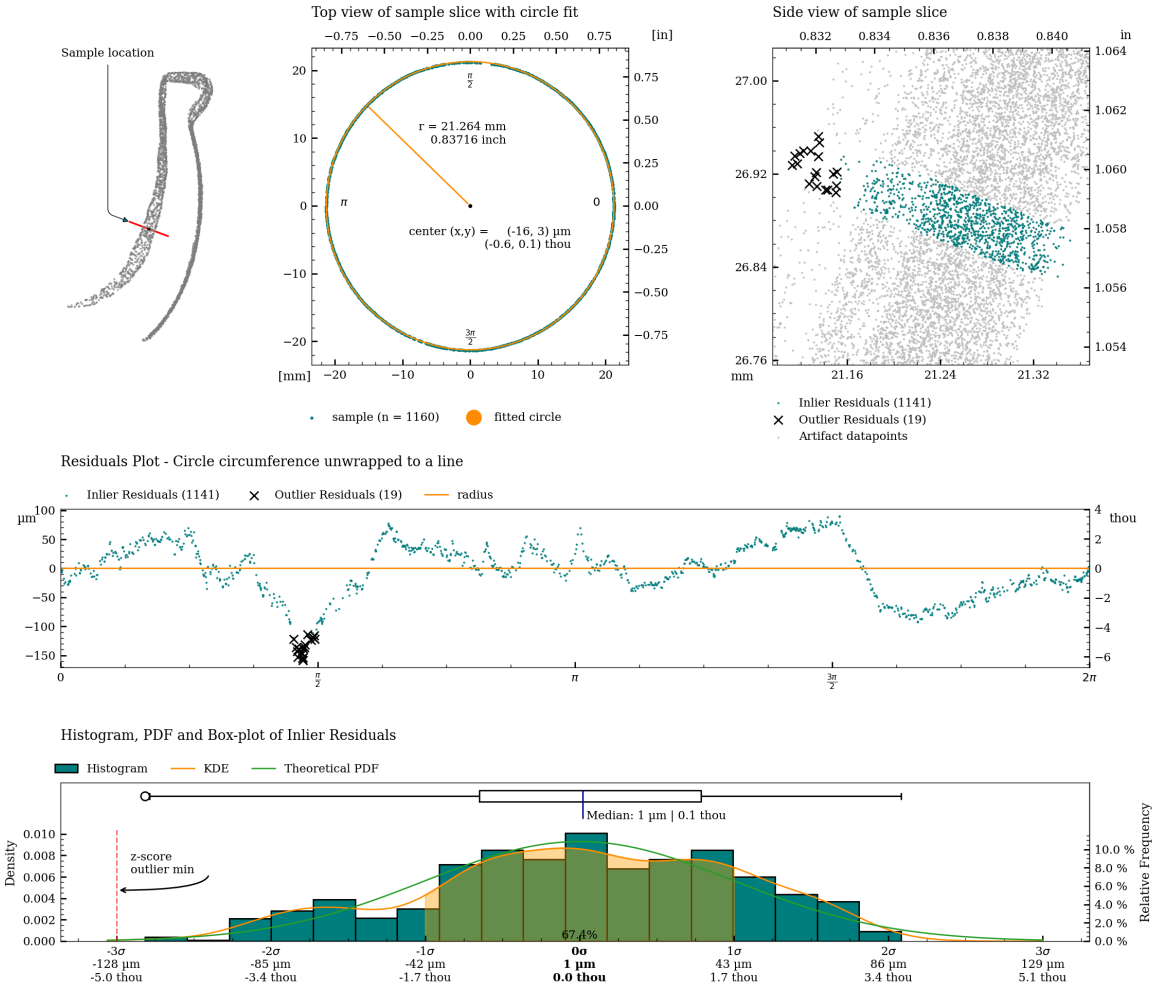

Figure 47: Detailed plot of concentricity measurement for c08_s.

Concentricity analysis of c09

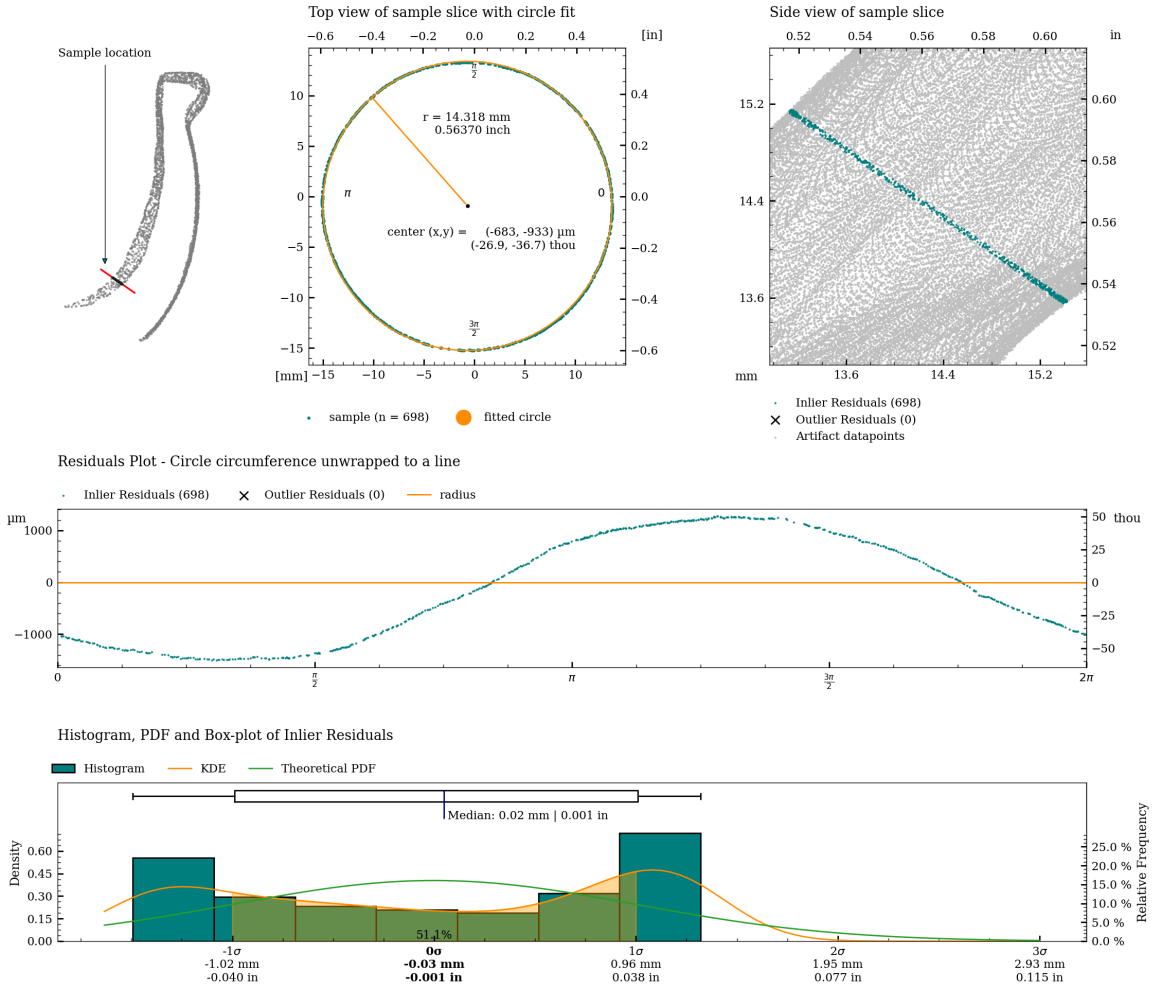

Figure 48: Detailed plot of concentricity measurement for c09.

Concentricity analysis of c09_s

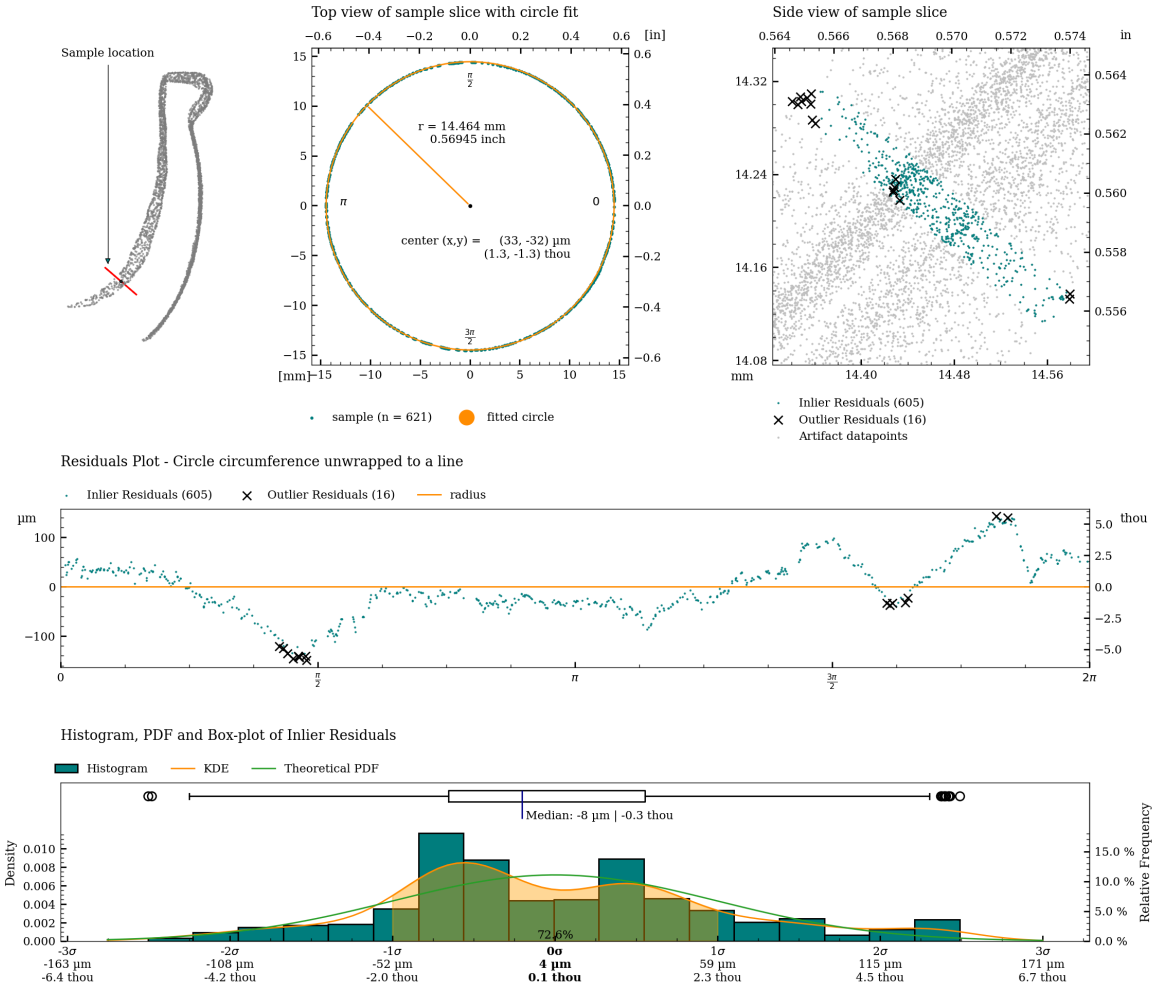

Figure 49: Detailed plot of concentricity measurement for c09_s.

Coaxiality

Coaxiality refers to the straightness and consistency of a central line running through the center of the vase. It measures how aligned the core of the vase remains along its vertical axis.

The coaxiality measurements are calculated using RANSAC (Random sample consensus) algorithm for outlier detection on least squares circle regression on cross-sections of the vessel (excluding potential handles), to estimate the best fit circle centers for each slice of the vessel. A best-fit line connects these centers, showing whether the vessels's shape twists or remains straight. This concept helps describe the symmetry and structural uniformity in a visual and analytical way.

Coaxiality is measured for:

- The exterior surface (excluding handles)
- The interior surface

	Exterior		**Interior**		**Interior separate**	
Analyzed Slices		1167		870		882
Median sample size		1800		1316		1298
Slice Height	50 µm	2.0 thou	50 µm	2.0 thou	50 µm	2.0 thou
Statistics with Z-axis as Reference						
Median Absolute Deviation (MAD)	104 µm	4.1 thou	1107 µm	43.6 thou	26 µm	1.0 thou
Standard Deviation (SD)	232 µm	9.2 thou	339 µm	13.3 thou	19 µm	0.7 thou
Root Mean Square Deviation (RMSD)	293 µm	11.6 thou	1168 µm	46.0 thou	36 µm	1.4 thou
Statistics with Best Fit Central Axis as Reference						
Best fit Central Axis Equation (in metric coordinate system with unit [mm])	x = 0.007 + t-0.00048 y = -0.017 + t0.00215 z = 0.000 + t1.00000		x = -1.118 + t-0.01500 y = -1.288 + t-0.01045 z = 0.000 + t-0.99983		x = 0.033 + t0.00094 y = -0.034 + t-0.00101 z = 0.000 + t-1.00000	
Axis tilt		−0.028°		−0.868°		0.054°
Median Absolute Deviation (MAD)	132 µm	5.2 thou	188 µm	7.4 thou	26 µm	1.0 thou
Standard Deviation (SD)	202 µm	7.9 thou	213 µm	8.4 thou	16 µm	0.6 thou
Root Mean Square Deviation (RMSD)	268 µm	10.5 thou	312 µm	12.3 thou	32 µm	1.2 thou

Table 4: Coaxiality analysis of vessel MV006.

Coaxiality plots, exterior surface

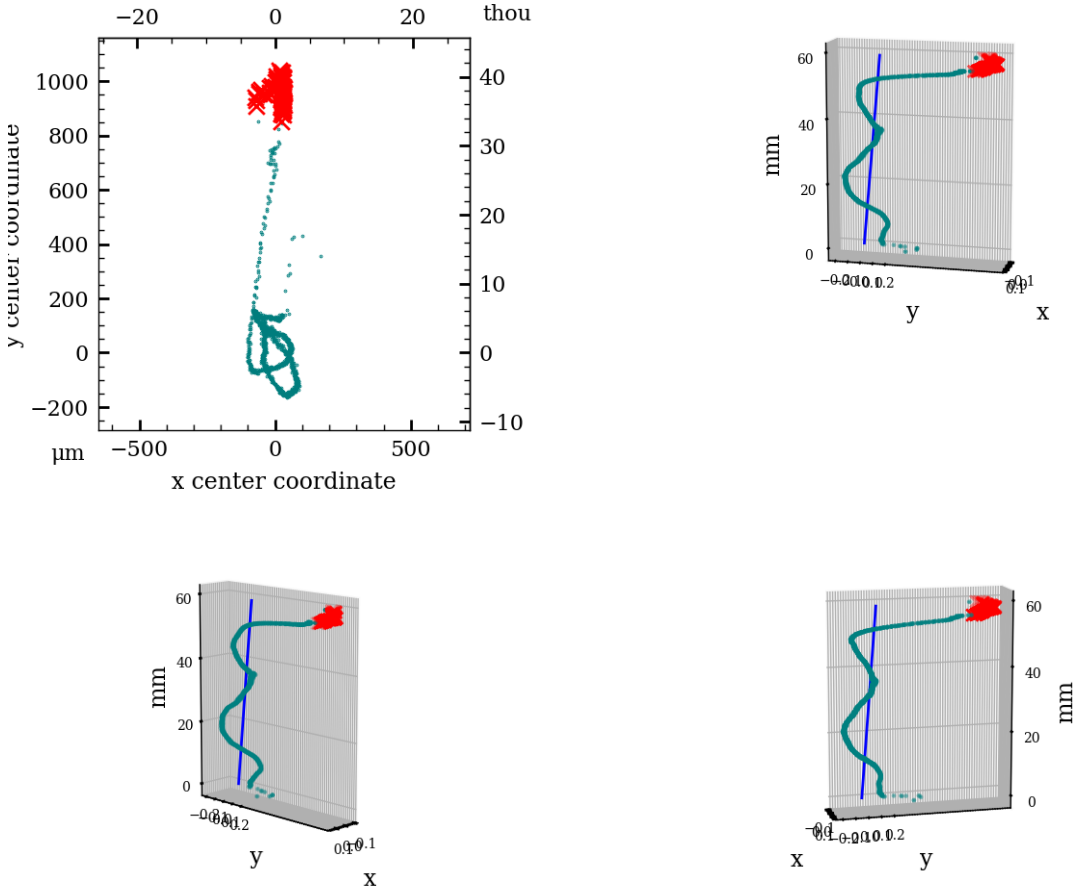

Coaxiality residuals from fitted axis, exterior surface

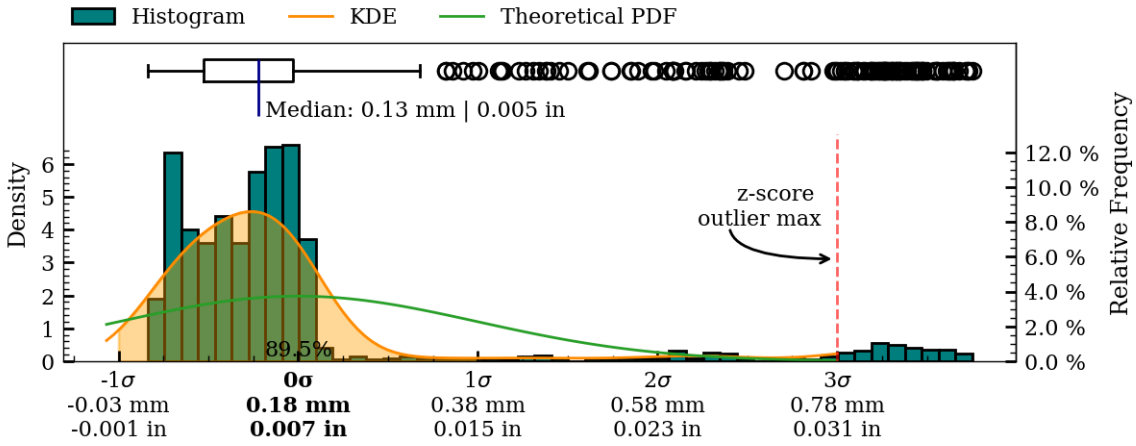

Figure 50: Coaxiality residual plots of exterior surface, MV006.

Coaxiality plots, interior surface

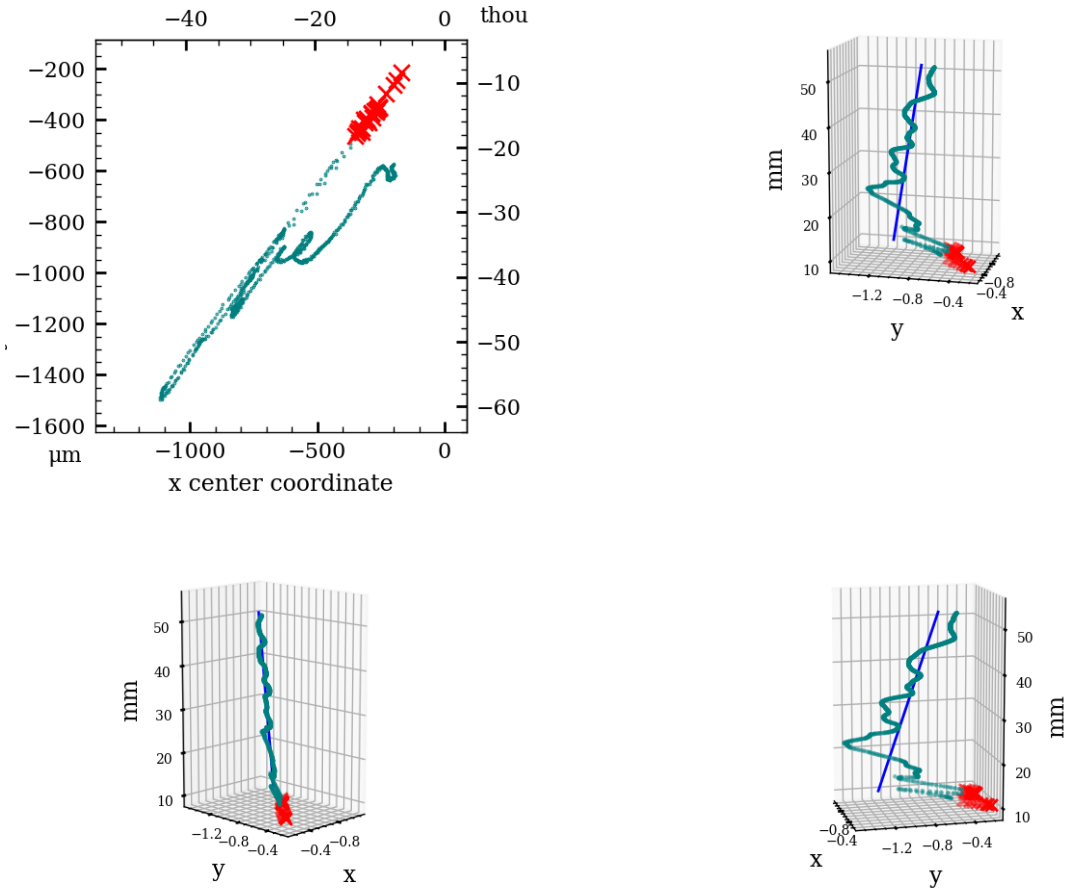

Coaxiality residuals from fitted axis, interior surface

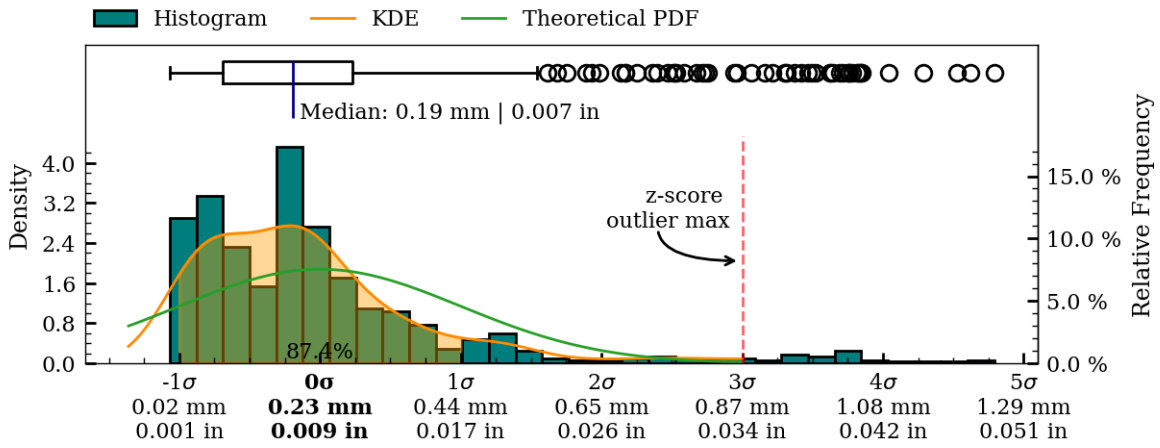

Figure 51: Coaxiality residual plots of interior surface, MV006.

Coaxiality plots, interior separately aligned surface

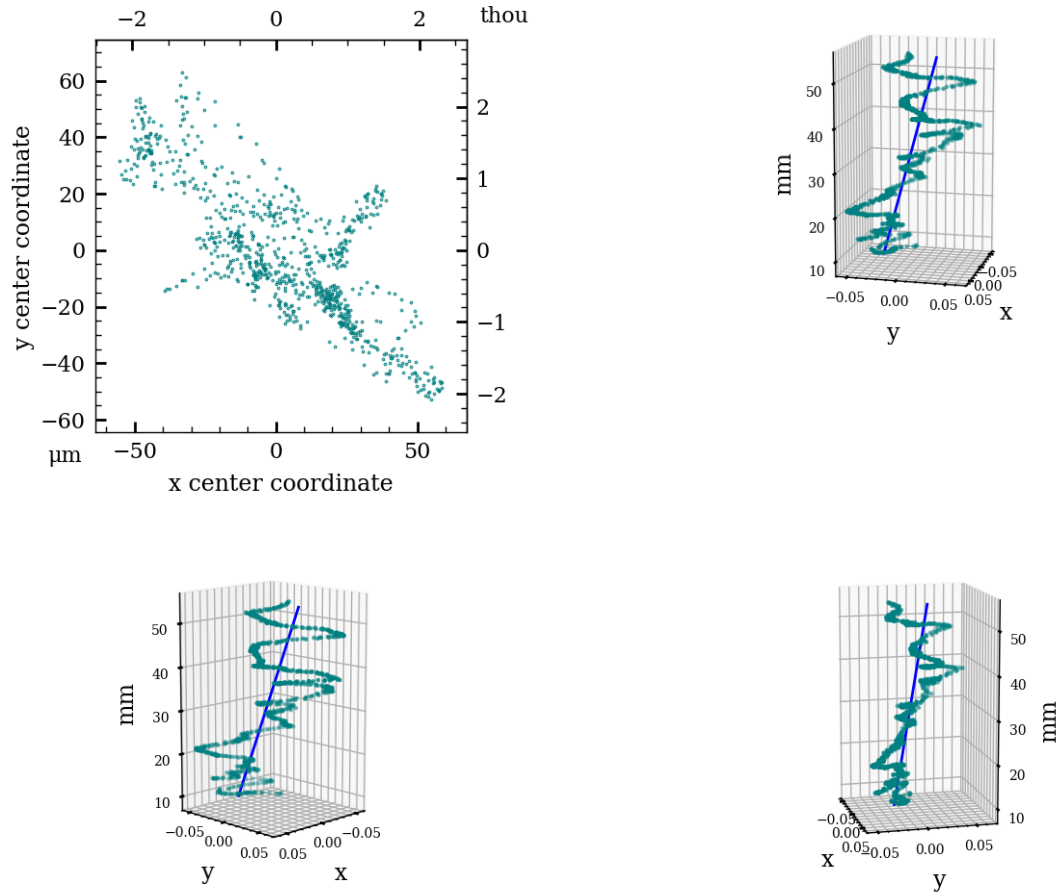

Coaxiality residuals from fitted axis, interior separately aligned surface

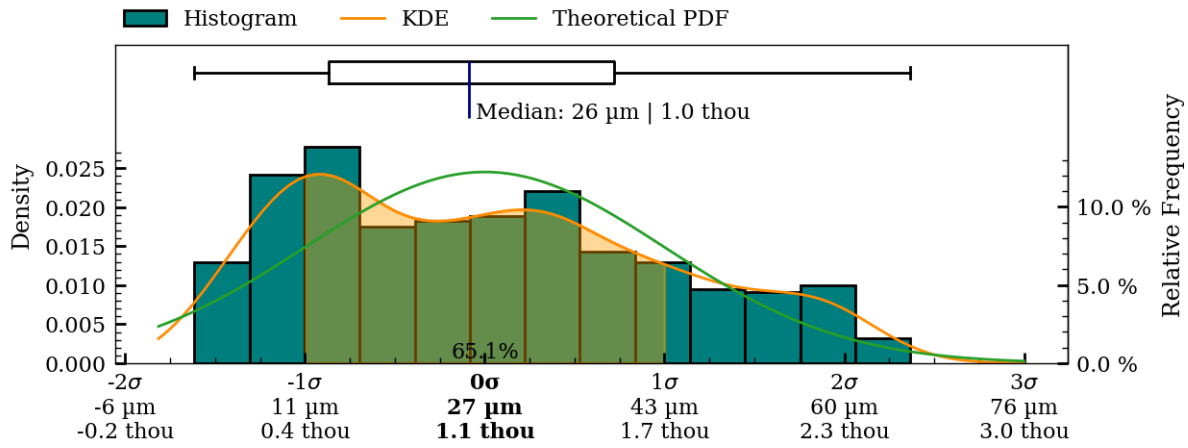

Figure 52: Coaxiality residual plots of interior_separate surface, MV006.

Surface Variability

To illustrate the overall surface deviations of the object, a surface variability heatmap has been created. This heatmap provides an accessible overview of the topography of the manufacturing precision and surface structure of the object.

The surface variability measurements are created by fitting a number of higher-order polynomials to the two-dimensional folded profile of the scan data. This process creates an idealized mathematical representation of actual surface curvature of object, and as such provides a continuous model representation of the actual object. It is important to note that only such a non-discretized representation is sufficient to avoid introducing inconsistently varying errors in the mapping of the final surface deviation results, that the rendered heatmaps are based on.

To produce the final surface variability map, the distance from each scanned vertex to the fitted polynomial is calculated and used as the mapping function input, for applying colours to the surface of the object.

It is important to note that this variability map does not describe deviations from the original *intended* shape of the artifact (if any), as this shape (the *intended design*, so to speak) will have been lost to time. It does however provide a very informative visualization of the texture and structure of the surface and very importantly, *does* hightlight potential manufacturing-relevant patterns in the surface texture (if present). Such patterns are, as an example, clearly evident on the interior surface of artifact PV001.

Exterior surface

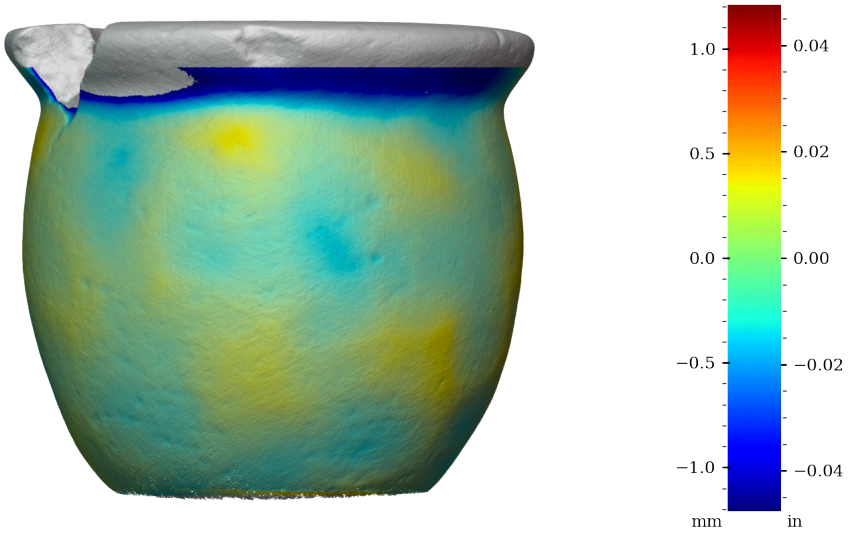

Figure 53: Surface variability heatmap of MV006, front view

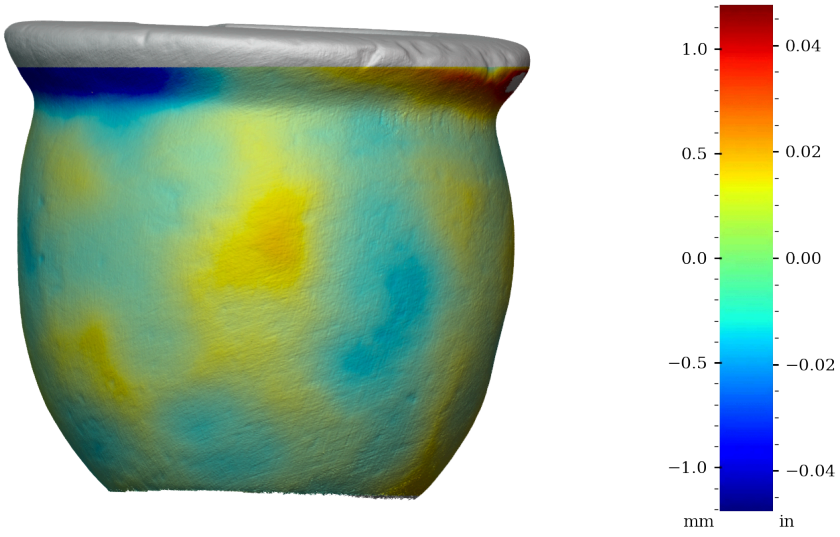

Figure 54: Surface variability heatmap of MV006, rotated 90°

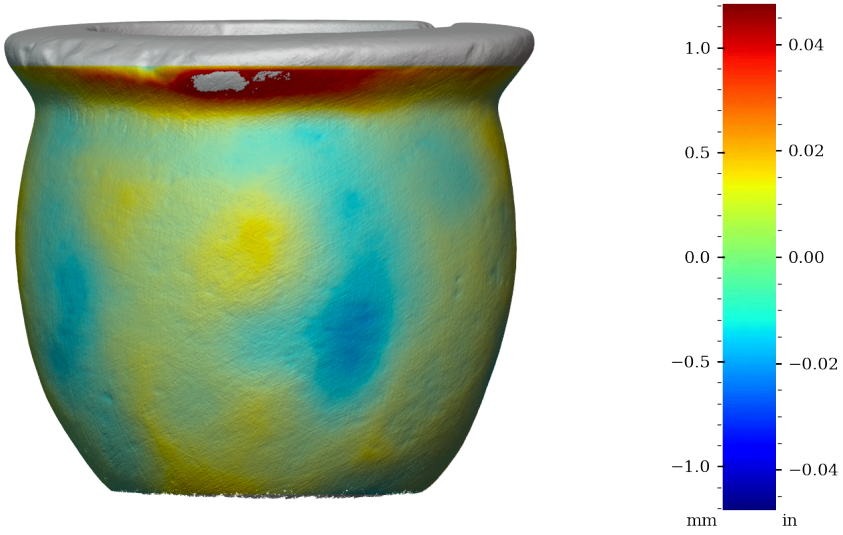

Figure 55: Surface variability heatmap of MV006, rotated 180°

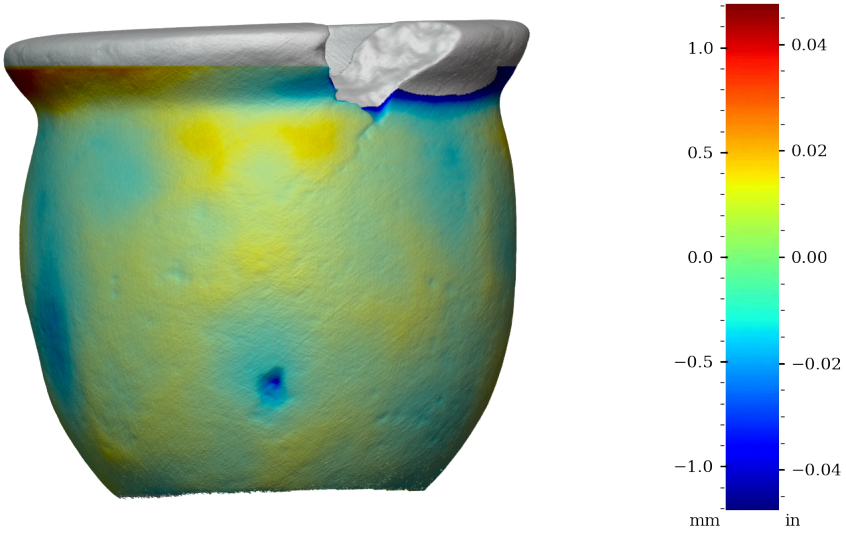

Figure 56: Surface variability heatmap of MV006, rotated 270°

Interior surface

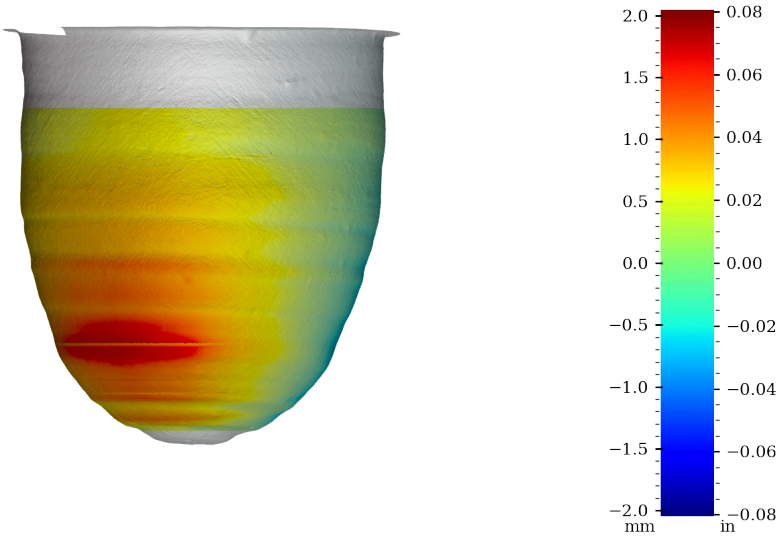

Figure 57: Surface variability heatmap of MV006, front view

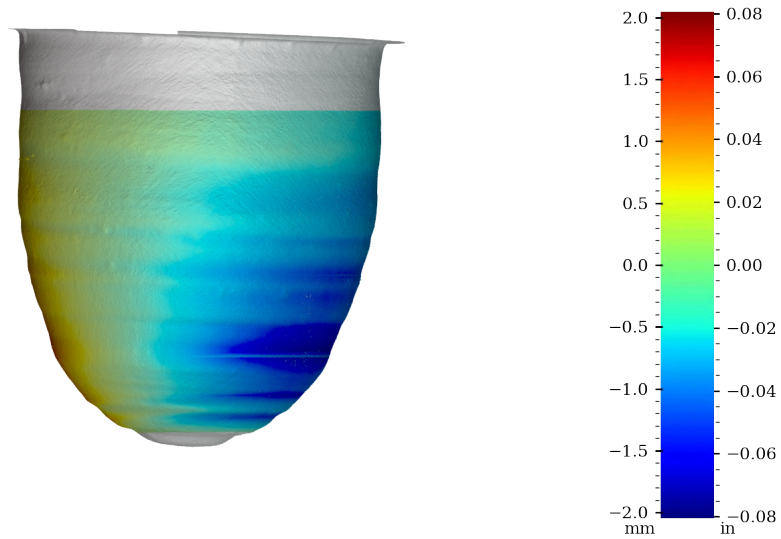

Figure 58: Surface variability heatmap of MV006, rotated 90°

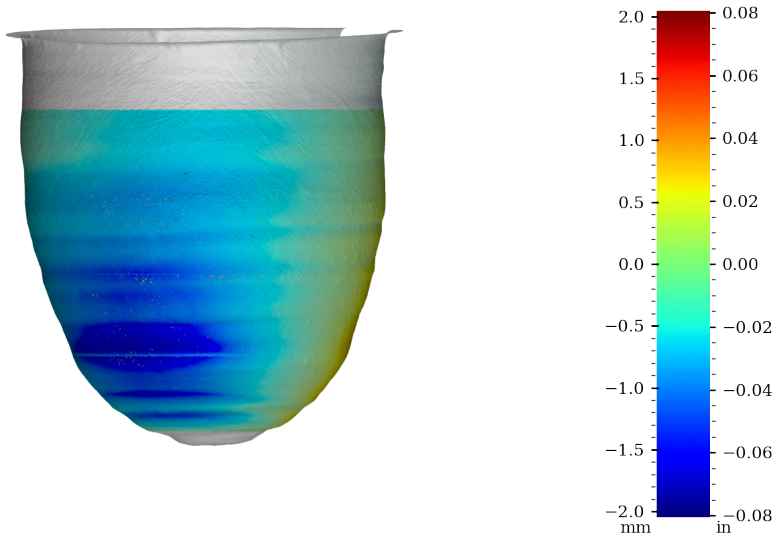

Figure 59: Surface variability heatmap of MV006, rotated 180°

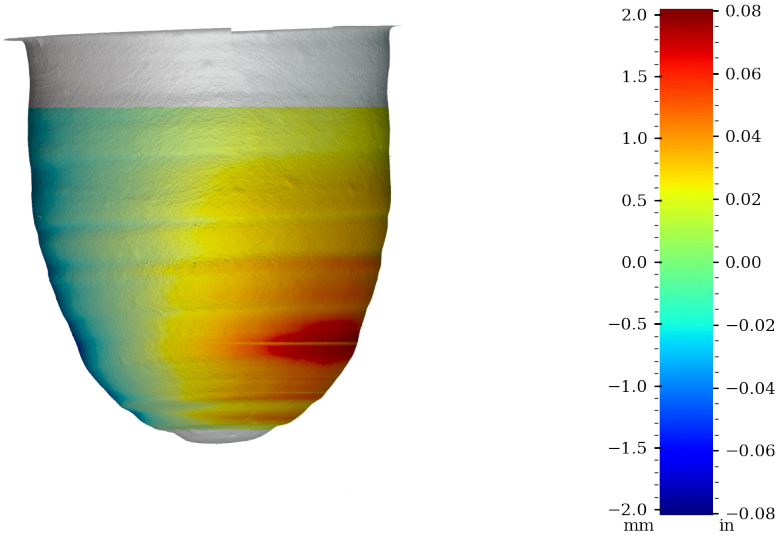

Figure 60: Surface variability heatmap of MV006, rotated 270°

Interior surface aligned separately

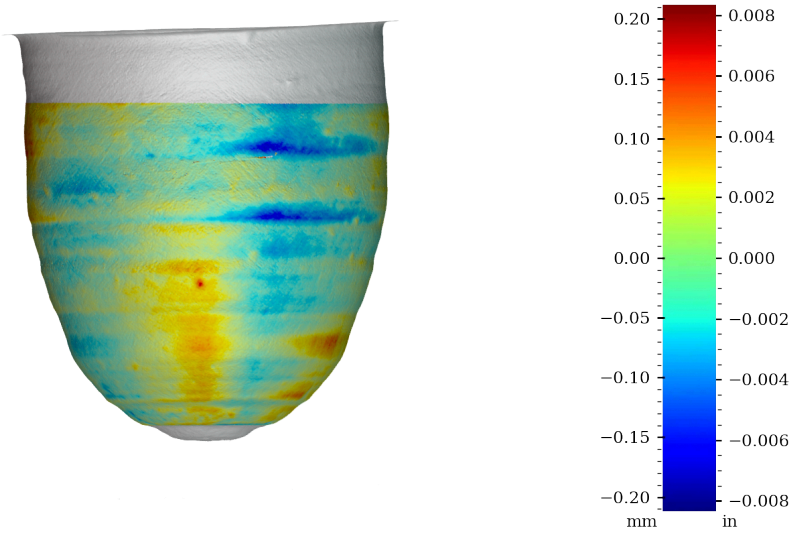

Figure 61: Surface variability heatmap of MV006, front view

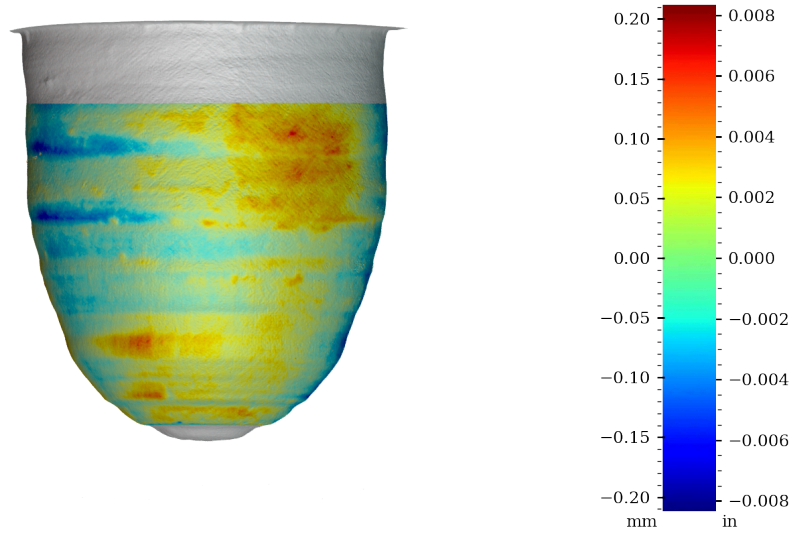

Figure 62: Surface variability heatmap of MV006, rotated 90°

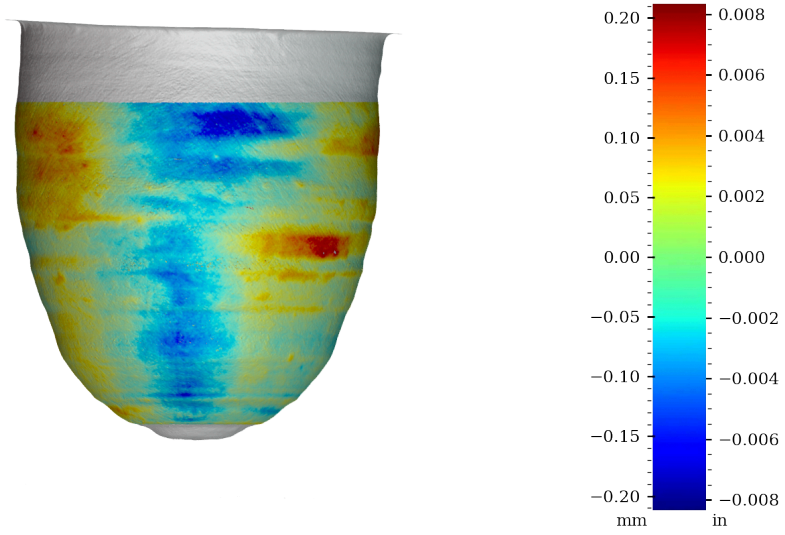

Figure 63: Surface variability heatmap of MV006, rotated 180°

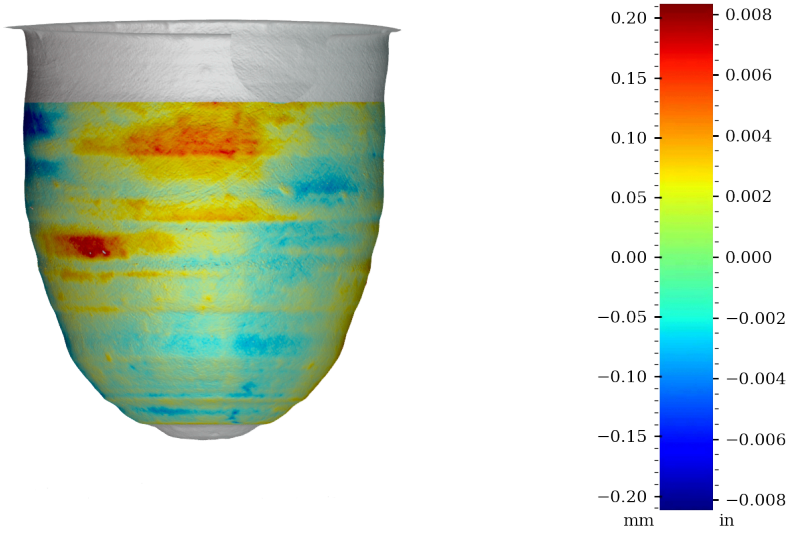

Figure 64: Surface variability heatmap of MV006, rotated 270°

Surface variability statistics

Area	MSD	RMSD	SD	Median AD	Range	Min	Max	Sample size
	mm^2	mm	mm	mm	mm	mm	mm	
Exterior	0.0912	0.302	0.222	0.085	2.907	−1.592	1.315	2252063
Interior	0.7930	0.890	0.461	0.357	4.013	−2.048	1.966	1190605
Interior separate	0.0036	0.060	0.037	0.023	1.128	−0.802	0.326	1191112
	in^2	in	in	in	in	in	in	
Exterior	0.000141	0.0119	0.0087	0.0034	0.1144	−0.0627	0.0518	2252063
Interior	0.001229	0.0351	0.0181	0.0141	0.1580	−0.0806	0.0774	1190605
Interior separate	0.000006	0.0024	0.0015	0.0009	0.0444	−0.0316	0.0128	1191112

Table 5: Surface variability statistics, MV006

Table 5 shows the statistics of the distance from the scan vertices to the best fit object model. These statistics are briefly explained below.

Histogram, KDE and Box-plot of measured surface variability - exterior surface

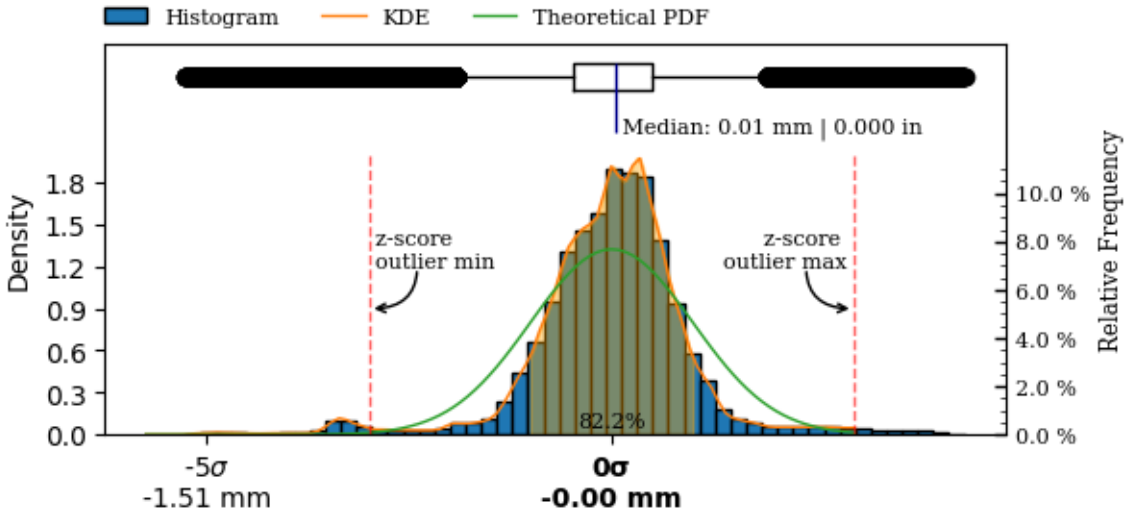

Figure 65: Exterior surface variability boxplot, kds and histogram.

Histogram, KDE and Box-plot of measured surface variability - interior surface

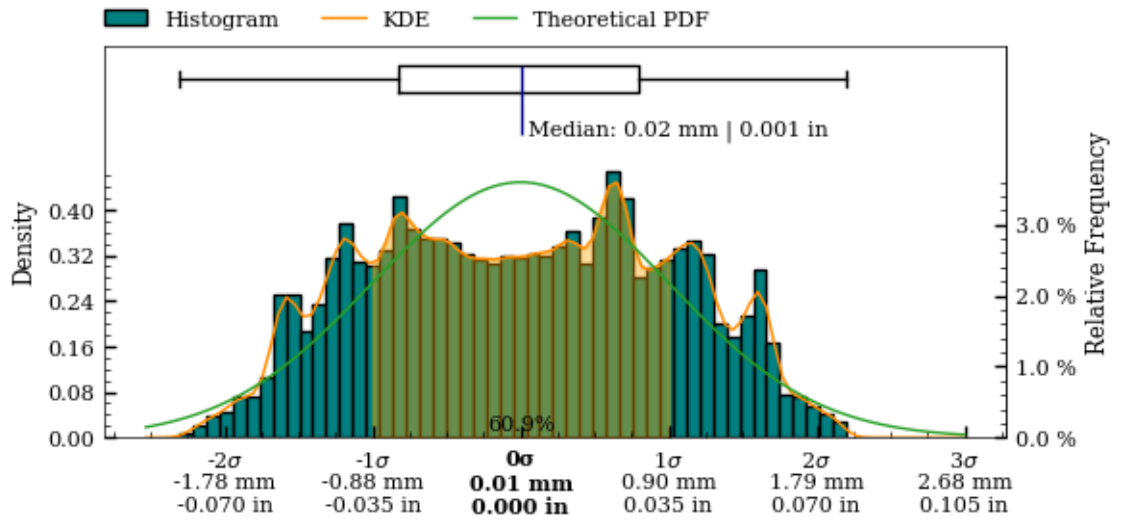

Figure 66: Interior surface variability boxplot, kds and histogram.

Histogram, KDE and Box-plot of measured surface variability - interior separately aligned surface

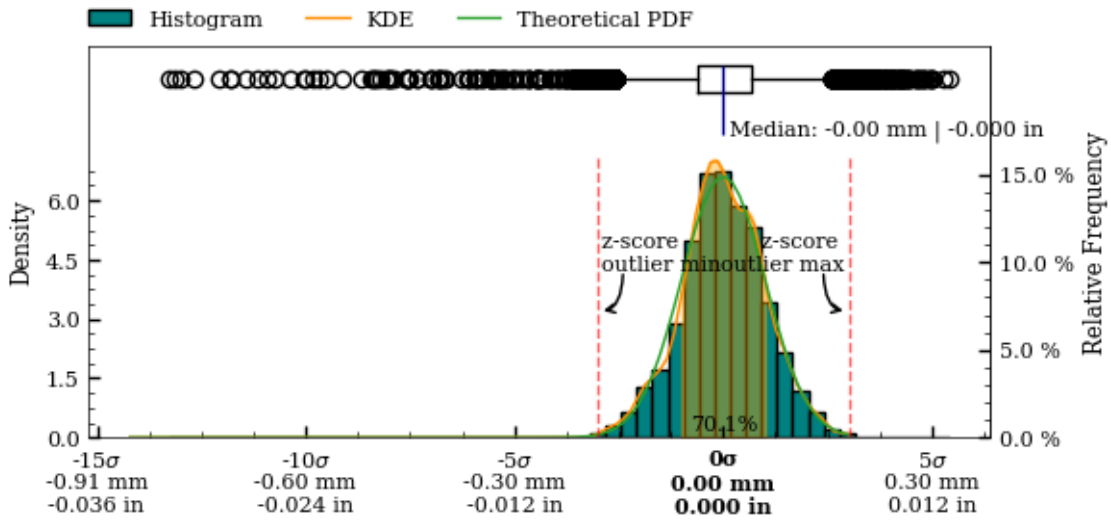

Figure 67: Interior separately aligned surface variability boxplot, kds and histogram.

Precision Score Of The Artifact

To enable valid comparison of the manufacturing precision of different artifacts, a metric that robustly quantifies the overall precision of the object is required. The considerations for such a metric will be explored in this section.

Based on these considerations, a *Precision Score* metric will be defined.

For an object to be described as having been manufactured with high precision, several qualities must be present *concurrently*, and throughout the *entire* geometry of the final object. A given object may exhibit high levels of one or more *components* of precision, but be lacking in others. For example:

- An object may present high levels of coaxialility, but lack circularity.
- An object may exhibit good circularity, but show imperfections in the surface structure.
- An object may be smoothed to perfection *without* any circularity or coaxiality.
- An object may exhibit high levels of all of the above metrics in *some* areas, but not in others.

Therefore, a precision score metric **must** account for *all* aspects of the individual, underlying precision metrics (circularity, concentricity, coaxiality and surface variability) throughout the *entire* surface area of the object.

The composite high order polynomial model, used to generate the surface variability map (described in Surface Variability, p. 52) is the best continuous mathematical representation of the object available to us (lacking any original design plans, as would normally be available in metrological analysis). This idealized model encompasses all of the above component metrics.

In the creation of the model, all scan data-points are taken into account (excluding areas with extensive damage), making it the best possible idealized representation we can achieve. When this model has been accurately created, the deviation between the model and the scanned data-points can be calculated over the non-discretized polynomials, *without* the need for an "original" CAD model (and importantly, unless such a CAD model *actually* corresponded to the original design intent, it would be an insufficient comparison basis).

Within the context of defining a valid, overall precision metric, this approach satisfies the incorporation of all of the necessary metrics:

- **Circularity**: Because the reconstructed polynomial model is revolved around the Z-plane, the idealized representation is perfectly circular, and thus incorporates the circularity component.
- **Concentricity and coaxiality**: Because the Z-axis (datum axis) is the center axis of the model, it incorporates the concentricity and coaxiality components.
- **Surface variability**: Because the model is continuous and non-discretized, it can be used accurately for all points of the scan data, and incorporates the surface variability component.

The level of precision ultimately achieved in a physical object does not share a linear relationship with its manufacturing requirements. Since continuously higher levels of final precision becomes progressively harder to achieve, an overall precision metric must take this relationship into account.

A robust statistical metric that satisfies this requirement is the *Mean Squared Deviation* (MSD or MSE). Here specifically, we can utilize the mean square of the deviations between the model ($\hat{y}$) and the data-points (y_i).

Combining all of the above considerations, we can express a well-defined *Precision Score* metric, that provides an immediately accessible way to understand the overall precision of an object, while being statistically valid. Since the Mean Squared Deviation tends towards zero as the overall precision increases, the inverse of the Mean Squared Deviation is taken to obtain a precision score metric that increases as precision increases[12]:

$$\text{Precision Score} = \frac{n}{\sum_{i=1}^{n} (y_i - \hat{y})^2}$$

[12] The precision score unit is $\frac{1}{\text{mm}^2}$

The precision score of MV006 have been calculated separately for:

- Precision score, exterior surface: 11
- Precision score, separately aligned interior surface: 274
- Precision score, interior surface: 1.26
- Precision score, full surface: 16

The precision score of a Zeiss 1.00000 inch reference sphere have been calculated to 43,943 (RMSE = 0.00477 mm / 0.00010 in). The scan was obtained by Max Fomitchev-Zamilov using a Keyence VL –500 scanner with a rated accuracy of 10 microns. The precision analysis of the reference sphere scan indicates at the maximum possible precision score obtainable.

Table 6 shows the precision score of this artifact (MV006), compared to the two most precise, and the two least precise vessels currently analyzed.

Artifact			Material	Precision Score	Link to Report
	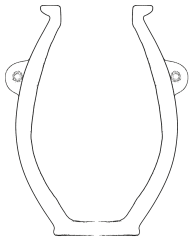	PV001	Red Granite	**1980** Full: 1177 Exterior: 1980 Interior separate: 798 Interior: 722	Report Publication
	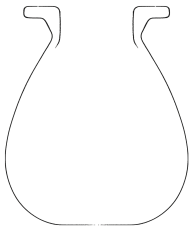	PV006	Dark grey granite	**621** Full: 610 Exterior: 621 Interior separate: 479 Interior: 152	Report Publication
	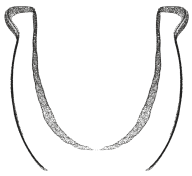	MV006	Basalt	**11** Full: 16 Exterior: 11 Interior separate: 274 Interior: 1.26	Report Publication
		RV003	Marble breccia	**1.46** Full: 1.49 Exterior: 1.46 Interior separate: 1.53 Interior: 0.54	Report Publication
	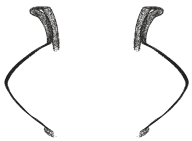	MV010	Calcite (Egyptian Alabaster)	**1.17** Full: 1.32 Exterior: 1.17 Interior separate: 11 Interior: 0.17	Report Publication

Analysis Roadmap

While the current iteration of this work already provides valuable results, continued future additions and improvements will enhance their utility further. This section details planned iterative updates and improvements, to both the reports themselves, and to the underlying methodology and software they are created with.

Alignment Section
- Detailed exploration of different circle regression algorithms
- If handles are present on the vessel, exploring alignment of the vessels so the handle positions match each other
- Add optimization of the perpendicular surface deviation, with the best results of the coaxial alignment
- Align by minimizing circularity results (of rotated sample slice, to compensate for sample height distortions)

Measurements of Precision
- Section detailing how measurements perpendicular to the surface curvature are obtained
- Detailed surface area analysis, exploring the residual patterns throughout subsequent sample slices of the artifact surface
- Wall thickness deviation color map
- Robust outlier identification on circularity, to better handle analysis of damaged areas of the artifacts in addition to removal of interior crystalline structure points present in CT scans
- Layout updates to the charts and tables

Visibility of Outliers and Damaged Sections
- Identification and marking of damaged parts
- Visualization of outliers on the artifact surface

Exploration of Mathematical Primitives
- Analysis of selected curvatures and flat surfaces on the vessel in both the horizontal and vertical planes
  - Circles
  - Parabolas
  - Ellipsoids
  - Hyperbolas
  - Cones
- Implementation of robust regressions models suitable for this domain, based on RANSAC.

Metrics on Primary Features
- Measurements of features in the horizontal plane
- Measurements of features in the vertical plane
- Measurements of angles
- Measurements of volume

Exploration of Potential Design Ratios
- π, φ, e, 1, 2, 3, 4 etc.

Raw Dataset Attachments
- Including all measurement and sample coordinates as CSV-files embedded in the report
- Including an STL file of the aligned object alongside the report, for easier external replication and validation of the research results

Appendix A - Comparison Of Circularity Measurements (Z-plane vs. surface-perpendicular)

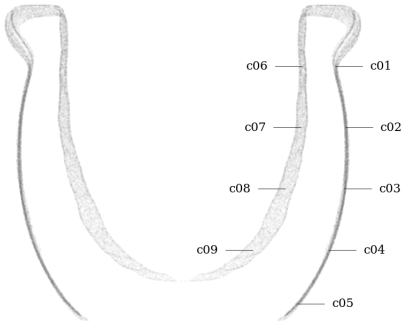

Figure 68: Circularity measurement sample locations, full mesh aligned to exterior surface

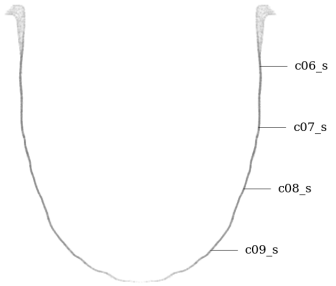

Figure 69: Circularity measurement sample location, separately aligned interior mesh

Samples perpendicular to the surface curvature

Tag	Area	Measured deviation[8]	Residuals				Sample size	Slice		
			Range	RMSD[9]	MAD[10]	SD		Height	Z coord.	Radius[11]
		mm	mm	mm	mm	mm		mm	mm	mm
c01	exterior	Ø62.863±0.516	1.012	0.276	0.111	0.149	1763	0.050	52.209	31.432
c02	exterior	Ø67.109±0.436	0.812	0.167	0.060	0.094	1960	0.050	39.545	33.555
c03	exterior	Ø66.558±0.503	0.818	0.191	0.076	0.117	2010	0.050	26.881	33.279
c04	exterior	Ø60.183±0.756	1.124	0.187	0.075	0.116	1645	0.050	14.218	30.091
c05	exterior	Ø47.151±0.437	0.714	0.167	0.078	0.107	1108	0.050	3.154	23.576
c06	interior	Ø49.366±0.754	1.408	0.460	0.155	0.203	1499	0.050	52.209	24.683
c06_s	interior sep.	Ø49.324±0.195	0.323	0.073	0.030	0.043	1434	0.050	52.209	24.662
c07	interior	Ø48.678±1.141	2.165	0.761	0.217	0.327	1447	0.050	39.545	24.339
c07_s	interior sep.	Ø48.756±0.141	0.255	0.056	0.024	0.031	1429	0.050	39.545	24.378
c08	interior	Ø42.346±1.493	2.937	1.017	0.385	0.455	1123	0.050	26.881	21.173
c08_s	interior sep.	Ø42.516±0.153	0.248	0.046	0.020	0.028	1160	0.050	26.881	21.258
c09	interior	Ø28.936±1.626	2.778	0.999	0.298	0.430	698	0.050	14.218	14.468
c09_s	interior sep.	Ø28.916±0.148	0.292	0.059	0.017	0.036	621	0.050	14.218	14.458

Table 7: Detailed circularity measurements at selected samples in z-plane, vessel MV006.

Samples in the Z-plane

Tag	Area	Measured deviation[8]	Residuals				Sample size	Slice		
			Range	RMSD[9]	MAD[10]	SD		Height	Z coord.	Radius[11]
		mm	mm	mm	mm	mm		mm	mm	mm
c01	exterior	Ø62.972±0.570	1.017	0.283	0.134	0.166	1779	0.050	52.209	31.486
c02	exterior	Ø67.096±0.454	0.823	0.171	0.063	0.097	1973	0.050	39.545	33.548
c03	exterior	Ø66.651±0.559	0.828	0.194	0.063	0.130	1992	0.050	26.881	33.325
c04	exterior	Ø60.251±0.759	1.126	0.198	0.086	0.128	1921	0.050	14.218	30.125
c05	exterior	Ø47.106±0.587	1.007	0.216	0.103	0.144	1869	0.050	3.154	23.553
c06	interior	Ø49.423±0.784	1.408	0.468	0.151	0.208	1528	0.050	52.209	24.711
c06_s	interior sep.	Ø49.349±0.207	0.323	0.075	0.028	0.047	1446	0.050	52.209	24.674
c07	interior	Ø48.754±1.191	2.209	0.771	0.224	0.336	1438	0.050	39.545	24.377
c07_s	interior sep.	Ø48.756±0.134	0.258	0.057	0.024	0.031	1444	0.050	39.545	24.378
c08	interior	Ø42.310±1.597	3.173	1.101	0.398	0.496	1324	0.050	26.881	21.155
c08_s	interior sep.	Ø42.526±0.161	0.258	0.049	0.021	0.030	1307	0.050	26.881	21.263
c09	interior	Ø28.944±2.248	4.216	1.458	0.449	0.634	1177	0.050	14.218	14.472
c09_s	interior sep.	Ø28.905±0.216	0.422	0.079	0.029	0.048	1159	0.050	14.218	14.452

Table 8: Detailed circularity measurements at selected samples perpendicular to vessel curvature, vessel MV006.

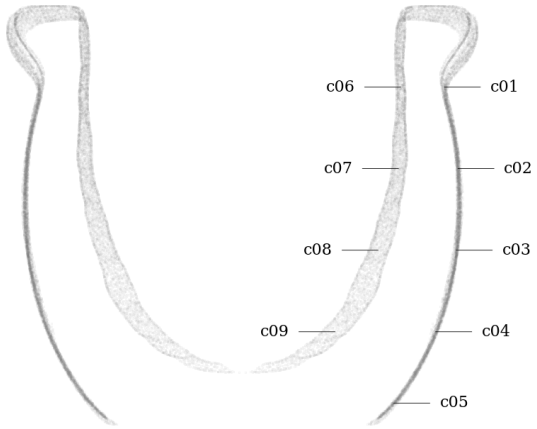

Figure 70: Circularity measurement sample locations, full mesh aligned to exterior surface

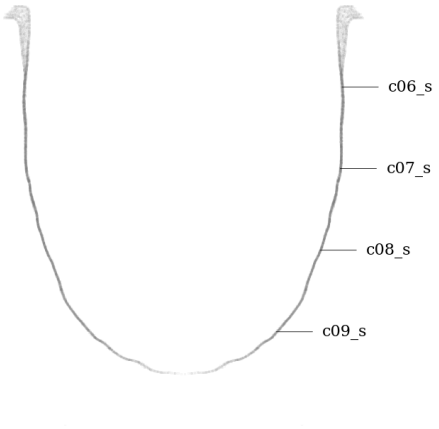

Figure 71: Circularity measurement sample location, separately aligned interior mesh

Samples perpendicular to the surface curvature

Tag	Area	Measured deviation[8]	Residuals				Sample size	Slice		
			Range	RMSD[9]	MAD[10]	SD		Height	Z coord.	Radius[11]
		in	in	in	in	in		in	in	in
c01	exterior	Ø2.4749±0.0203	0.0398	0.0109	0.0044	0.0059	1763	0.0020	2.0555	1.2375
c02	exterior	Ø2.6421±0.0172	0.0320	0.0066	0.0024	0.0037	1960	0.0020	1.5569	1.3210
c03	exterior	Ø2.6204±0.0198	0.0322	0.0075	0.0030	0.0046	2010	0.0020	1.0583	1.3102
c04	exterior	Ø2.3694±0.0298	0.0442	0.0073	0.0030	0.0045	1645	0.0020	0.5598	1.1847
c05	exterior	Ø1.8564±0.0172	0.0281	0.0066	0.0031	0.0042	1108	0.0020	0.1242	0.9282
c06	interior	Ø1.9435±0.0297	0.0555	0.0181	0.0061	0.0080	1499	0.0020	2.0555	0.9718
c06_s	interior sep.	Ø1.9419±0.0077	0.0127	0.0029	0.0012	0.0017	1434	0.0020	2.0555	0.9709
c07	interior	Ø1.9164±0.0449	0.0853	0.0300	0.0085	0.0129	1447	0.0020	1.5569	0.9582
c07_s	interior sep.	Ø1.9195±0.0055	0.0100	0.0022	0.0010	0.0012	1429	0.0020	1.5569	0.9598
c08	interior	Ø1.6672±0.0588	0.1156	0.0400	0.0152	0.0179	1123	0.0020	1.0583	0.8336
c08_s	interior sep.	Ø1.6739±0.0060	0.0098	0.0018	0.0008	0.0011	1160	0.0020	1.0583	0.8369
c09	interior	Ø1.1392±0.0640	0.1094	0.0393	0.0117	0.0169	698	0.0020	0.5598	0.5696
c09_s	interior sep.	Ø1.1384±0.0058	0.0115	0.0023	0.0007	0.0014	621	0.0020	0.5598	0.5692

Table 9: Detailed circularity measurements at selected samples in z-plane, vessel MV006.

Samples in the Z-plane

Tag	Area	Measured deviation[8]	Residuals				Sample size	Slice		
			Range	RMSD[9]	MAD[10]	SD		Height	Z coord.	Radius[11]
		in	in	in	in	in		in	in	in
c01	exterior	Ø2.4792±0.0224	0.0400	0.0111	0.0053	0.0065	1779	0.0020	2.0555	1.2396
c02	exterior	Ø2.6416±0.0179	0.0324	0.0067	0.0025	0.0038	1973	0.0020	1.5569	1.3208
c03	exterior	Ø2.6240±0.0220	0.0326	0.0076	0.0025	0.0051	1992	0.0020	1.0583	1.3120
c04	exterior	Ø2.3721±0.0299	0.0443	0.0078	0.0034	0.0050	1921	0.0020	0.5598	1.1860
c05	exterior	Ø1.8546±0.0231	0.0397	0.0085	0.0041	0.0057	1869	0.0020	0.1242	0.9273
c06	interior	Ø1.9458±0.0309	0.0554	0.0184	0.0059	0.0082	1528	0.0020	2.0555	0.9729
c06_s	interior sep.	Ø1.9429±0.0082	0.0127	0.0030	0.0011	0.0019	1446	0.0020	2.0555	0.9714
c07	interior	Ø1.9195±0.0469	0.0870	0.0303	0.0088	0.0132	1438	0.0020	1.5569	0.9597
c07_s	interior sep.	Ø1.9195±0.0053	0.0102	0.0022	0.0010	0.0012	1444	0.0020	1.5569	0.9598
c08	interior	Ø1.6657±0.0629	0.1249	0.0434	0.0157	0.0195	1324	0.0020	1.0583	0.8329
c08_s	interior sep.	Ø1.6743±0.0063	0.0101	0.0019	0.0008	0.0012	1307	0.0020	1.0583	0.8371
c09	interior	Ø1.1395±0.0885	0.1660	0.0574	0.0177	0.0250	1177	0.0020	0.5598	0.5698
c09_s	interior sep.	Ø1.1380±0.0085	0.0166	0.0031	0.0011	0.0019	1159	0.0020	0.5598	0.5690

Table 10: Detailed circularity measurements at selected samples perpendicular to vessel curvature, vessel MV006.

Comparison of circularity on the full vessel surface

Metric

Samples perpendicular to the surface curvature

Area	Range			Standard Deviation			RMSD			Slices	Slice height
	Median	Min.	Max.	Median	Min.	Max.	Median	Min.	Max.		
	mm	mm	mm	mm	mm	mm	mm	mm	mm		mm
Exterior	0.854	0.567	2.229	0.114	0.068	0.335	0.193	0.143	0.728	1167	0.050
Interior	2.243	1.023	3.626	0.338	0.128	0.533	0.745	0.283	1.119	870	0.050
Interior separate	0.270	0.150	0.939	0.031	0.018	0.073	0.055	0.028	0.101	882	0.050

Table 11: Detailed circularity measurements at selected samples in z-plane, vessel MV006.

Samples in the z-plane

Area	Range			Standard Deviation			RMSD			Slices	Slice height
	Median	Min.	Max.	Median	Min.	Max.	Median	Min.	Max.		
	mm	mm	mm	mm	mm	mm	mm	mm	mm		mm
Exterior	0.903	0.629	3.570	0.122	0.083	0.554	0.206	0.159	1.084	1165	0.050
Interior	3.064	1.365	4.478	0.475	0.198	1.040	1.045	0.442	1.574	876	0.050
Interior separate	0.311	0.199	1.217	0.038	0.023	0.117	0.065	0.040	0.209	876	0.050

Table 12: Detailed circularity measurements at selected samples perpendicular to vessel curvature, vessel MV006.

Imperial

Samples perpendicular to the surface curvature

Area	Range			Standard Deviation			RMSD			Slices	Slice height
	Median	Min.	Max.	Median	Min.	Max.	Median	Min.	Max.		
	in	in	in	in	in	in	in	in	in		in
Exterior	0.854	0.567	2.229	0.114	0.068	0.335	0.193	0.143	0.728	1167	0.050
Interior	2.243	1.023	3.626	0.338	0.128	0.533	0.745	0.283	1.119	870	0.050
Interior separate	0.270	0.150	0.939	0.031	0.018	0.073	0.055	0.028	0.101	882	0.050

Table 13: Detailed circularity measurements at selected samples in z-plane, vessel MV006.

Samples in the z-plane

Area	Range			Standard Deviation			RMSD			Slices	Slice height
	Median	Min.	Max.	Median	Min.	Max.	Median	Min.	Max.		
	in	in	in	in	in	in	in	in	in		in
Exterior	0.903	0.629	3.570	0.122	0.083	0.554	0.206	0.159	1.084	1165	0.050
Interior	3.064	1.365	4.478	0.475	0.198	1.040	1.045	0.442	1.574	876	0.050
Interior separate	0.311	0.199	1.217	0.038	0.023	0.117	0.065	0.040	0.209	876	0.050

Table 14: Detailed circularity measurements at selected samples perpendicular to vessel curvature, vessel MV006.

Circularity analysis of exterior surface - perpendicular to surface curvature

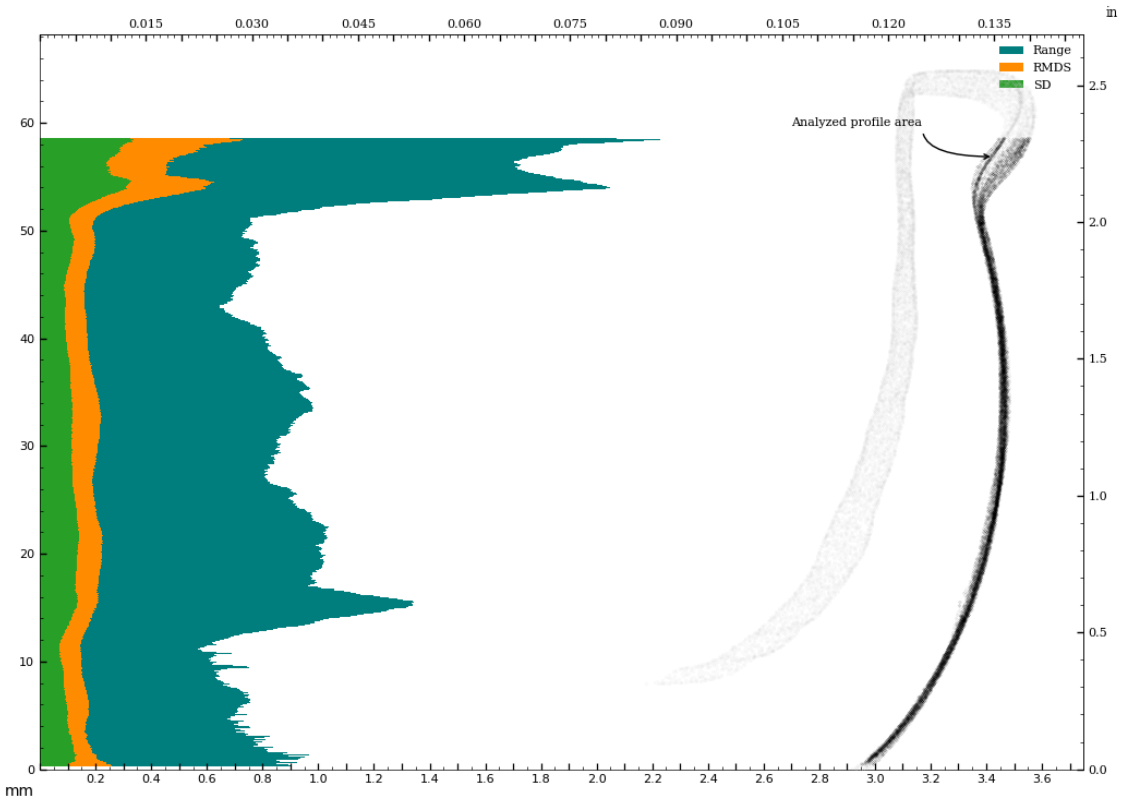

Figure 72: Circularity of exterior surface - perpendicular to surface curvature.

Circularity analysis of exterior surface - in z-plane

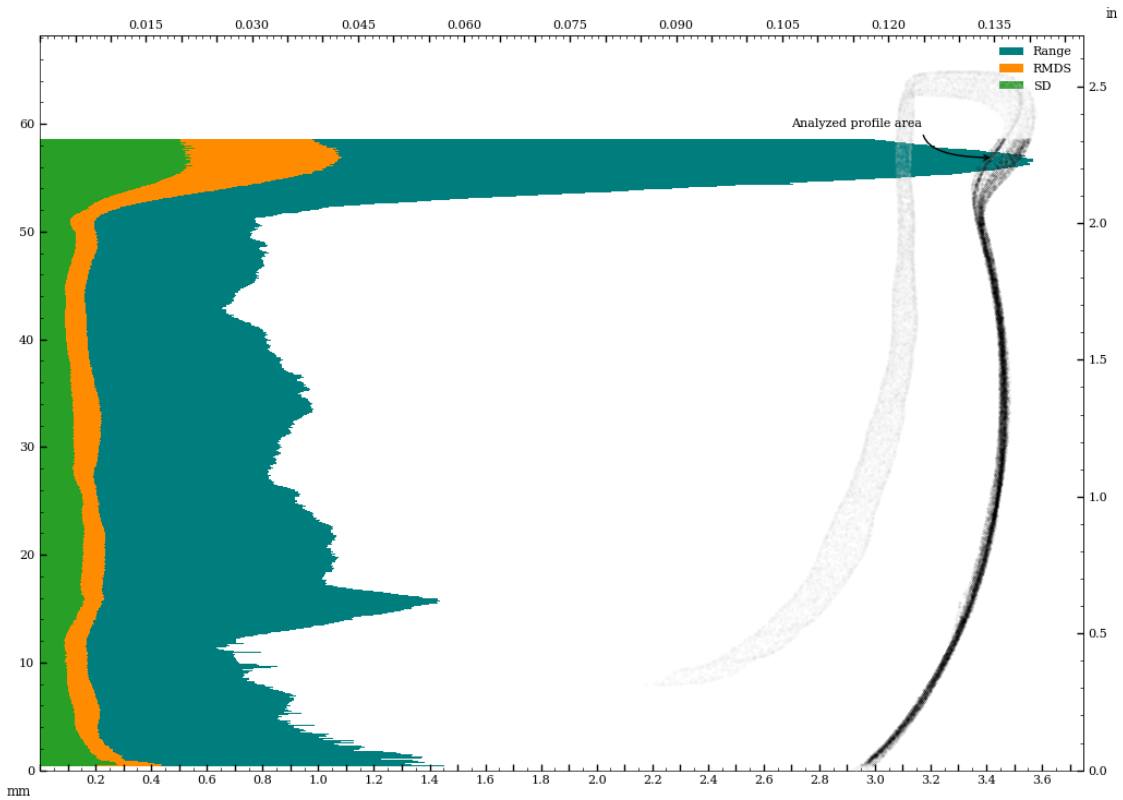

Figure 73: Circularity of exterior surface - in z-plane.

Circularity analysis of exterior surface, perpendicular to surface curvature, Standard Deviation and Root Mean Squared Deviation

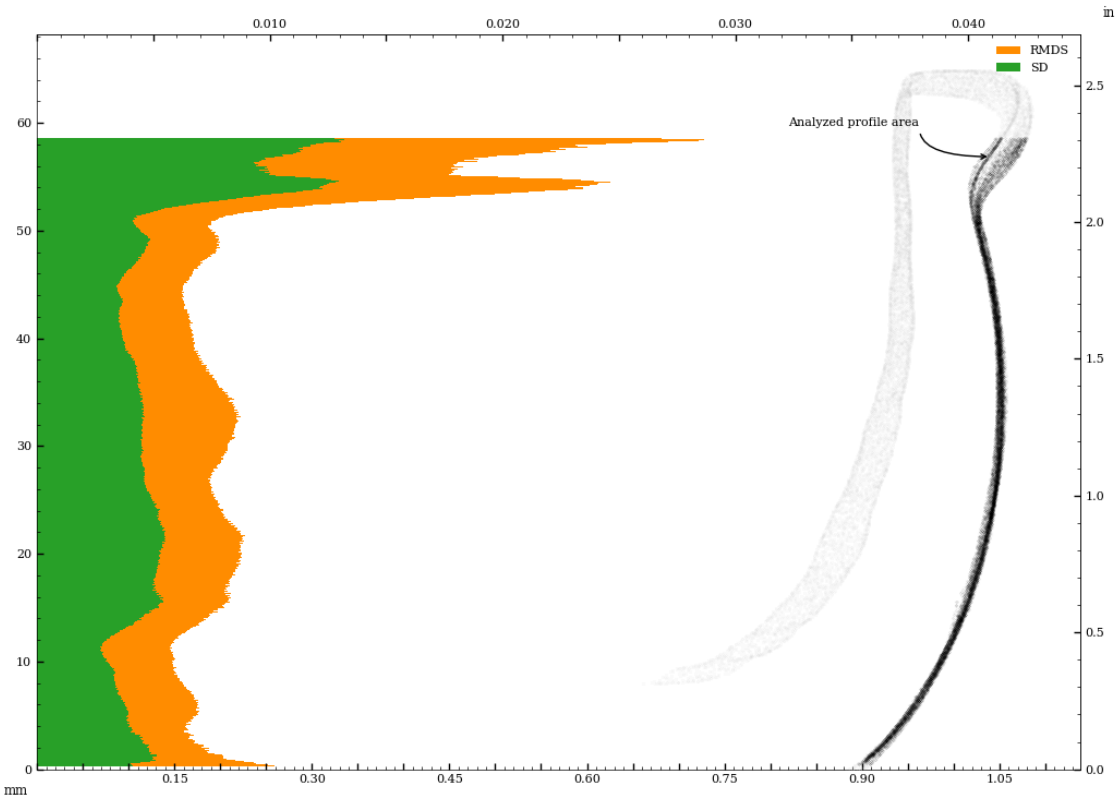

Figure 74: Vessel circularity of exterior surface, perpendicular to surface curvature, standard deviation and median absolute deviation.

Circularity analysis of exterior surface, in z-plane, Standard Deviation and Root Mean Squared Deviation

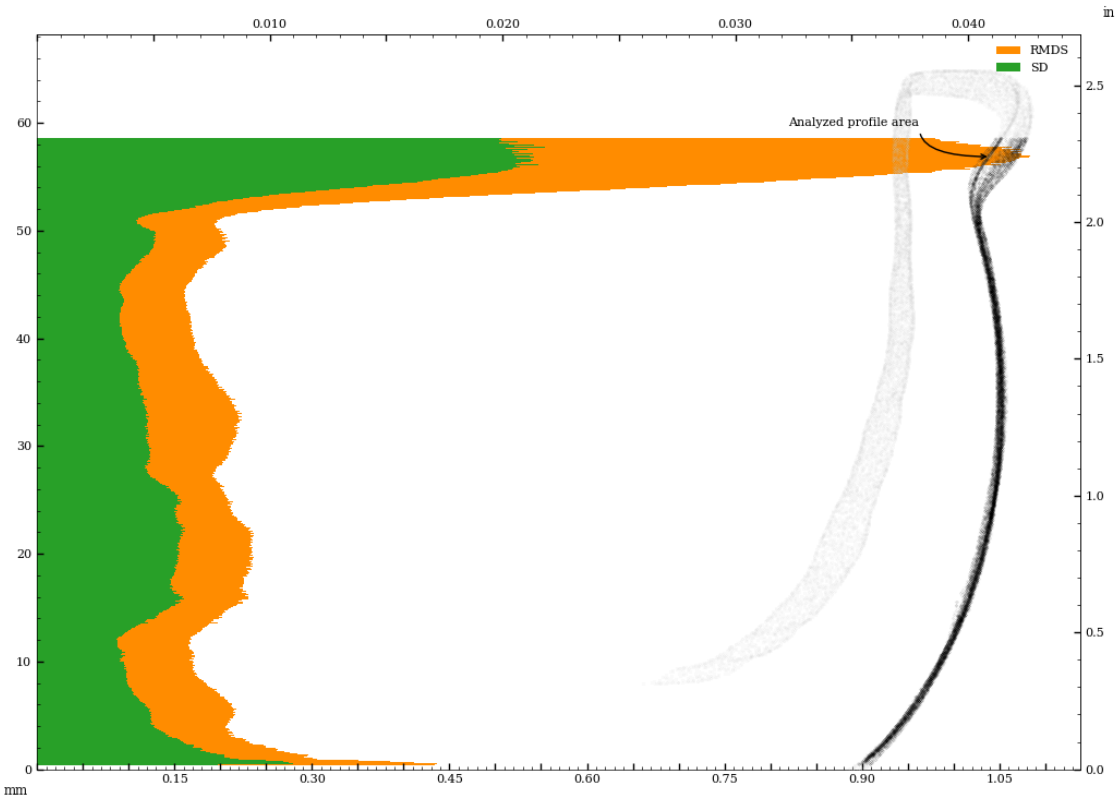

Figure 75: Vessel circularity of exterior surface, in z-plane, standard deviation and median absolute deviation.

Circularity analysis of interior surface - perpendicular to surface curvature

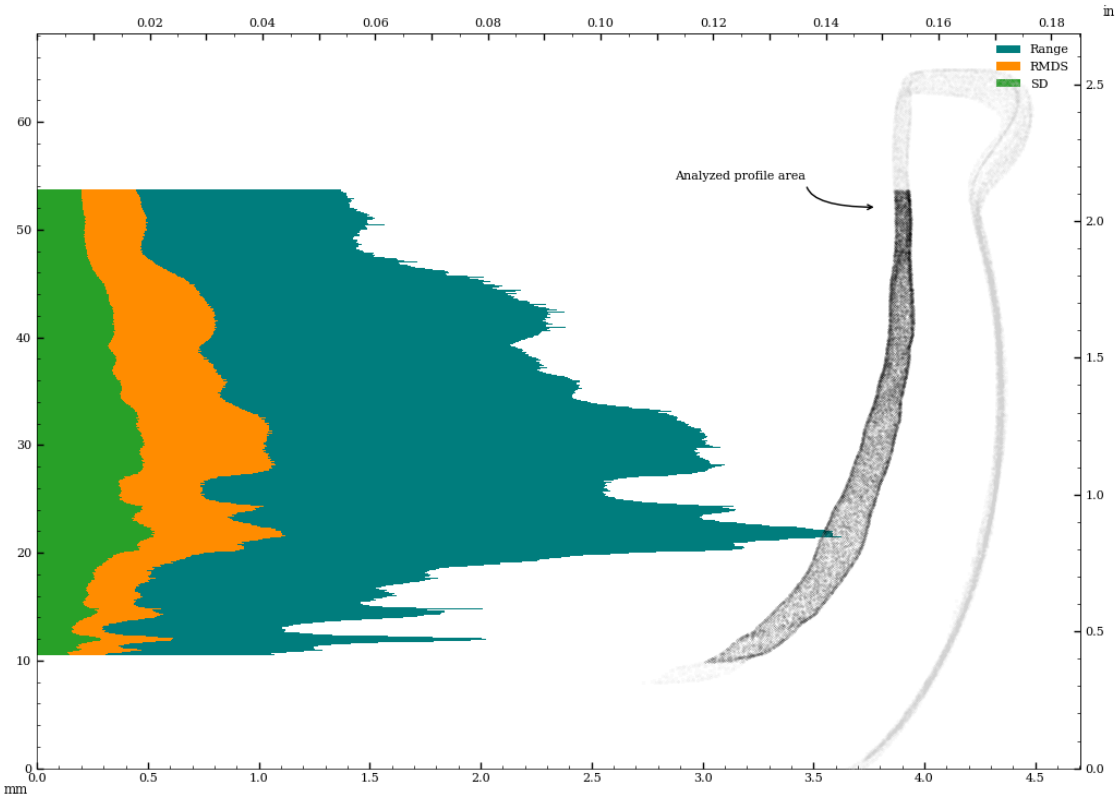

Figure 76: Circularity of interior surface - perpendicular to surface curvature.

Circularity analysis of interior surface - in z-plane

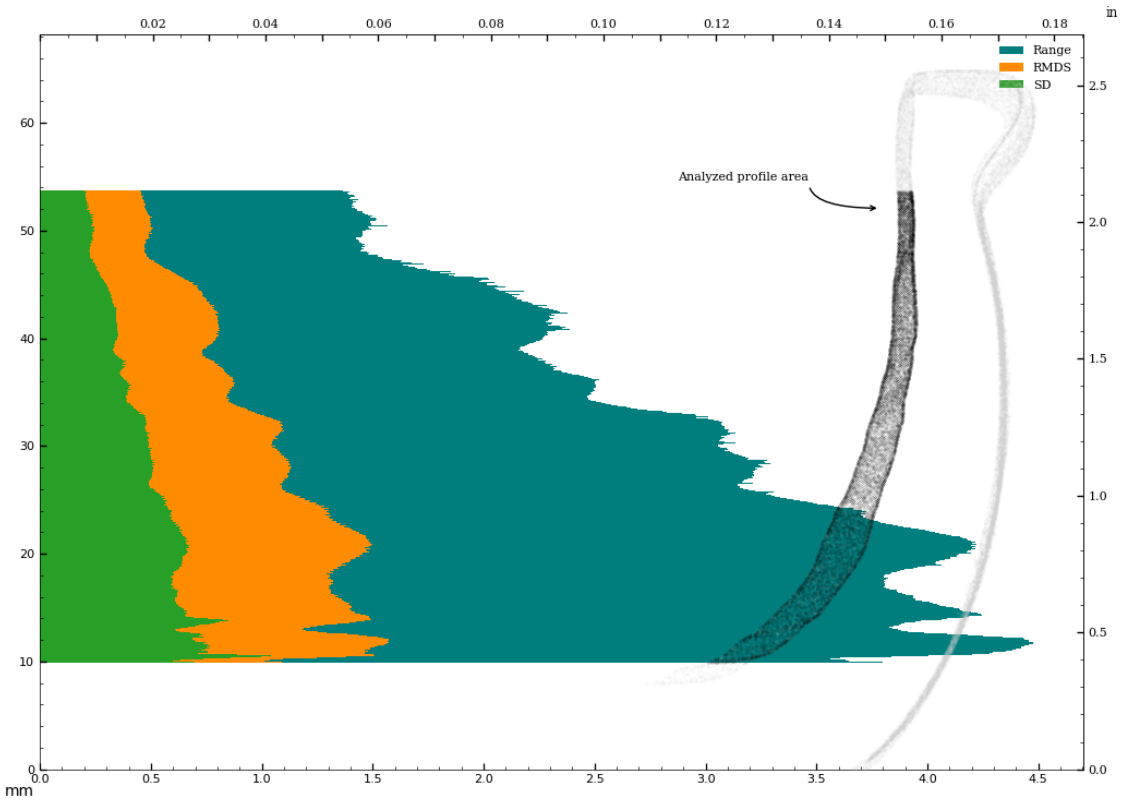

Figure 77: Circularity of interior surface - in z-plane.

Circularity analysis of interior surface, perpendicular to surface curvature, Standard Deviation and Root Mean Squared Deviation

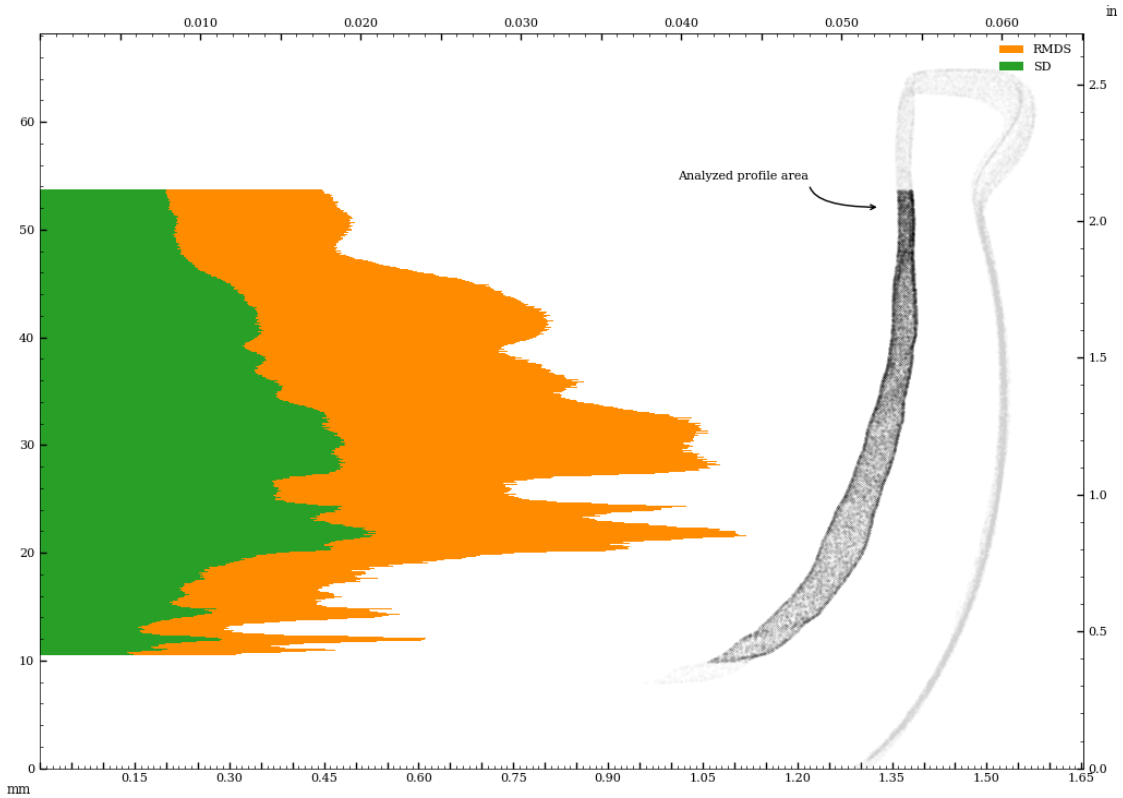

Figure 78: Vessel circularity of interior surface, perpendicular to surface curvature, standard deviation and median absolute deviation.

Circularity analysis of interior surface, in z-plane, Standard Deviation and Root Mean Squared Deviation

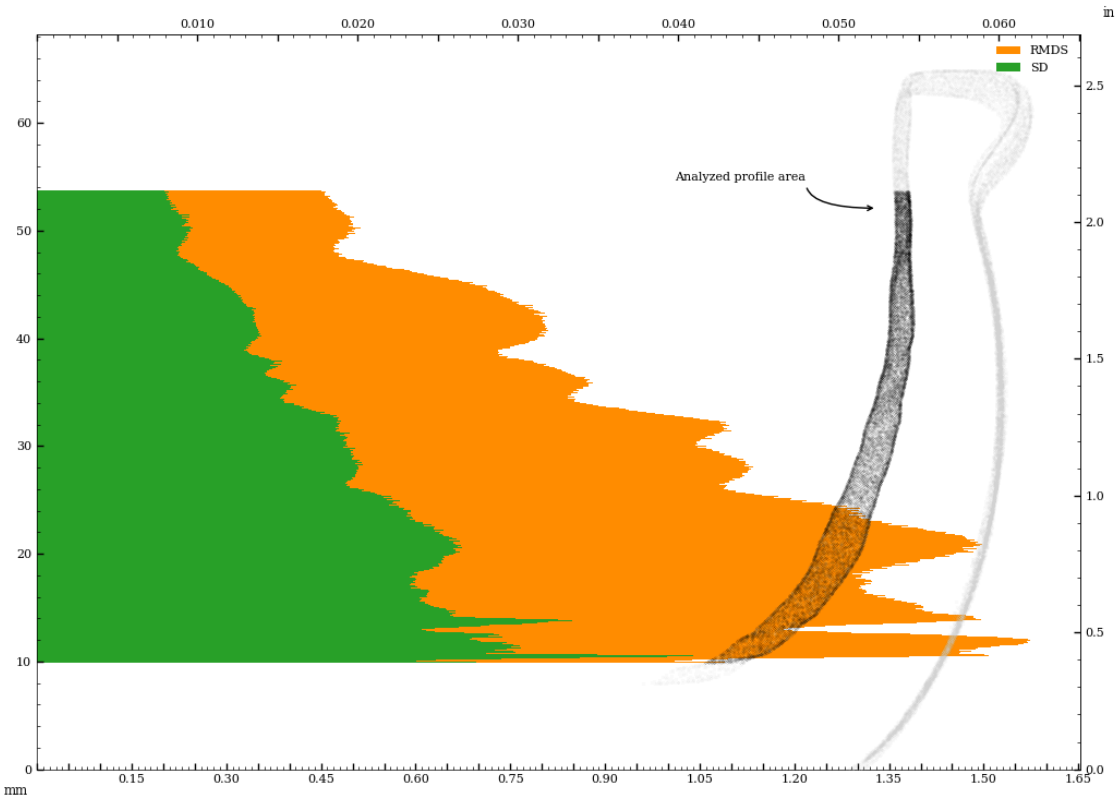

Figure 79: Vessel circularity of interior surface, in z-plane, standard deviation and median absolute deviation.

Circularity analysis of interior separately aligned surface - perpendicular to surface curvature

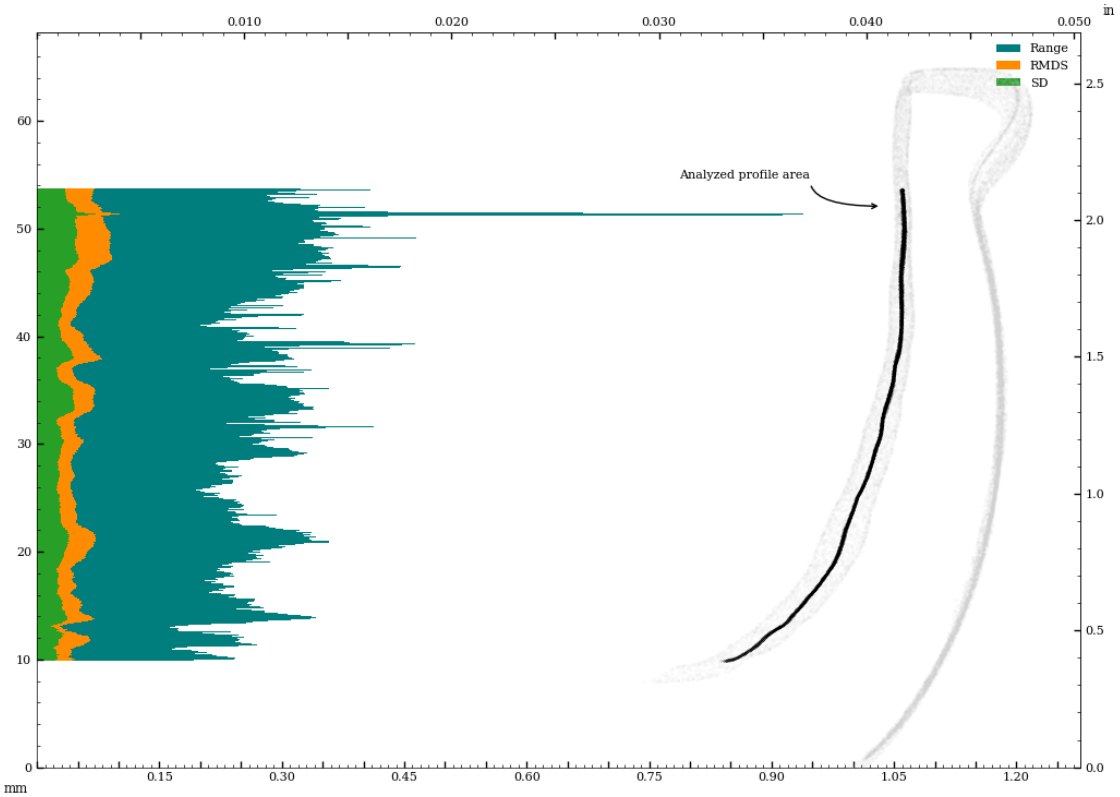

Figure 80: Circularity of interior_separate surface - perpendicular to surface curvature.

Circularity analysis of interior separately aligned surface - in z-plane

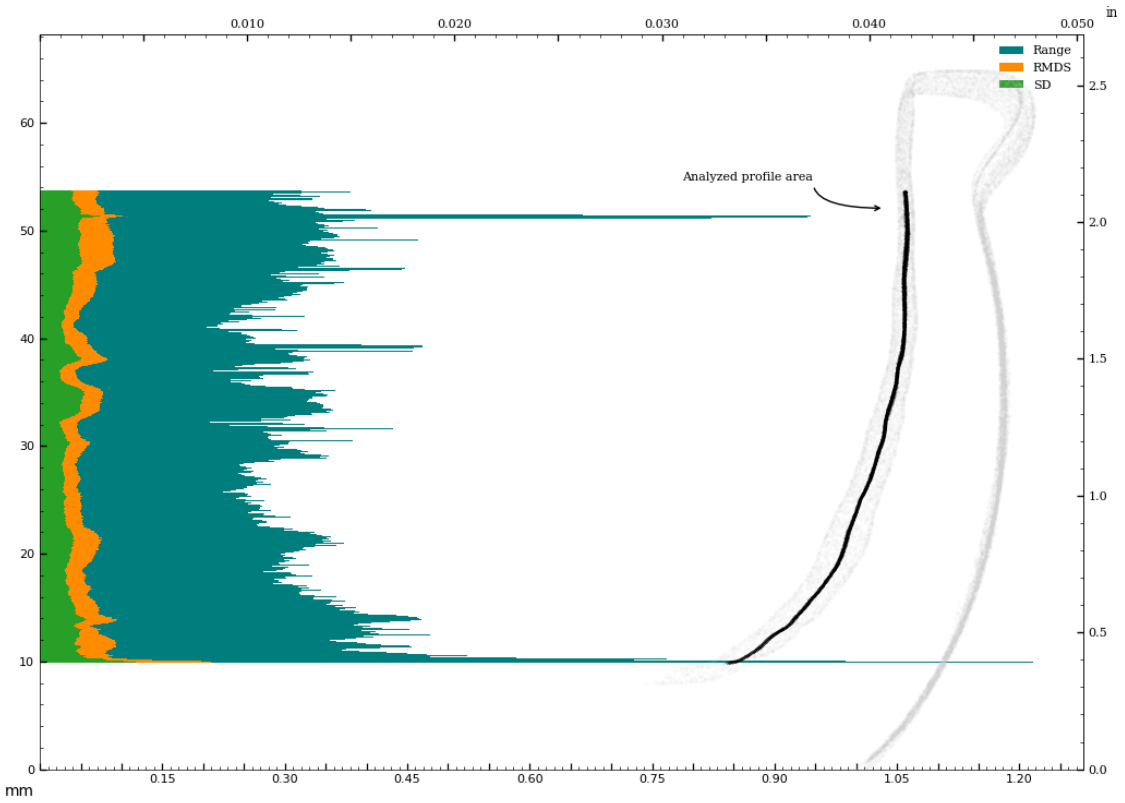

Figure 81: Circularity of interior_separate surface - in z-plane.

Circularity analysis of interior separately aligned surface, perpendicular to surface curvature, Standard Deviation and Root Mean Squared Deviation

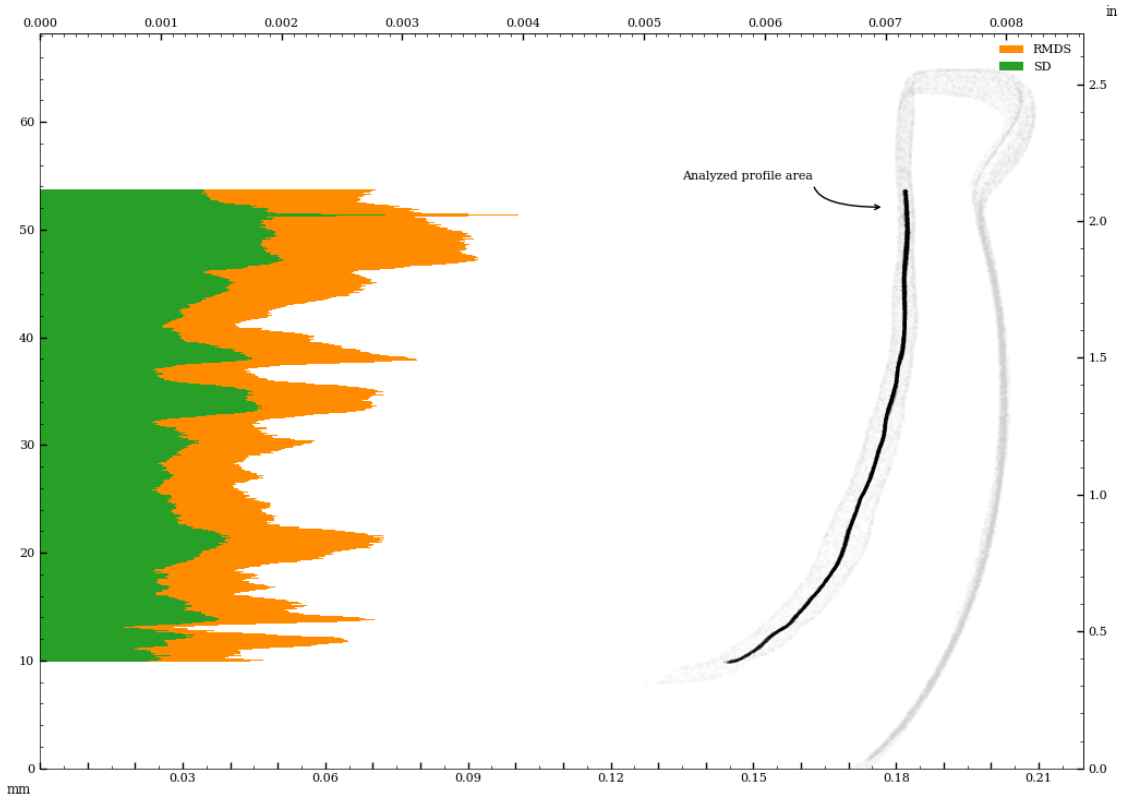

Figure 82: Vessel circularity of interior_separate surface, perpendicular to surface curvature, standard deviation and median absolute deviation.

Circularity analysis of interior separately aligned surface, in z-plane, Standard Deviation and Root Mean Squared Deviation

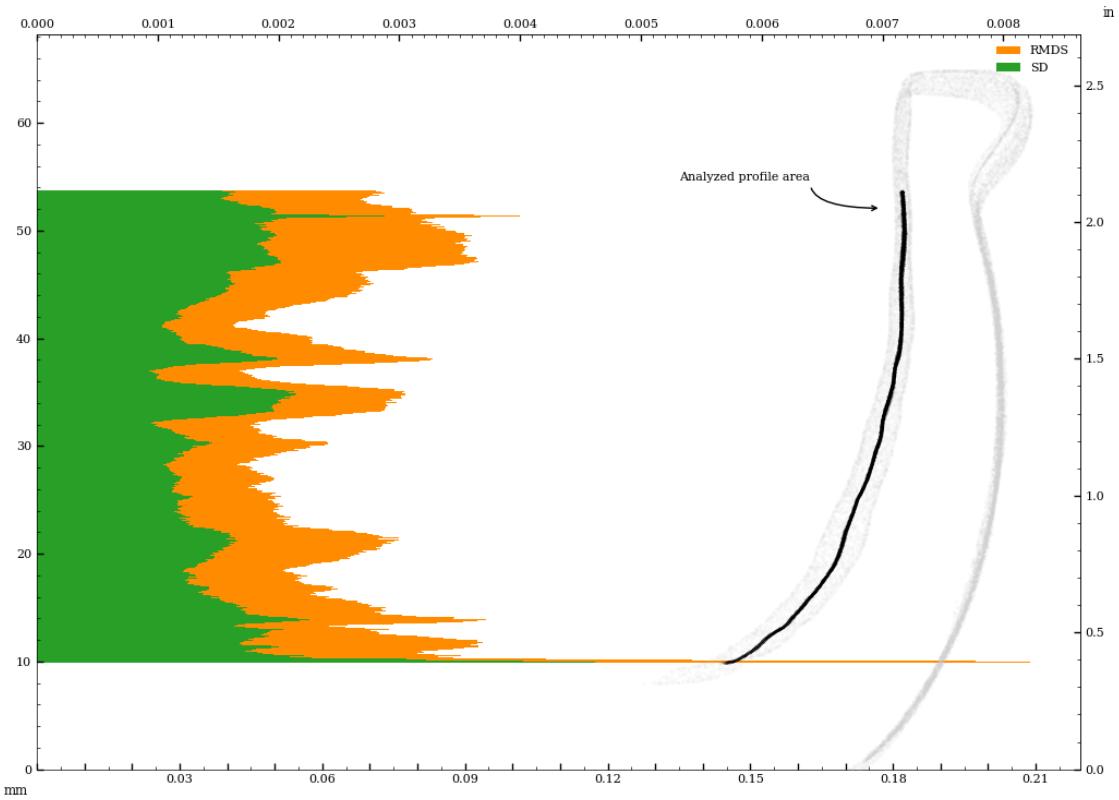

Figure 83: Vessel circularity of interior_separate surface, in z-plane, standard deviation and median absolute deviation.

Appendix B - Comparison Of Concentricity Measurements (Z-plane vs. surface-perpendicular)

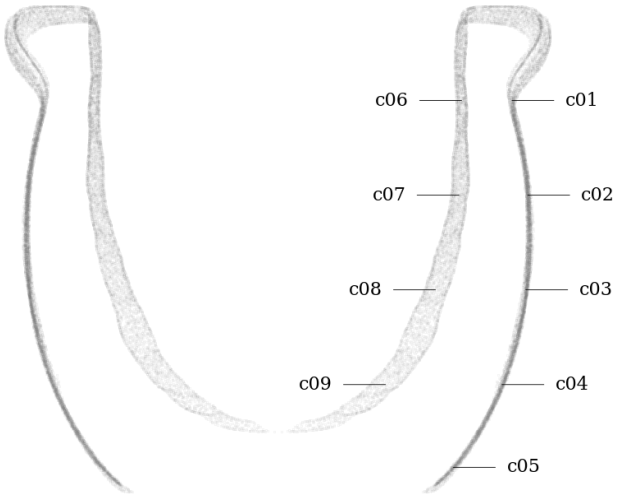

Figure 84: Circularity measurement sample locations, full mesh aligned to exterior surface

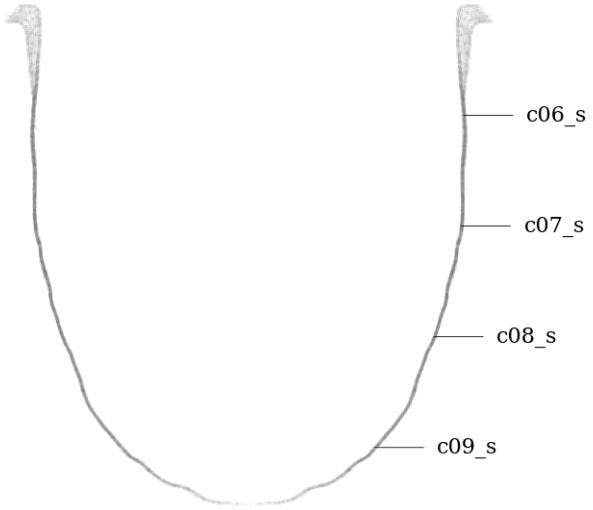

Figure 85: Circularity measurement sample location, separately aligned interior mesh

Concentricity measurements perpendicular to surface curvature

Tag	Reference	Deviation	Sample size	Circle fit residuals analysis for sample listed in Tag column						
				Range full	Range inliers	RMSD full	RMDS inliers	SD full	SD inliers	Center (x,y)
		mm		mm	mm	mm	mm	mm	mm	µm
c01	z-axis	0.307	1779	1.812	1.812	0.485	0.485	0.238	0.238	−67, 300
c02	z-axis	0.064	1973	0.844	0.844	0.188	0.188	0.108	0.108	47, 44
c03	z-axis	0.064	1992	0.830	0.822	0.212	0.210	0.128	0.127	−29, −57
c04	z-axis	0.094	1921	1.069	1.013	0.197	0.192	0.125	0.120	79, −51
c05	z-axis	0.233	1869	1.636	1.636	0.376	0.376	0.226	0.226	−31, 231
c06	z-axis	0.642	1528	3.017	3.017	1.046	1.050	0.450	0.451	−197, −611
c06_s	z-axis	0.021	1446	0.366	0.366	0.079	0.079	0.047	0.047	4, −20
c07	z-axis	1.073	1438	4.662	4.662	1.667	1.667	0.728	0.728	−577, −904
c07_s	z-axis	0.022	1444	0.302	0.302	0.064	0.064	0.036	0.036	−5, 22
c08	z-axis	1.549	1324	6.636	6.636	2.341	2.336	1.047	1.050	−918, −1248
c08_s	z-axis	0.017	1307	0.254	0.215	0.048	0.046	0.029	0.027	−16, 6
c09	z-axis	2.071	1177	8.845	8.845	3.121	3.120	1.381	1.381	−1229, −1668
c09_s	z-axis	0.081	1159	0.493	0.469	0.097	0.095	0.065	0.063	54, −60
c01	c06	0.920								131, 910
c02	c07	1.136								624, 949
c03	c08	1.486								889, 1191
c04	c09	2.079								1307, 1617

Concentricity measurements in z-plane

Tag	Reference	Deviation	Sample size	Circle fit residuals analysis for sample listed in Tag column						
				Range full	Range inliers	RMSD full	RMDS inliers	SD full	SD inliers	Center (x,y)
		mm		mm	mm	mm	mm	mm	mm	µm
c01	z-axis	0.307	1779	1.812	1.812	0.485	0.485	0.238	0.238	−67, 300
c02	z-axis	0.064	1973	0.844	0.844	0.188	0.188	0.108	0.108	47, 44
c03	z-axis	0.064	1992	0.830	0.822	0.212	0.210	0.128	0.127	−29, −57
c04	z-axis	0.094	1921	1.069	1.013	0.197	0.192	0.125	0.120	79, −51
c05	z-axis	0.233	1869	1.636	1.636	0.376	0.376	0.226	0.226	−31, 231
c06	z-axis	0.642	1528	3.017	3.017	1.046	1.050	0.450	0.451	−197, −611
c06_s	z-axis	0.021	1446	0.366	0.366	0.079	0.079	0.047	0.047	4, −20
c07	z-axis	1.073	1438	4.662	4.662	1.667	1.667	0.728	0.728	−577, −904
c07_s	z-axis	0.022	1444	0.302	0.302	0.064	0.064	0.036	0.036	−5, 22
c08	z-axis	1.549	1324	6.636	6.636	2.341	2.336	1.047	1.050	−918, −1248
c08_s	z-axis	0.017	1307	0.254	0.215	0.048	0.046	0.029	0.027	−16, 6
c09	z-axis	2.071	1177	8.845	8.845	3.121	3.120	1.381	1.381	−1229, −1668
c09_s	z-axis	0.081	1159	0.493	0.469	0.097	0.095	0.065	0.063	54, −60
c01	c06	0.920								131, 910
c02	c07	1.136								624, 949
c03	c08	1.486								889, 1191
c04	c09	2.079								1307, 1617

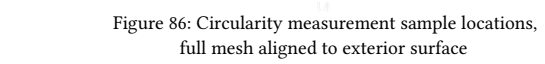

Figure 86: Circularity measurement sample locations, full mesh aligned to exterior surface

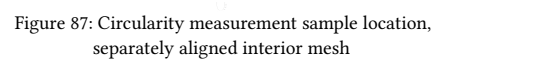

Figure 87: Circularity measurement sample location, separately aligned interior mesh

Concentricity measurements perpendicular to surface curvature

Tag	Reference	Deviation	Sample size	Circle fit residuals analysis for sample listed in Tag column						
				Range full	Range inliers	RMSD full	RMDS inliers	SD full	SD inliers	Center (x,y)
		in		in	in	in	in	in	in	thou
c01	z-axis	0.0121	1779	0.0713	0.0713	0.0191	0.0191	0.0094	0.0094	−2.6, 11.8
c02	z-axis	0.0025	1973	0.0332	0.0332	0.0074	0.0074	0.0043	0.0043	1.8, 1.8
c03	z-axis	0.0025	1992	0.0327	0.0323	0.0083	0.0083	0.0050	0.0050	−1.1, −2.3
c04	z-axis	0.0037	1921	0.0421	0.0399	0.0078	0.0075	0.0049	0.0047	3.1, −2.0
c05	z-axis	0.0092	1869	0.0644	0.0644	0.0148	0.0148	0.0089	0.0089	−1.2, 9.1
c06	z-axis	0.0253	1528	0.1188	0.1188	0.0412	0.0413	0.0177	0.0178	−7.8, −24.0
c06_s	z-axis	0.0008	1446	0.0144	0.0144	0.0031	0.0031	0.0019	0.0019	0.2, −0.8
c07	z-axis	0.0422	1438	0.1835	0.1835	0.0656	0.0656	0.0287	0.0287	−22.7, −35.6
c07_s	z-axis	0.0009	1444	0.0119	0.0119	0.0025	0.0025	0.0014	0.0014	−0.2, 0.9
c08	z-axis	0.0610	1324	0.2613	0.2613	0.0922	0.0920	0.0412	0.0413	−36.1, −49.2
c08_s	z-axis	0.0007	1307	0.0100	0.0084	0.0019	0.0018	0.0012	0.0011	−0.6, 0.3
c09	z-axis	0.0816	1177	0.3482	0.3482	0.1229	0.1228	0.0544	0.0544	−48.4, −65.7
c09_s	z-axis	0.0032	1159	0.0194	0.0184	0.0038	0.0037	0.0026	0.0025	2.1, −2.4
c01	c06	0.0362								5.1, 35.8
c02	c07	0.0447								24.6, 37.4
c03	c08	0.0585								35.0, 46.9
c04	c09	0.0819								51.5, 63.7

Concentricity measurements in z-plane

Tag	Reference	Deviation	Sample size	Circle fit residuals analysis for sample listed in Tag column						
				Range full	Range inliers	RMSD full	RMDS inliers	SD full	SD inliers	Center (x,y)
		in		in	in	in	in	in	in	thou
c01	z-axis	0.0121	1779	0.0713	0.0713	0.0191	0.0191	0.0094	0.0094	−2.6, 11.8
c02	z-axis	0.0025	1973	0.0332	0.0332	0.0074	0.0074	0.0043	0.0043	1.8, 1.8
c03	z-axis	0.0025	1992	0.0327	0.0323	0.0083	0.0083	0.0050	0.0050	−1.1, −2.3
c04	z-axis	0.0037	1921	0.0421	0.0399	0.0078	0.0075	0.0049	0.0047	3.1, −2.0
c05	z-axis	0.0092	1869	0.0644	0.0644	0.0148	0.0148	0.0089	0.0089	−1.2, 9.1
c06	z-axis	0.0253	1528	0.1188	0.1188	0.0412	0.0413	0.0177	0.0178	−7.8, −24.0
c06_s	z-axis	0.0008	1446	0.0144	0.0144	0.0031	0.0031	0.0019	0.0019	0.2, −0.8
c07	z-axis	0.0422	1438	0.1835	0.1835	0.0656	0.0656	0.0287	0.0287	−22.7, −35.6
c07_s	z-axis	0.0009	1444	0.0119	0.0119	0.0025	0.0025	0.0014	0.0014	−0.2, 0.9
c08	z-axis	0.0610	1324	0.2613	0.2613	0.0922	0.0920	0.0412	0.0413	−36.1, −49.2
c08_s	z-axis	0.0007	1307	0.0100	0.0084	0.0019	0.0018	0.0012	0.0011	−0.6, 0.3
c09	z-axis	0.0816	1177	0.3482	0.3482	0.1229	0.1228	0.0544	0.0544	−48.4, −65.7
c09_s	z-axis	0.0032	1159	0.0194	0.0184	0.0038	0.0037	0.0026	0.0025	2.1, −2.4
c01	c06	0.0362								5.1, 35.8
c02	c07	0.0447								24.6, 37.4
c03	c08	0.0585								35.0, 46.9
c04	c09	0.0819								51.5, 63.7